

การสังเคราะห์และสมบัติเชิงแสงของพอร์ไฟรินที่มีวงเอกไซไซคลิกแอโรแมติก

นางสาวชมภัทร เมตตาประเสริฐ

วิทยานิพนธ์นี้เป็นส่วนหนึ่งของการศึกษาตามหลักสูตรปริญญาวิทยาศาสตรมหาบัณฑิต

สาขาวิชาเคมี ภาควิชาเคมี

คณะวิทยาศาสตร์ จุฬาลงกรณ์มหาวิทยาลัย

ปีการศึกษา 2552

ลิขสิทธิ์ของจุฬาลงกรณ์มหาวิทยาลัย

SYNTHESIS AND OPTICAL PROPERTIES OF PORPHYRINS WITH EXOCYCLIC
AROMATIC RINGS

Miss Chommapat Mettaprasert

A Thesis Submitted in Partial Fulfillment of the Requirements
for the Degree of Master of Science Program in Chemistry

Department of Chemistry

Faculty of Science

Chulalongkorn University

Academic Year 2009

Copyright of Chulalongkorn University

Thesis Title SYNTHESIS AND OPTICAL PROPERTIES OF
 PORPHYRINS WITH EXOCYCLIC AROMATIC RINGS
By Miss Chommapat Mettaprasert
Field of Study Chemistry
Thesis Advisor Assistant Professor Worawan Bhanthumnavin, Ph.D.

Accepted by the Faculty of Science, Chulalongkorn University in
Partial Fulfillment of the Requirements for the Master's Degree

.....Dean of the Faculty of Science
(Professor Supot Hannongbua, Dr. rer. nat.)

THESIS COMMITTEE

.....Chairman
(Associate Professor Sirirat Kokpol, Ph.D.)

.....Thesis Advisor
(Assistant Professor Worawan Bhanthumnavin, Ph.D.)

.....Examiner
(Associate Professor Buncha Pulpoka, Ph.D.)

.....External Examiner
(Assistant Professor Radchada Bunttem, Ph.D.)

ชมภัทพร เมตตดาประเสริฐ: การสังเคราะห์และสมบัติเชิงแสงของพอร์ไฟรินที่มีวงเอกไซไซ-
คลิกแอโรแมติก. (SYNTHESIS AND OPTICAL PROPERTIES OF PORPHYRINS
WITH EXCOCYCLIC RINGS) อ.ที่ปรึกษาวิทยานิพนธ์หลัก: ผศ.ดร.วรวรรณ
พินธุมนาวิน, 75 หน้า.

ได้สังเคราะห์สารประกอบพอร์ไฟรินที่มีหมู่แทนที่ที่ตำแหน่งมีโซเป็นวงแอโรแมติกและมีวงเอกไซไซคลิกพีแนนทริน ซึ่งการขยายระบบพายคอนจูเกตนี้ส่งผลต่อสมบัติทางอิเล็กทรอนิกส์พีแนนโทโร[9,10-c]พอร์โรล-1-คาร์บอกซีเลตได้จากปฏิกิริยาการควบแน่นบาร์ตันซาร์ดของ9-ไนโทโร-พีแนนทรินกับเอทิลไอโซไซยาโนแอซีเตตในผลได้ปริมาณผลิตภัณฑ์ที่สูง จากนั้นกำจัดหมู่คาร์บอกซีเลตโดยการรีฟลักซ์กับโพแทสเซียมไฮดรอกไซด์ในเอทิลลีนไกลคอลและผลิตภัณฑ์ที่ได้คือพีแนนโทโร[9,10-c]พอร์โรล ซึ่งเป็นพรีเคอร์เซอร์ของพอร์ไฟริน มีโซเททระแอริลเททระพีแนนโทโรพอร์ไฟรินเตรียมจากปฏิกิริยาควบแน่นระหว่างอนุพันธ์พอร์โรลกับแอริลแอลดีไฮด์ที่ต้องการ ณ อุณหภูมิต่ำโดยใช้โบรอนไตรฟลูออไรด์เป็นตัวเร่งปฏิกิริยา ได้พิกัสเจอร์เอกลักษณะอนุพันธ์พอร์ไฟรินกลุ่มนี้ด้วยเทคนิคโปรตอนเอ็นเอ็มอาร์สเปกโตรสโกปี เทคนิคยูวี-วิชีเบิลสเปกโตรสโกปี ฟลูออเรสเซนซ์สเปกโตรสโกปีและมัลติทอพแมสสเปกโตรเมทรี จากการศึกษาสมบัติกายภาพเชิงแสงของอนุพันธ์พอร์ไฟรินที่สังเคราะห์ได้พบว่าการเพิ่มวงเอกไซไซคลิกแอโรแมติกติดกับวงพอร์ไฟรินส่งผลให้ยูวี-วิชีเบิลสเปกตรัมเลื่อนไปทางความยาวคลื่นที่มากขึ้นและเข้าใกล้ช่วงอินฟราเรด สมบัติการดูดกลืนแสงในช่วงนี้ทำให้อนุพันธ์พอร์ไฟรินที่สังเคราะห์ได้มีศักยภาพที่จะนำไปประยุกต์ใช้งานได้หลายรูปแบบรวมถึงการนำไปใช้งานทางการแพทย์

ภาควิชาเคมี..... ลายมือชื่อนิสิต.....
สาขาวิชา.....เคมี..... ลายมือชื่ออ.ที่ปรึกษาวิทยานิพนธ์หลัก.....
ปีการศึกษา 2552.....

5072254323 : MAJOR CHEMISTRY

KEYWORDS: PORPHYRINS / RING-FUSED PORPHYRINS / PHENANTHRENE

CHOMMAPAT METTAPRASERT: SYNTHESIS AND OPTICAL PROPERTIES OF PORPHYRINS WITH EXOCYCLIC AROMATICS RINGS.
 THESIS ADVISOR: ASST. PROF. WORAWAN BHANTHUMNAVIN,
 Ph.D., 75 pp.

A series of *meso*-aryl substituted porphyrin with fused phenanthrene subunits have been synthesized to obtain insights into the influence of conjugated porphyrin systems on the electronic properties. Barton-Zard condensation of 9-nitrophenanthrene with ethyl isocyano-acetate afforded phenanthro[9,10-*c*]pyrrole-1-carboxylate in good yield. Cleavage of the ester moiety with KOH in refluxing ethylene glycol gave phenanthro[9,10-*c*]pyrrole as a precursor of porphyrins. *meso*-Tetraaryltetraphenanthroporphyrin can be obtained using Lindsey condensation of phenanthro[9,10-*c*]pyrrole with aryl aldehyde at low temperature using boron trifluoride as catalyst. These compounds were characterized by ¹H-NMR, and UV-visible spectroscopies, and MALDI-TOF mass spectrometry. The UV-visible spectra of highly conjugated porphyrins showed that ring fusion had a profound impact on the producing bathochromic shift of the Soret and Q bands into the near-infrared region. Absorption in this area is useful for wide applications in many fields including biomedicine and materials.

Department : Chemistry Student's Signature :

Field of Study : Chemistry Advisor's Signature :

Academic Year : 2009

ACKNOWLEDGEMENTS

I would like to express my sincere and deep gratitude to my thesis advisors, Assistant Professor Dr. Worawan Bhanthumnavin for valuable suggestions, encouragement and kindness throughout the course of this work. I am also truthfully grateful to the members of the thesis committee, Associate Professor Dr. Sirirat Kokpol, Associate Professor Dr. Buncha Pulpoka, and Assistant Professor Dr. Radchada Buntem for reviewing my thesis and giving valuable suggestions and comments.

Furthermore, I am sincerely thankful to Associate Prof. Santi Pippyang and the members of the Natural Product Research Unit (NPRU) for providing some equipments for my research as well as members of the Organic Synthesis Research Unit (OSRU) especially Mr. Wuttichai Reainthippayasakul for useful suggestion and kindness.

Lastly, I would like to acknowledge financial assistance for this project provided by the Center for Petroleum, Petrochemicals and Advanced Materials at Chulalongkorn University. Finally, this thesis would not have been possible without the support, understanding and kindness from my family members and my colleagues throughout my entire study.

CONTENTS

	Page
ABSTRACT (THAI)	iv
ABSTRACT (ENGLISH).....	v
ACKNOWLEDGEMENTS	vi
CONTENTS.....	vii
LIST OF TABLES	x
LIST OF FIGURES	xi
LIST OF ABBREVIATIONS	xii
CHAPTER I INTRODUCTION	1
1.1 Porphyrins	1
1.2 Structure and Nomenclature of Porphyrins.....	2
1.3 Photophysical properties of Porphyrins	3
1.4 Porphyrins with Exocyclic Aromatic Rings	5
1.5 Application of Porphyrins	8
1.5.1 Dye-sensitized Solar Cells (DSSCs).....	8
1.5.2 Photodynamic Therapy (PDT).....	9
1.5.3 Photosensitizer Properties in Photodynamic Therapy.....	10
1.6 Objectives.....	12
CHAPTER II EXPERIMENTAL	13
2.1 Materials and Chemicals	13
2.2 Instruments and Equipments	14
2.3 Synthesis of 9-Nitrophenanthrene (1)	15
2.4 Synthesis of Ethyl Phenanthro[9,10- <i>c</i>]pyrrole-1-carboxylate (2).....	16
2.5 Synthesis of Phenanthro[9,10- <i>c</i>]pyrrole (3).....	17
2.6 Synthesis of <i>meso</i> -Tetraphenyltetraphenanthroporphyrin Derivatives.....	17
2.6.1 Synthesis of <i>meso</i> -Tetraphenyltetraphenanthroporphyrin (TPTPP, 4)...	17
2.6.2 Synthesis of Cu(II)- <i>meso</i> -Tetraphenyltetraphenanthroporphyrin (Cu-TPTPP, 5).....	18

	Page
2.6.3 Attempted Synthesis of Zn(II)- <i>meso</i> -Tetraphenyltetraphenanthroporphyrin (Zn-TPTPP, 6).....	19
2.7 Synthesis of <i>meso</i> -Tetramethoxycarbonylphenyltetraphenanthroporphyrin Derivatives	20
2.7.1 Synthesis of <i>meso</i> -Tetramethoxycarbonylphenyltetraphenanthroporphyrin (TMCPTPP, 7)	20
2.7.2 Synthesis of Cu(II)- <i>meso</i> -Tetramethoxycarbonylphenyltetraphenanthroporphyrin (Cu-TMCPTPP, 8)	21
2.7.3 Synthesis of <i>meso</i> -Tetramethoxycarbonylphenyltetraphenanthroporphyrin (Zn-TMCPTPP, 9)	22
2.7.4 Synthesis of <i>meso</i> -Tetramethoxycarbonylphenyltetraphenanthroporphyrin (Co-TMCPTPP, 10)	23
2.8 Synthesis of <i>meso</i> -Tetracarboxylphenyltetraphenanthroporphyrin (TCPTPP, 11).....	24
2.8.1 Attempts to use Lindsey's Method	24
2.8.2 Attempts to use Adler-Longo's Method.....	25
2.8.3 Hydrolysis of <i>meso</i> -Tetramethoxycarbonylphenyltetraphenanthroporphyrin (TMCPTPP, 7)	25
2.9 Investigation of Photophysical Properties.....	26
2.9.1 UV-Visible Spectroscopy	26
2.9.2 Fluorescence Spectroscopy	27
CHAPTER III RESULTS AND DISCUSSION.....	28
3.1 Concept of Molecular Design.....	28
3.2 Synthesis of Ring Extended Pyrrole	29
3.3 Synthesis of <i>meso</i> -Tetraphenyltetraphenanthroporphyrin Derivatives.....	33
3.3.1 Synthesis of <i>meso</i> -Tetraphenyltetraphenanthroporphyrin (TPTPP, 4)... ..	33
3.3.2 Synthesis of Cu(II)- <i>meso</i> -Tetraphenyltetraphenanthroporphyrin (Cu-TPTPP, 5).....	36
3.3.3 Synthesis of Zn(II)- <i>meso</i> -Tetraphenyltetraphenanthroporphyrin (Zn-TPTPP, 6).....	37

	Page
3.4 Synthesis of <i>meso</i> -Tetramethoxycarbonylphenyltetraphenanthroporphyrin Derivatives	39
3.4.1 Synthesis of <i>meso</i> -Tetramethoxycarbonylphenyltetraphenanthroporphyrin (TMCPTPP, 7)	39
3.4.2 Synthesis of Cu(II)- <i>meso</i> -Tetramethoxycarbonylphenyltetraphenanthroporphyrin (Cu-TMCPTPP, 8).....	43
3.4.3 Synthesis of Zn(II)- <i>meso</i> -Tetramethoxycarbonylphenyltetraphenanthroporphyrin (Zn-TMCPTPP, 9).....	43
3.4.4 Synthesis of Co(II)- <i>meso</i> -Tetramethoxycarbonylphenyltetraphenanthroporphyrin (Co-TMCPTPP, 10).....	44
3.5 Synthesis of <i>meso</i> -Tetracarboxyphenyltetraphenanthroporphyrin (TCPTPP, 11).....	45
3.6 Solubility of <i>meso</i> -Tetraaryltetraphenanthroporphyrin Series	47
3.7 Investigation of Photophysical Properties.....	49
3.7.1 UV-Visible Spectroscopy	49
3.7.2 Fluorescence Spectroscopy.....	54
 CHAPTER IV CONCLUSION.....	 55
 REFERENCES.....	 56
 APPENDIX	 60
 VITAE	 75

LIST OF TABLES

Table		Page
2.1	The amounts of porphyrins which were used in the preparation of the stock solutions.....	27
3.1	The conditional summary of phenanthro[9,10- <i>c</i>]pyrrole synthesis.....	32
3.2	The conditional summary of TPTPP synthesis.....	33
3.3	The conditional summary of TMCPTPP synthesis.....	40
3.4	The MALDI-TOF mass data of synthesized <i>meso</i> -tetraaryltetra-phenanthroporphyrin derivatives.....	47
3.5	The solubility of all synthesized porphyrins.....	47
3.6	Absorption maxima of the solutions of all synthesized porphyrins at a 10^{-5} M concentration and their color in solution.....	50

LIST OF FIGURES

Figure		Page
1.1	Structure of chlorophylls and haeme.....	2
1.2	Structure and nomenclature of porphyrin in Fischer's system relative to IUPAC system.....	3
1.3	The Gouterman's four orbital model and the electronic absorption spectrum of a simple porphyrin.....	4
1.4	The electronic transitions energy diagram.....	5
1.5	The structures of tetrabenzoporphyrin (TBP) and tetranaphtho- porphyrins (TNPs).....	6
1.6	The structures of tetraacenaphthoporphyrin (TANP), tetraphenyl- tetraacenaphthoporphyrin (TPTANP) and tetraphenanthro- porphyrin (TPP).....	7
1.7	The structure and synthetic method of <i>meso</i> -tetraaryltetra- phenanthroporphyrin.....	8
1.8	The basic scheme of tumour phototherapy using a photosensitizer..	10
1.9	The general structure of target porphyrins.....	12
3.1	The general structure of target molecule.....	30
3.2	Reagents and conditions for the synthesis of phenanthro[9,10- <i>c</i>]- pyrrole.....	29
3.3	The ¹ H NMR spectra of mixture, 9-nitrophenanthrene and 3-nitro- phenanthrene.....	30
3.4	The ¹ H NMR of 9-nitrophenanthrene (1).....	30
3.5	The ¹ H NMR of 3-nitrophenanthrene.....	31
3.6	The ¹ H NMR of ethyl phenanthro[9,10- <i>c</i>]pyrrole-1-carboxylate (2).....	32
3.7	The ¹ H NMR of phenanthro[9,10- <i>c</i>]pyrrole (3).....	33
3.8	The MALDI-TOF mass spectrum of TPTPP from entry 1.....	34

Figure	Page	
3.9	The absorption spectra of synthesized TPTPP (4) and TPTPP from You group in dichloromethane.....	35
3.10	The MALDI-TOF mass spectrum of Cu-TPTPP crude.....	37
3.11	The UV-visible absorption spectrum of Cu-TPTPP (5).....	37
3.12	The MALDI-TOF mass spectrum of Zn-TPTPP by using CHCl ₃ as a solvent.....	38
3.13	The MALDI-TOF mass spectrum of Zn-TPTPP by using DMF as solvent.....	39
3.14	The MALDI-TOF mass spectrum of the resulting solution in the entry 4.....	41
3.15	The ¹ H NMR spectrum of TMCPTPP (7) in deuteriochloroform	42
3.16	The MALDI-TOF mass spectrum of Zn-TMCPTPP by using CHCl ₃ as a solvent.....	44
3.17	The MALDI-TOF mass spectrum of Co-TMCPTPP at 2 h, 4 h and 7 h.....	45
3.18	The MALDI-TOF mass spectrum of dication TCPTPP	46
3.19	The structure of <i>meso</i> -tetraphenanthroporphyrin	48
3.20	The difference in degree of π - π stacking interactions between (a) <i>meso</i> -tetraphenanthroporphyrin and (b) <i>meso</i> -tetraaryltetra-phenanthroporphyrin.....	49
3.21	UV-visible absorption spectra of TPTPP, TMCPTPP and TCPTPP in dichloromethane.....	51
3.22	UV-visible absorption spectra of (a) TMCPTPP and (b) <i>meso</i> -tetraphenanthroporphyrin in 1% TFA-chloroform.....	52
3.23	UV-visible absorption spectra of TMCPTPP, Cu-TMCPTPP, Zn-TMCPTPP and Co-TMCPTPP in dichloromethane.....	53
A-1	The ¹ H-NMR spectrum of 9-nitrophenanthrene (1).....	61
A-2	The ¹³ C-NMR spectrum of 9-nitrophenanthrene (1).....	61

Figure		Page
A-3	The ¹ H-NMR spectrum of ethyl phenanthro[9,10- <i>c</i>]pyrrole-1-carboxylate (2).....	62
A-4	The ¹³ C-NMR spectrum of ethyl phenanthro[9,10- <i>c</i>]pyrrole-1-carboxylate (2).....	62
A-5	The ESI mass spectrum of ethyl phenanthro[9,10- <i>c</i>]pyrrole-1-carboxylate (2).....	63
A-6	The ¹ H-NMR spectrum of phenanthro[9,10- <i>c</i>]pyrrole (3).....	63
A-7	The ¹³ C-NMR spectrum of phenanthro[9,10- <i>c</i>]pyrrole (3).....	64
A-8	The ESI mass spectrum of phenanthro[9,10- <i>c</i>]pyrrole(3).....	64
A-9	The MALDI-TOF mass spectrum of TPTPP (4).....	65
A-10	The UV-visible spectrum of TPTPP (4).....	65
A-11	The MALDI-TOF mass spectrum of Cu-TPTPP (5).....	66
A-12	The UV-visible spectrum of Cu-TPTPP (5).....	66
A-13	The ¹ H-NMR spectrum of TMCPTPP (7).....	67
A-14	The MALDI-TOF mass spectrum of TMCPTPP (7).....	67
A-15	The UV-visible spectrum of TMCPTPP (7).....	68
A-16	The ¹ H-NMR spectrum of Cu-TMCPTPP (8).....	68
A-17	The MALDI-TOF mass spectrum of Cu-TMCPTPP (8).....	69
A-18	The UV-visible spectrum of Cu-TMCPTPP (8).....	69
A-19	The ¹ H-NMR spectrum of Zn-TMCPTPP (9).....	70
A-20	The MALDI-TOF mass spectrum of Zn-TMCPTPP (9).....	70
A-21	The UV-visible spectrum of Zn-TMCPTPP (9).....	71
A-22	The ¹ H-NMR spectrum of Co-TMCPTPP (10).....	71
A-23	The MALDI-TOF mass spectrum of Co-TMCPTPP (10).....	72
A-24	The UV-visible spectrum of Co-TMCPTPP (10).....	72
A-25	The ¹ H-NMR spectrum of TCPTPP (11).....	73
A-26	The MALDI-TOF mass spectrum of TCPTPP (11).....	73
A-27	The UV-visible spectrum of TCPTPP (11).....	74

LIST OF ABBREVIATIONS

Å	angstroms
α	alpha
Abs	absorbance
Ar	aryl or aromatic group
β	beta
br	broad
°C	degree Celsius
CDCl ₃	deuterated chloroform
cm	centimeter
d	doublet (NMR)
dd	doublet of doublet (NMR)
δ	delta
DBU	1,8-diazabicyclo[5.4.0]undec-7-ene
DDQ	2,3-dichloro-5,6-dicyanobenzoquinone
DMF	<i>N,N</i> -dimethylformamide
DMSO	dimethylsulfoxide
DSSC	dye-sensitized solar cell
eq.	equivalent
ESI-MS	electrospray ionization mass spectrometry
Et	ethyl
g	gram
γ	gamma

h	hour
HOMO	highest occupied molecular orbital
Hz	hertz
<i>J</i>	coupling constant
LOMO	lowest unoccupied molecular orbital
m	multiplet (NMR)
<i>m</i> -	meta
M	molar
$[M]^+$	molecular ion
MALDI-TOF-MS	matrix assisted laser desorption ionization time-of-flight mass spectrometry
mg	milligram
MHz	megahertz
min	minute
mL	milliliter
mmol	millimole
mol	mole
m/z	mass per charge ratio
nm	nanometer
NMR	nuclear magnetic resonance
<i>o</i> -	ortho
OAc	acetate
<i>p</i> -	para
PDT	photodynamic therapy
Ph	phenyl

ppm	part per million
rt	room temperature
s	second
s	singlet (NMR)
t	triplet (NMR)
TFA	trifluoroacetic acid
THF	tetrahydrofuran
TLC	thin layer chromatography
TMS	trimethylsilyl
μL	microliter
UV	ultraviolet
λ	wavelength
δ	chemical shift
π	pi
%	percent

CHAPTER I

INTRODUCTION

1.1 Porphyrins

Porphyrins and their analogues constitute one of the most important families of aromatic macrocycles. The word *porphyrin* is derived from the Greek *porphura* that was used to describe the colour purple [1]. Porphyrins are widespread compounds in nature, where they play essential functions for life. A free-base porphyrin in which metal is inserted in its cavity is called metalloporphyrin. The metal complexes are fundamental importance in the development of life, due to their roles as mediators in biological oxidation reactions. The chlorophylls are magnesium(II)-porphyrin complexes that are central in the transformation of solar energy in bacteria, algae and plants. The haems are iron(II)-porphyrin complexes responsible for the oxygen carrying properties of haemoglobin and myoglobin. Haem is also the prosthetic group in the cytochromes, responsible for electron transport, reduction of oxygen and hydroxylation reactions. Vitamin B₁₂ is a cobalt(III) complex of a compound related to haem. Iron complexes in the haemoprotein, and magnesium complexes in the chlorophylls are shown in **Figure 1.1**.

All porphyrins are intensely colored due to their large π -conjugated system. They are sometimes known as “the pigments and the colors of life”. This reflects the importance of porphyrins as they play a key role in our biological functions. In fact, our life relies on biological processes which are either performed by or catalyzed by porphyrin-containing substances. They have also been reported to accumulate in tumors and it is possibly effective radiosensitizers [2].

As “the pigments and the colors of life”, porphyrins have been intensely one of the subjects that interests chemists and biochemists worldwide. Recently, various porphyrin derivatives have been synthesized and found useful in several applications. Nevertheless, many researchers are still working on porphyrins to reveal many mystery functions that will play an important role to our life in the future.

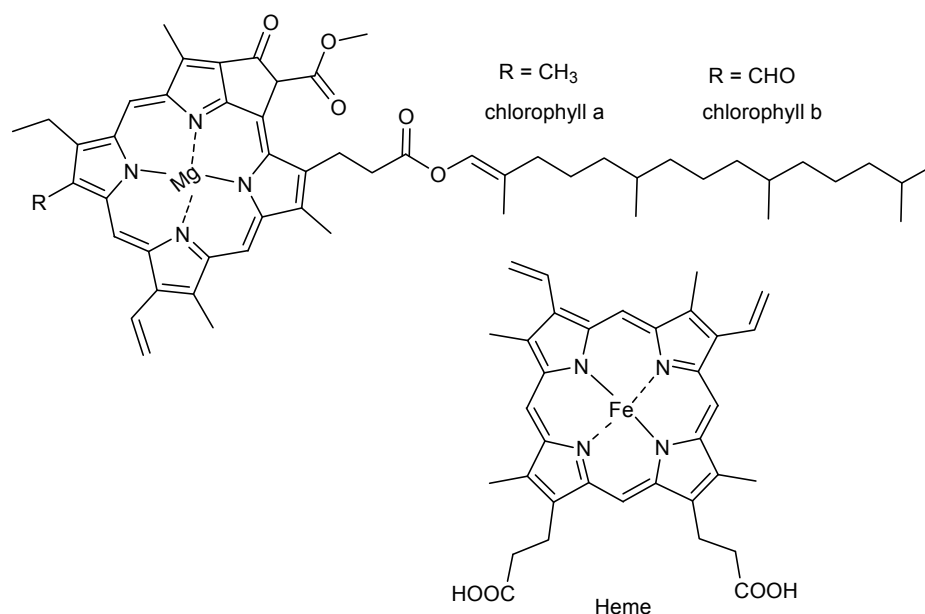


Figure 1.1 Structure of chlorophylls and haem

1.2 Structure and Nomenclature of Porphyrins

The basic structure of porphyrins consists of four pyrrole units linked by four methine bridges between the α -positions of the five-membered pyrrole rings. The first system of nomenclature for porphyrin was created by Hans Fischer (**Figure 1.2**). In this system, each position on the pyrrole fragments where a substituent could go are given a number from 1 to 8 and the bridging carbon atoms (*meso*-position) named α , β , γ , and δ whereas the pyrrole positions next to each nitrogen atom are remained unnumbered. The Fischer system is straightforward for naming simple porphyrins. However, when the complexity of a porphyrin derivative increases, the system becomes too complicated and even contradictory. A new, more systematic nomenclatures was introduced which numbered all the atoms in the macrocycle and cut down on the number of trivial names. These recommendations provide for naming porphyrins, hydroporphyrins, ring contracted or expanded porphyrins, porphyrins fused with other rings, skeletally replaced porphyrins and porphyrin-metal coordination complexes together with corresponding linear arrangements of three and four pyrrole rings. The application of these recommendations permits these substances to be named more systematically using fewer trivial names. These may seem a senseless change for a systematic nomenclature based on 1-24 numbering system (**Figure 1.2**) which is developed by a

joint commission on biochemical nomenclature, consisting of the International Union of Pure and Applied Chemistry (IUPAC) and the International Union of Biochemistry (IUB) [1].

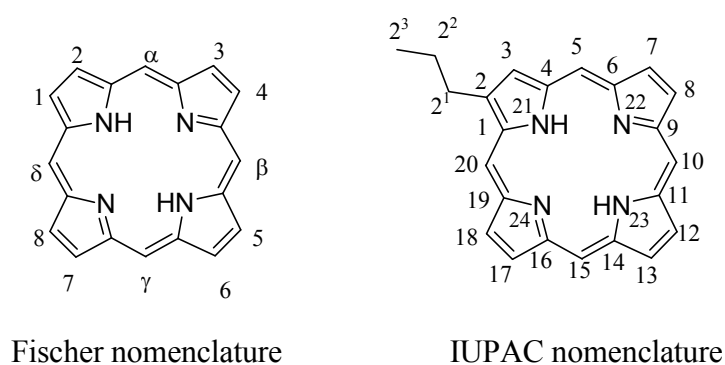


Figure 1.2 Structure and nomenclature of porphyrin in Fischer's system relative to IUPAC system

The 1-24 numbering system is adopted for the porphyrin nucleus. The 2, 3, 7, 8, 12, 13, 17, and 18 positions have commonly been referred to generically as “ β -positions”. Similarly, the 1, 4, 6, 9, 11, 14, 16, and 19 positions have been referred to generically as “ α -positions”, while the 5, 10, 15, and 20 positions have been referred to generically as “*meso*-positions”. However, in order to avoid possible ambiguity with stereochemical designations, the use of these generic terms is discouraged.

1.3 Photophysical Properties of Porphyrins

Porphyrins and their related derivatives have an extensive system of delocalized π electrons, hence these macrocyclic compounds display interesting and extraordinary photophysical properties, especially as shown in their UV-visible absorption and emission spectra.

Generally, the electron absorption spectrum of a typical porphyrin such as octaethylporphyrinatozinc(II) (ZnOEP) consists of a strong transition to the second excited state ($S_0 \rightarrow S_2$) at about 400 nm called the Soret or B band and a weak transition to the first excited state ($S_0 \rightarrow S_1$) at around 500-700 nm called the Q band. Both Soret and Q bands arise from π - π^* transitions and can be explained by considering the four

frontier orbitals (the “Gouterman’s four orbital model”, as shown in **Figure 1.3**): two π orbitals (a_{1u} and a_{2u}) and a degenerate pair of π^* orbitals (e_{gx} and e_{gy}). The two highest occupied π orbitals happen to have about the same energy. One might imagine that this would lead to two almost coincident absorption bands due to $a_{1u} \rightarrow e_g$ and $a_{2u} \rightarrow e_g$ transitions, but in fact these two transitions mix together by a process known as configurational interaction, resulting in two bands with very different intensities and wavelengths. The constructive interference leads to the intense short-wavelength Soret band, while the weak long-wavelength Q band results from destructive combinations. The two types of position on the porphyrin periphery are referred to as *meso*- and β -positions. The a_{1u} orbital has nodes at all four *meso*-positions whereas the a_{2u} orbital has high coefficients at these sites [3]. Moreover, Q band that showed at the longest wavelength is called Q band I and the next peak is named Q band II as shown in the absorption spectrum in **Figure 1.3**.

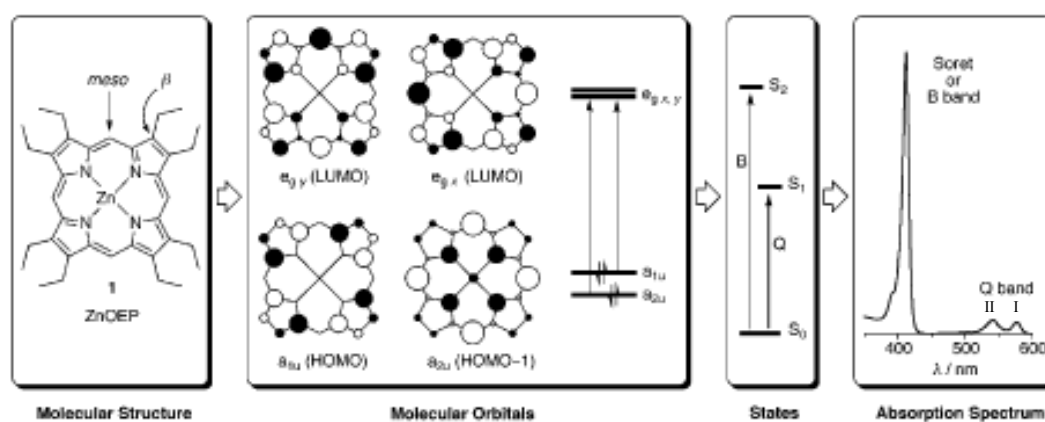


Figure 1.3 The Gouterman’s four orbital model and the electronic absorption spectrum of a simple porphyrin [3]

For the description of the emission phenomenon and photophysical parameters is best made with the use of the energy diagram as shown in **Figure 1.4** [4]. Starting with excitation from the ground state S_0 to to any singlet excited state S_1 or S_2 leads to very fast radiationlessly decay to the first excited singlet state S_1 . From the first excited singlet state S_1 , the molecule can emit fluorescence radiation $S_1 \rightarrow S_0$ at the rate k_F , can be nonradiative process such as internal conversion from $S_1 \rightarrow S_0$ at the rate k_{ic} , or can

internally convert to the lowest triplet $S_1 \rightarrow T_1$ at the rate k_{isc} . The first excited singlet state S_1 decays between 10^{-12} and 10^{-7} s, after which, if the system is still excited, it exists in the lowest triplet state T_1 . From the first triplet state T_1 , the molecule can emit phosphorescence radiation $T_1 \rightarrow S_0$ at the rate k_p , can radiationlessly decay $T_1 \rightarrow S_0$ at the rate k_{ip} . Thus, only the relaxation process from S_1 to S_0 with rate k_F can emit fluorescence radiation. In the case of porphyrins, the internal conversion from the second excited state to the first excited state ($S_2 \rightarrow S_1$) is rapid; hence, fluorescence is only detected from the first excited state S_1 [5].

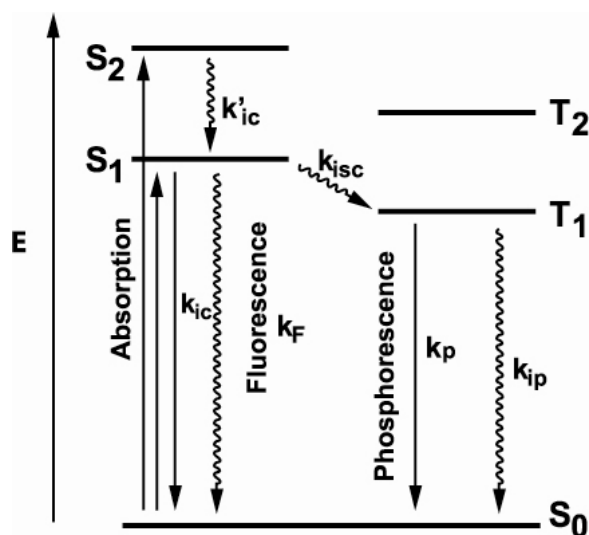


Figure 1.4 The electronic transitions energy diagram

1.4 Porphyrins with Exocyclic Aromatic Rings

Modified porphyrin chromophores with strong absorption in the red/near-infrared region can be approached in different ways, which include expanding the basic tetrapyrrolic macrocycle by adding extra pyrrolic fragments [6], manipulating porphyrin planarity [7], introducing *meso*-alkynyl substituents [8], as well as, extending the porphyrin core by fusing it with external aromatic fragments [9, 10]. The latter is called “ π -extended porphyrins”, which has drawn much attention in recent years. One of the most effective and promising synthetic approaches might be the fusion of aromatic rings at the β -pyrrolic position which lead to a significant alternation in the electronic

and optical properties. These enhanced absorption in near-infrared region is generally useful for several applications.

The best known representatives of this class of compounds are symmetrically π -extended porphyrins such as tetrabenzoporphyrins (TBP) and tetranaphthoporphyrins (TNP) in **Figure 1.5**, whose optical and other properties attract interest in material research, biomedical imaging and sensing, up-conversion of noncoherent near-infrared light and photodynamic therapy [9, 11]. Moreover, numerous π -extended porphyrins with fused acenaphthylene [12, 13], phenanthrene [14, 15], anthracene [16] have been investigated.

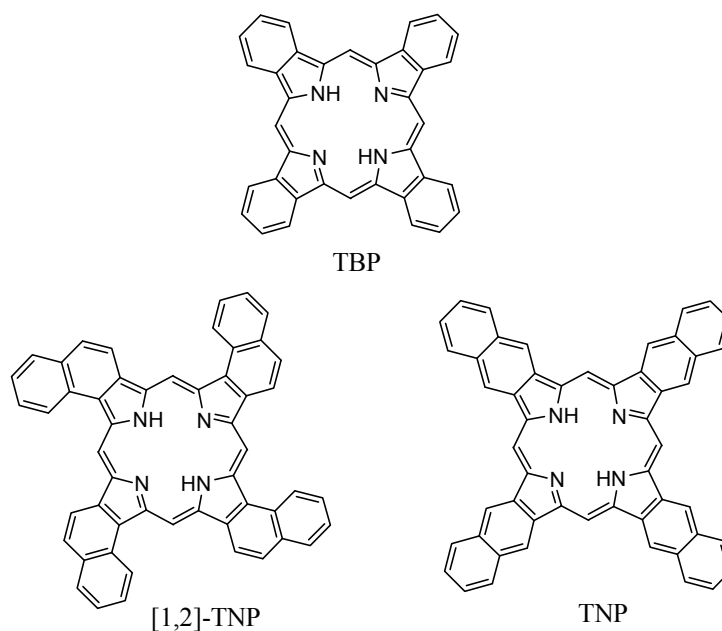


Figure 1.5 The structures of tetrabenzoporphyrin (TBP) and tetranaphthoporphyrins (TNPs)

A drawback can occur when the π -expansion induces strong π - π stacking between molecules which results in low solubility of the porphyrins and difficulties in purification. To overcome these obstacles, *meso*-substituted porphyrins has been designed and prepared. For example, tetraacenaphthoporphyrin (TANP) is highly insoluble in most organic solvents, whereas tetraphenyltetraacenaphthoporphyrin (TPTANP) can dissolve in organic solvents. Their structures are shown in **Figure 1.6**.

In the latter case, phenyl groups are unable to lie in the same plane as the porphyrin macrocycle, they should disrupt intermolecular π - π stacking and hence might have the added advantage of strongly influencing the compound with significantly increased solubility [12].

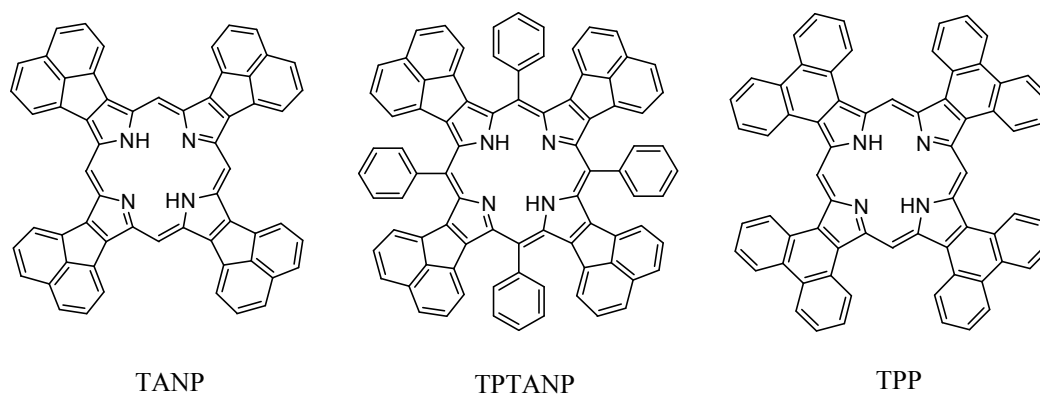


Figure 1.6 The structures of tetraacenaphthoporphyrin (TANP), tetraphenyltetraacenaphthoporphyrin (TPTANP) and tetraphenanthroporphyrin (TPP)

In 1995, Lash and Novak [14] had been interested in developing synthetic routes to new highly conjugated porphyrin systems, tetraphenanthroporphyrin (TPP) structure of which is shown in **Figure 1.6**. This porphyrin was shown the electronic spectrum in trifluoroacetic acid/chloroform dramatically red-shifted absorption bands compared to those of any previously reported porphyrin structure. The Soret band was observed at 482 nm and two bathochromically shifted Q bands were observed at 615 and 688 nm. However, tetraphenanthroporphyrin was virtually insoluble in most organic solvents similarly to tetraacenaphthoporphyrin as mentioned before.

Subsequently, Xu group [15] synthesized *meso*-aryl substituted tetraphenanthroporphyrin series to develop solubility properties in organic solvent. The synthetic route of these porphyrins (**Figure 1.7**) are not complicated compared to synthetic routes for porphyrins with different exocyclic rings [13, 17]. Moreover, they revealed that the compound has a surprisingly red-shifted absorption spectra. Q band I almost reached 800 nm.

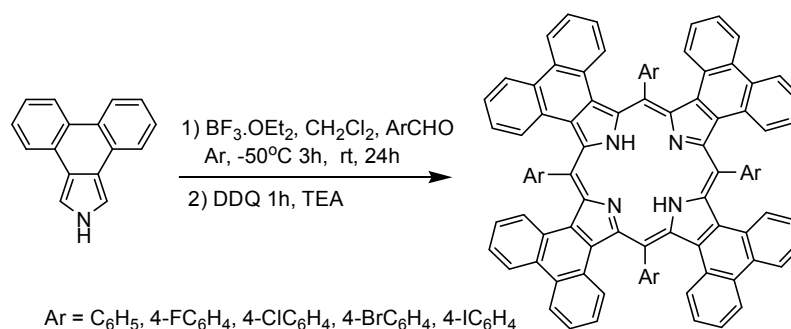


Figure 1.7 The structure and synthetic method of *meso*-tetraaryltetraphenanthroporphyrin

1.5 Application of Porphyrins

Porphyrin and metalloporphyrin represent a large family of functional molecular materials with high chemical and thermal stability. These compounds are objects of great interest for chemists, physicists, biochemists, and industrial scientists because of their potential role in emerging technologies including dye-sensitized solar cells (DSSCs) [18, 19], organic light-emitting diodes (OLED) technology [20, 21], gas sensors [22, 23], fluorescence probes [24] and biomedical applications such as photosensitizers in photodynamic therapy [25, 26]. Applications of porphyrins in DSSCs and photodynamic therapy are further described.

1.5.1 Dye-sensitized Solar Cells (DSSCs)

Generally, molecules that will be used as a dye for DSSC should absorb across the entire visible spectrum, bind strongly to the semiconductor surface, have a suitably high redox potential for regeneration following excitation and be stable over many years of exposure to sunlight. Consequently, a wide varieties of dyes with different binding groups and the linkers have mentioned. Anchoring to TiO₂ as semiconductor surface has been achieved through a number of functional groups such as salicylate, carboxylic acid, sulphonic acid, phosphonic acid, and acetylacetonate derivatives. The most widely used and successful to date of these functional groups are carboxylic acid and phosphonic acid [18]. Therefore, the use of porphyrins as light harvests on semiconductors is particularly attractive given their primary role in photosynthesis and

the relative ease with which a variety of covalent or noncovalent porphyrin arrays can be constructed.

1.5.2 Photodynamic Therapy (PDT)

Phototherapy is the use of visible or near-visible light as a therapeutic agent in clinical medicine. It falls into two categories: *direct*, without an administered photosensitizer; and *indirect*, where the effect is achieved *via* an administered photosensitizer which is the effective light absorber. The indirect category is useful to make the distinction because the administration of both sensitizing drug and a dose of light means that consideration must be given to additional parameters (e.g. chemical structure of the photosensitizer, length of drug-light interval). Hence, the basic idea of tumour phototherapy is this: (1) find a good photosensitizer which shows some selectivity for photodamage to tumor tissue; (2) inject the photosensitizer and wait for a certain time; and (3) irradiate the tumour with visible light to generate singlet oxygen which will destroy the tumour [27].

Photodynamic therapy (PDT) is a new modal cancer treatment leading to the selective destruction of malignancies by visible light in the presence of a photosensitizer and oxygen. Upon the irradiation of visible light with appropriate wavelength, the activated photosensitizer can drive molecular oxygen into excited triplet state and the electron transfers energy into ground state molecular oxygen to produce singlet oxygen. Thereby, the generated singlet oxygen plays an important role in cytotoxic effects on tumour tissues while sparing healthy adjacent areas. The basic scheme of tumour phototherapy using a photosensitizer is shown in **Figure 1.8**.

The first generation of photosensitizer is a mixture of haematoporphyrin derivatives; Photofin [26-28] which, however, presents several undesirable properties. Those are three important disadvantages. Firstly, it is not very selective and causes skin sensitivity for some weeks. Secondly, the absorption band in the red (Q band I approximately 630 nm) is weak. Thirdly, it is complex and variable mixtures from which it has not proved possible to isolate a single highly active constituent [27]. These limitations of the first generation led to a development of a new generation photosensitizers to offer potential advantages over the first generation photosensitizers.

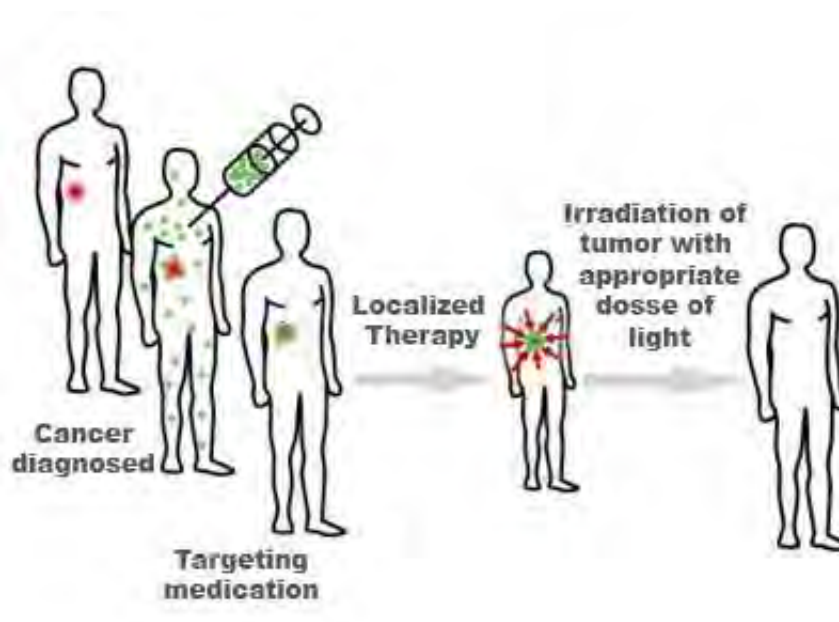


Figure 1.8 The basic scheme of tumour phototherapy using a photosensitizer

1.5.3 Photosensitizer Properties in Photodynamic Therapy

Second generation photosensitizers with improved PDT properties are under widely investigation from the past until now. The design features of second generation photosensitizers for photodynamic therapy will be discussed which appear to be as follows.

Single substance

The preference must be single substances because this simplifies the interpretation of dose-response relationships in a situation which is already much more complex than usual because of the extra variables to do with light treatment (*e.g.* drug light interval, wavelength, total energy). In general, most of the second generation photosensitizers which belong to porphyrin series broadly defined because porphyrin systems is a good singlet oxygen generator.

Toxicity and Stability

It is clearly desirable that the substance for photosensitizer should has zero or very low cytotoxicity in the absence of light so that light activation produces maximum benefits. Moreover, it should be rapidly excreted from the body.

Photophysical Parameters

A new drug as photosensitizer for PDT critically depends on its photophysical parameters that are triplet yield, life time, and energy. It should have a high quantum yield of triplet state formation and a long triplet life. While the energy of the triplet needs to be $\geq 94 \text{ kJ mol}^{-1}$ for efficient energy transfer to ground state dioxygen. For singlet oxygen reactions, the key parameter overall is the quantum yield (Φ_{Δ}) of singlet oxygen.

Hydrophobicity and Hydrophilicity

Most amphiphilic substances have some selectivity for the tumour and are rapidly cleared from the body. Many macrocyclic compounds including porphyrins are hydrophobic, this means that hydrophilic substituents are needed to achieve the correct amphiphilic balance. For example, hydrophilic properties of porphyrins can be improved by introducing polar substituents. Sulfonic acid, carboxylic acid, hydroxyl, and quaternary ammonium salt have been the substituents most studied and differential interactions have been observed at the molecular, cellular and the tumour tissue level [29].

Red Absorption

On account of both absorption and scattering of light by tissue increase as the wavelength decreases, the most efficiently excited sensitizers are those which have strong absorption bands at red end of the visible spectrum. Isomeric and expanded porphyrin systems are attractive as potential PDT photosensitizers because they generally absorb at wavelength at or above 700 nm. That is important to be available for singlet oxygen production with commensurately less being lost to tissue absorption and scatter [29].

1.6 Objectives

This research is aimed to synthesize an extensive series of porphyrin with exocyclic phenanthrene rings and their metal complexes. The general structure of these porphyrins is illustrated in **Figure 1.9**. All of the synthesized porphyrins will be characterized by ^1H NMR spectroscopy and MALDI-TOF mass spectrometry. Moreover, UV-visible absorption spectroscopy and fluorescence spectroscopy are also used to investigate their photophysical properties. Effects of metal ions as well as various aryl substituents at *meso*-positions of synthesized porphyrins on photophysical properties will be discussed.

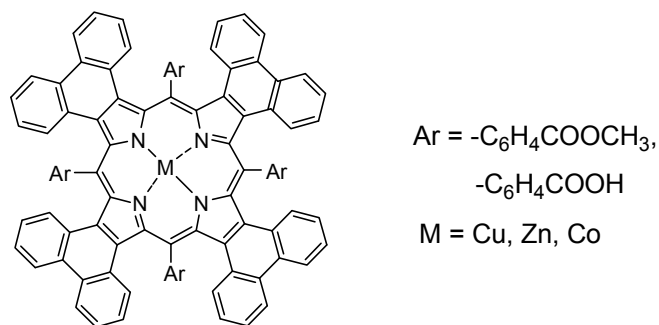


Figure 1.9 The general structure of target porphyrins

CHAPTER II

EXPERIMENTAL

2.1 Materials and Chemicals

Dried glassware were used in all reactions. The progress of the reactions and all separation techniques could be monitored by thin layer chromatography (TLC) performed on Merck D.C. silica gel 60 F₂₅₄ 0.2 mm precoated aluminium sheets. The plates were visualized by the use of a UV lamp (254 nm), or by dipping in a solution of potassium permanganate in sulfuric acid or vanillin in ethanolic sulfuric acid. Column chromatography was performed on Merck 70-230 mesh ASTM silica gel, while flash column chromatography was performed on Merck 230-400 mesh ASTM silica gel. Purification of some compounds was performed on Sephadex LH-20 purchased from Pharmacia. Preparative thin layer chromatography was coated on the 20×20 cm² glass plate by Merck silica gel 60 GF₂₅₄.

Solvents for synthesis and crystallization including chloroform, dichloromethane, *N,N*-dimethylformamide (DMF), ethanol, ethylene glycol, tetrahydrofuran (THF), and toluene were AR grade. While solvents for chromatography including hexanes, ethyl acetate, dichloromethane, and methanol were commercial grade and were distilled before use.

All chemicals were reagent grade and were used without further purification. They were purchased from the following vendors:

- Acros Organics (New Jersey, USA): acetyl chloride
- Aldrich Chemical Co., Inc. (Steinheim, Germany): ethyl isocynoactate
- BDH Chemicals Ltd. (Poole, England) : glacial acetic acid, phenanthrene
- Carlo Erba Reagenti (Milan, Italy): potassium hydroxide, triethylamine, dicholoromethane

- Fluka Chemical Corp. (Buchs, Switzerland): anhydrous magnesium sulfate, boron trifluoride diethyl etherate, 4-carboxybenzaldehyde, cobalt(II) acetate tetrahydrate, copper(II) acetate, 1,8-diazabicyclo[5.4.0]undec-7-ene (DBU), 2,3-dichloro-5,6-dicyano-*p*-benzoquinone (DDQ), *N,N*-dimethylformamide (DMF), triethylamine, trifluoroacetic acid (TFA), zinc(II) acetate dihydrate
- Labscan Asia Co., Ltd. (Bangkok, Thailand): chloroform, dichloromethane, tetrahydrofuran
- Merck Co., Ltd. (Darmstadt, Germany): benzaldehyde, ethanol, ethylene glycol, methanol, methyl-4-formylbenzoate, nitric acid, toluene
- Riedel-de Haën AG (Seelze, Germany): propionic acid
- Sigma Chemical Co., Inc. (St. Louis, Missouri, USA): dithranol
- Suksapan Panit (Bangkok, Thailand): sodium hydrogen carbonate
- Wilmad LabGlass SP Industries, Inc. (New Jersey, USA): deuterated chloroform, hexadeuterated dimethylsulfoxide

2.2 Instruments and Equipments

The weight of all chemicals was determined on a Precisa XT 220A electric balance. Evaporation of solvents was carried out on a Büchi Rotavapor R-200 equipped with a Büchi Heating Bath B-490 and a Büchi Recirculating Chiller B-740.

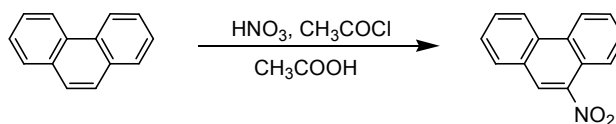
All reported ^1H and ^{13}C NMR were recorded using a Varian Mercury plus 400 NMR spectrometer operated at 400 MHz for ^1H and 100 MHz for ^{13}C nuclei in deuterated chloroform (CDCl_3) and hexadeuterated dimethylsulfoxide ($\text{DMSO}-d_6$). The chemical shifts (δ) are reported in parts per million (ppm) and are relative to tetramethylsilane (TMS) or relative to the reference peak of the deuterated solvent. Coupling constants (J) are given in hertz (Hz).

Mass spectra were obtained with Electrospray Ionization Mass Spectrometry (ESI-MS) by a Waters Micromass Quattro micro API Mass Spectrometer with an electrospray ion source, and ethyl acetate was used as a solvent. Mass spectra of porphyrins were determined on a Bruker Microflex Matrix Assists Laser Desorption Ionization Time-of-Flight Mass Spectrometer (MALDI-TOF-MS). The instrument was

equipped with a nitrogen laser to desorb and ionize the samples. A stainless steel target was used as the substrate on which the samples were deposited. Samples were prepared in dichloromethane and methanol solutions using dithranol as the matrix.

UV-visible absorption spectra were determined with a Varian Cary 100 Bio UV-visible Spectrophotometer. Both the deuterium and the visible lamps were used as light sources in this instrument. Fluorescence emission spectra were carried out using a Varian Cary eclipse fluorescence spectrophotometer. The light source is a pulsed xenon lamp and the detector is a photomultiplier tube.

2.3 Synthesis of 9-Nitrophenanthrene (1) [30]



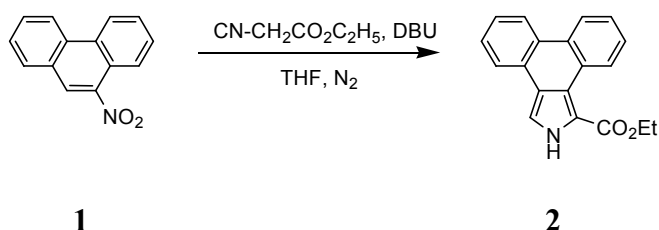
1

Nitric acid (6 mL) was added dropwise to a stirred acetyl chloride (12 mL). The mixture was added slowly during an approximately 1 h period into a solution of phenanthrene (8.000 g, 44.89 mmol) in glacial acetic acid (16 mL). The resulting mixture was heated between 40 and 50 °C for 4 h and then poured into iced water. The liquid was decanted off from the resulting yellow gum, and then the residual was dissolved in dichloromethane. The ice-water solution was extracted with dichloromethane, and the combined organic solutions were washed sequentially with water, 5% sodium bicarbonate solution, and water. The organic phase was dried over anhydrous MgSO₄, and the solvent was then removed using a rotary evaporator under vacuum to afford a yellow oil. The crude product was dissolved with a small amount of toluene then loaded on silica gel for a flash column chromatography (230-400 mesh silica) and eluted with hexanes. After the yellow nitrophenanthrene fraction started to elute, approximately 2.0 L of hexanes was collected. Evaporation of the solvent under reduced pressure, followed by recrystallization from 99% ethanol, gave the desired 9-nitrophenanthrene (**1**) (2.70 g, 29%) as yellow crystals.

¹H NMR (CDCl₃, 400 MHz): δ 7.70-7.86 (4H, m, Ar), 8.03 (1H, d, *J* = 8.2 Hz, Ar), 8.50 (1H, s, Ar), 8.52 (1H, m, Ar), 8.72 (1H, d, *J* = 8.4 Hz, Ar), 8.78 (1H, d, *J* =

7.6 Hz, Ar); ^{13}C NMR (CDCl_3 , 100 MHz): δ 122.8, 122.9, 123.1, 123.8, 125.3, 127.8, 127.9, 128.0, 128.7, 129.9, 131.0, 132.0.

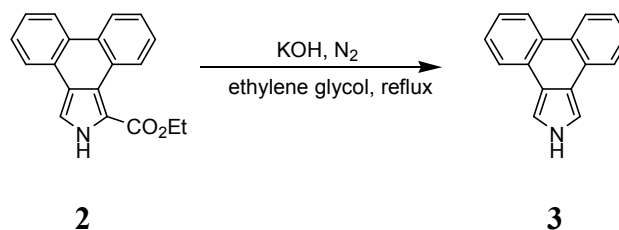
2.4 Synthesis of Ethyl Phenanthro[9,10-*c*]pyrrole-1-carboxylate (**2**) [30]



9-Nitrophenanthrene (**1**) (2.790 g, 12.50 mmol) was dissolved in dry THF (28 mL) under a N_2 atmosphere and then ethyl isocyanoacetate (1.35 mL, 12.35 mmol) was added. After that DBU (1.85 mL, 12.37 mmol) was added slowly into the solution and the solution was stirred at room temperature overnight. The solution was diluted with dichloromethane (20 mL), washed with distilled water three times, and dried over MgSO_4 . The solvent was removed using a rotary evaporator under vacuum to give a crude product as a brown solid. The crude product was recrystallized from toluene and washed well with toluene to give ethyl phenanthro[9,10-*c*]pyrrole-1-carboxylate (2.83 g, 79%) as a pale yellow solid.

^1H NMR (CDCl_3 , 400 MHz): δ 1.47 (3H, t, $J = 7.2$ Hz, CH_3), 4.47 (2H, q, $J = 7.2$ Hz, CH_2), 7.49-7.54 (2H, m, Ar), 7.58-7.66 (2H, m, Ar), 7.70 (1H, d, $J = 3.6$ Hz, Ar), 8.04 (1H, m, Ar), 8.52 (1H, m, Ar), 8.57 (1H, m, Ar), 9.81 (1H, d, $J = 6.3$ Hz, Ar), 9.91 (1H, br, NH); ^{13}C NMR (CDCl_3 , 100 MHz): δ 14.5, 60.7, 114.9, 115.9, 122.6, 122.8, 123.1, 123.4, 123.9, 125.7, 126.7, 126.9, 127.0, 127.4, 127.4, 128.3, 130.4, 160.5; ESI-MS: m/z $[\text{M}]^+$ Calcd for $\text{C}_{19}\text{H}_{15}\text{NO}_2$: 289.110, Found 288.251.

2.5 Synthesis of Phenanthro[9,10-*c*]pyrrole (**3**) [31]

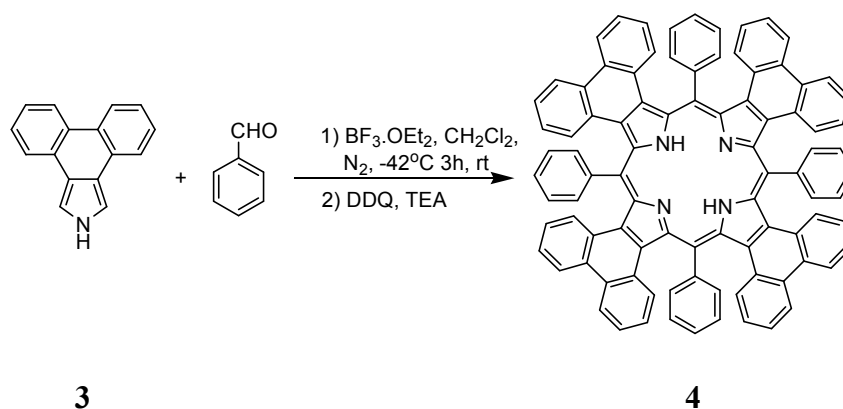


A mixture of ethyl phenanthro[9,10-*c*]pyrrole-1-carboxylate (**2**) (1.054 g, 3.63 mmol) and KOH (2.106 g, 37.55 mmol) in ethylene glycol (32 mL) were placed in a dried two-necked round bottom flask. Nitrogen gas was bubbled through the mixture for 10 min, and the resulting solution was refluxed on a preheated oil bath at 170 °C under a nitrogen atmosphere for an additional 30 min. The mixture was warmed to room temperature and then poured into an iced water. The resulting precipitate was collected by suction filtration and washed well with water to give phenanthro[9,10-*c*]pyrrole (**3**) (0.766 g, 97%) as a tan solid.

¹H NMR (CDCl₃, 400 MHz): δ 7.48 (4H, m, Ar), 7.55 (2H, d, *J* = 2.7 Hz, Ar), 8.05 (2H, d, *J* = 7.4 Hz, Ar), 8.47 (2H, d, *J* = 7.6 Hz, Ar), 8.89 (1H, br, *NH*); ¹³C NMR (CDCl₃, 100 MHz): δ 110.3, 119.8, 123.3, 123.6, 125.1, 126.9, 128.7, 128.8; ESI-MS: *m/z* [M]⁺ Calcd for C₁₆H₁₁N: 217.089, Found 218.183 [M+H]⁺.

2.6 Synthesis of *meso*-Tetraphenyltetraphenanthroporphyrin Derivatives

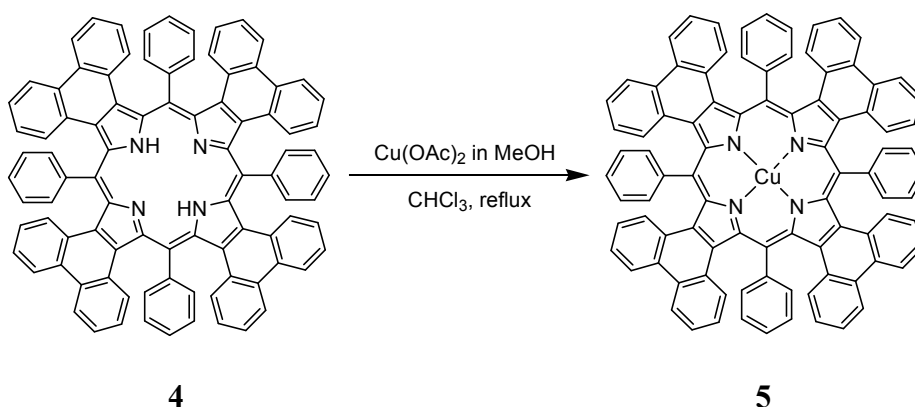
2.6.1 Synthesis of *meso*-Tetraphenyltetraphenanthroporphyrin (TTPPP, **4**) [15]



Phenanthro[9,10-*c*]pyrrole (**3**) (0.978 g, 4.50 mmol) was dissolved in 80 mL of CH₂Cl₂ under N₂ and was cooled to -45°C (acetonitrile-dry ice bath). A solution of benzaldehyde (0.45 mL, 4.45 mmol) in CH₂Cl₂ (1 mL) was added dropwise to the mixture, followed by an addition of BF₃·OEt₂ (0.57 mL, 4.50 mmol). The mixture was stirred at -45°C for 3 h after which the cool bath was removed. The mixture was left to react at ambient temperature under continuous stirring for 2 nights. DDQ (2.050 g, 9.00 mmol) was added, and the solution stirred for another 2 h. Five drops of triethylamine were then added. The residue was purified by short column chromatography (70-130 mesh silica, CH₂Cl₂, Hexanes:EtOAc 1:1, EtOAc). The dark red solution was collected and further purified by flash column chromatography (230-400 mesh silica, Hexanes:EtOAc 1:1) with subsequent crystallization by layering methanol onto concentrated CH₂Cl₂ solution. After filtration, the pure porphyrin could not be obtained.

MALDI-TOF-MS (dithranol): *m/z* [M]⁺ Calcd for C₉₂H₅₄N₄: 1214.435, Found 1215.889; UV-visible (CH₂Cl₂, nm): λ_{max} nm (ε) 579 (64302) (Soret), 727 (8626), 804 (15123) (Q).

2.6.2 Synthesis of Cu(II)-*meso*-Tetraphenyltetraphenanthroporphyrin (Cu-TPTPP, **5**)

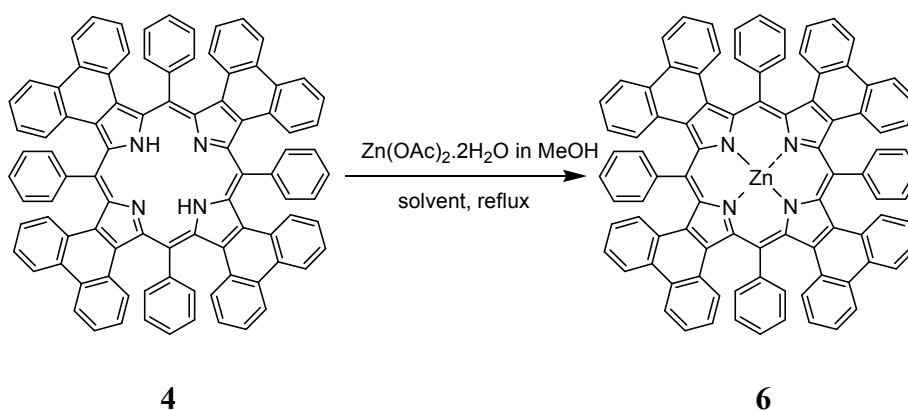


A solution of Cu(OAc)₂ (0.0252 g, 0.14 mmol) in MeOH (2 mL) was added to a boiling solution of *meso*-tetraphenyltetraphenanthroporphyrin (TPTPP, **4**) (0.7040 g, 0.024 mmol) in CHCl₃. The solution was refluxed at 60-70 °C for 1 h. After that the reaction was cooled down and extracted three times with distilled water. The organic layer was dried over MgSO₄. Further, purification by column chromatography (70-130

mesh silica, CH_2Cl_2) and Sephadex (LH-20, CH_2Cl_2 :MeOH 7:3), the pure desired complex porphyrin could not be obtained.

MALDI-TOF-MS (dithranol): m/z $[\text{M}]^+$ Calcd for $\text{C}_{92}\text{H}_{52}\text{CuN}_4$: 1275.349, Found 1279.176; UV-visible (CH_2Cl_2 , nm): λ_{max} nm 588 (Soret), 689 (Q).

2.6.3 Attempted synthesis of Zn(II)-*meso*-Tetraphenyltetraphenanthroporphyrin (Zn-TPTPP, 6)

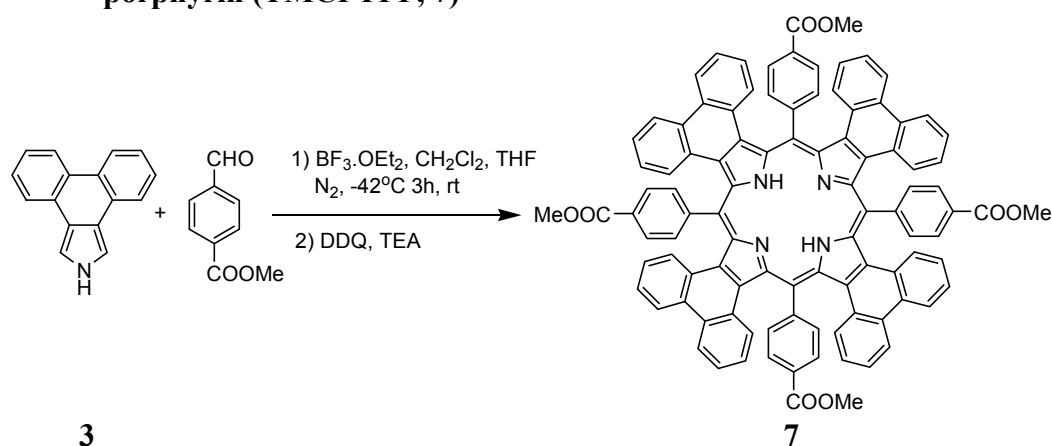


Method I : A solution of $\text{Zn}(\text{OAc})_2 \cdot 2\text{H}_2\text{O}$ (18.6 mg, 0.085 mmol) in MeOH (1 mL) was added to a boiling solution of *meso*-tetraphenyltetraphenanthroporphyrin (TPTPP, **4**) (29.6 mg, 0.024 mmol) in CHCl_3 . The mixture was refluxed at 60-70 °C for 1 h. After that an aliquot of the reaction mixture was taken out and monitored by MALDI-TOF mass spectrometry. The zinc complex of porphyrin and the unreacted free-base porphyrin were observed. The reflux was therefore continued overnight. The MALDI-TOF mass spectrum still showed an intense peak of starting material and a small peak of Zn-TPTPP.

Method II : A solution of $\text{Zn}(\text{OAc})_2 \cdot 2\text{H}_2\text{O}$ (22.8 mg, 0.10 mmol) in MeOH (1 mL) was added to a boiling solution of *meso*-tetraphenyltetraphenanthroporphyrin (TPTPP, **4**) (24.4 mg, 0.020 mmol) in DMF. The mixture was refluxed at 150-160 °C for 1 h. After that the reaction was monitored by MALDI-TOF spectrometry. The zinc complex of porphyrin peak could not be detected in the mass spectrum.

2.7 Synthesis of meso-Tetramethoxycarbonylphenyltetraphenanthroporphyrin Derivatives

2.7.1 Synthesis of meso-Tetramethoxycarbonylphenyltetraphenanthroporphyrin (TMCPTPP, 7)

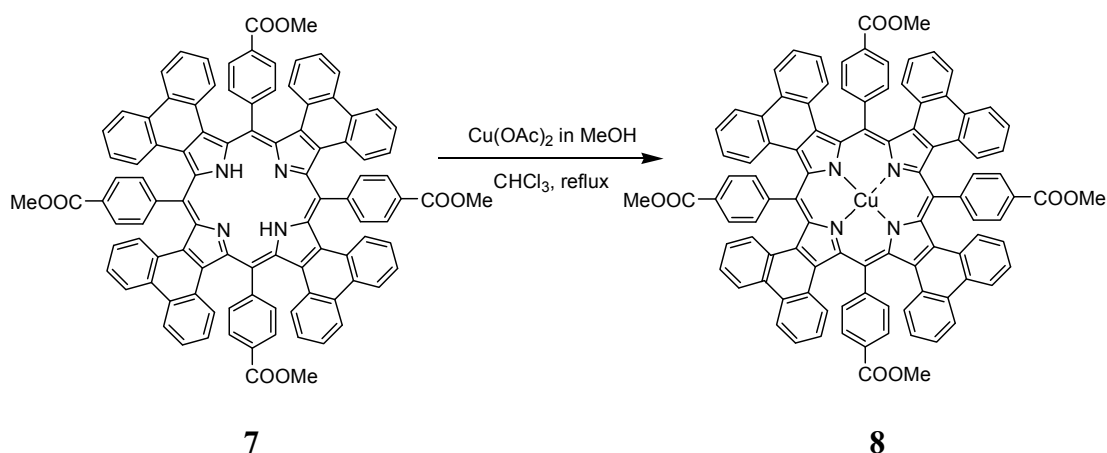


Phenanthro[9,10-*c*]pyrrole (**3**) (0.7641 g, 3.52 mmol) was dissolved in 400 mL of CH_2Cl_2 under N_2 in the dark room and was cooled to -45°C (acetonitrile-dry ice bath). The solution of methyl-4-formylbenzoate (0.5413 g, 3.30 mmol) in CH_2Cl_2 (3 mL) was added dropwise to the mixture, followed by an addition of $\text{BF}_3 \cdot \text{OEt}_2$ (0.22 mL, 1.74 mmol). The mixture was stirred at -45°C for 3 h after which the cooling bath was removed. The mixture was left to react at ambient temperature under continuous stirring 2 nights. DDQ (0.7820 g, 3.43 mmol) was added, and the solution stirred for another 3 h. Ten drops of triethylamine were then added. The resulting solution was extracted with 5% aqueous sodium bicarbonate solution and water. After drying over anhydrous MgSO_4 , the solution was evaporated under reduced pressure. Following the evaporation, the residue was purified by column chromatography (70-130 mesh silica), eluting with CH_2Cl_2 :petroleum ethers 19:1 then EtOAc. The dark blue solution was collected and further recrystallized twice by layering methanol onto concentrated CHCl_3 solution to give meso-tetramethoxycarbonylphenyltetraphenanthroporphyrin (**7**) (76.5 mg, 6%) as a dark red solid.

^1H NMR (TFA- CDCl_3 , 400 MHz): δ 1.23 (4H, s, NH), 4.26 (12H, s, CH_3), 6.75 (8H, t, $J = 7.7$ Hz, Ar), 7.29 (16H, m, Ar), 8.24 (8H, d, $J = 8.2$ Hz, Ar), 8.37 (8H, d, $J = 8.6$ Hz, Ar), 8.81 (8H, d, $J = 8.2$ Hz, Ar); MALDI-TOF-MS (dithranol): m/z $[\text{M}]^+$ Calcd

for $C_{100}H_{62}N_4O_8$: 1446.457, Found 1447.173; UV-visible (CH_2Cl_2 , nm): λ_{max} nm (ϵ) 586 (61861) (Soret), 719 (10421), 797 (12953) (Q).

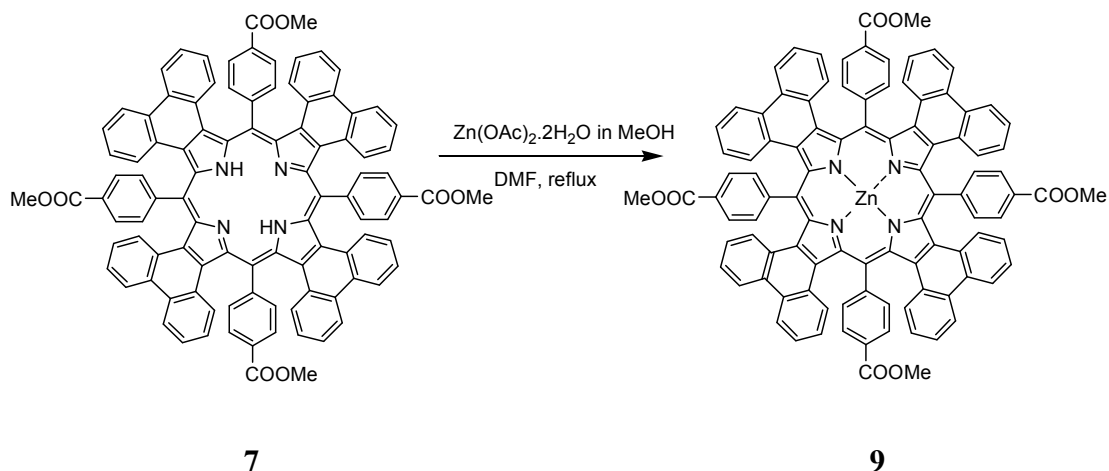
2.7.2 Synthesis of Cu(II)-*meso*-Tetramethoxycarbonylphenyltetraphenanthroporphyrin (Cu-TMCPTPP, **8**)



A solution of $Cu(OAc)_2$ (17.3 mg, 0.095 mmol) in MeOH (2 mL) was added to a boiling solution of *meso*-tetramethoxycarbonylphenyltetraphenanthroporphyrin (TMCPTPP, **7**) (40.5 mg, 0.028 mmol) in $CHCl_3$. The solution was refluxed at 60-70 °C for 1 h. After that the reaction was cooled down and extracted three times with distilled water. The organic layer was dried over $MgSO_4$ and concentrated under vacuum to give Cu(II)-*meso*-tetramethoxycarbonylphenyltetraphenanthroporphyrin (**8**) (38.9 mg, 92%) as a dark violet solid.

1H NMR ($CDCl_3$, 400 MHz): δ 3.97 (br), 6.79 (br), 7.86 (br), 8.59 (br),; MALDI-TOF-MS (dithranol): m/z $[M]^+$ Calcd for $C_{100}H_{60}CuN_4O_8$: 1507.371, Found 1507.758; UV-visible (CH_2Cl_2 , nm): λ_{max} nm (ϵ) 599 (52359) (Soret), 670 (12584) (Q).

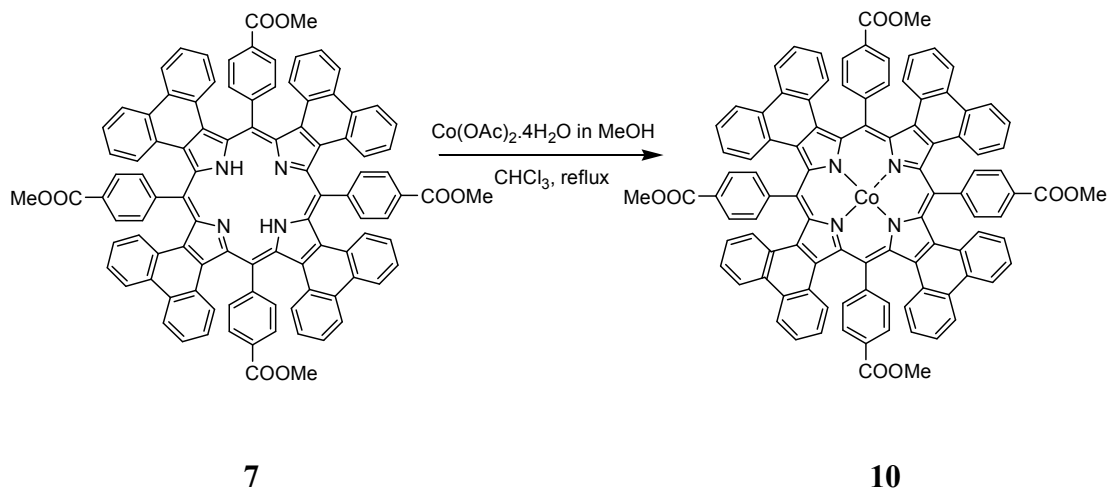
2.7.3 Synthesis of *meso*-Tetramethoxycarbonylphenyltetraphenanthroporphyrin (Zn-TMCPTPP, 9)



A solution of $\text{Zn(OAc)}_2 \cdot 2\text{H}_2\text{O}$ (22.7 mg, 0.10 mmol) in MeOH (2 mL) was added to a boiling solution of *meso*-tetramethoxycarbonylphenyltetraphenanthroporphyrin (TMCPTPP, **4**) (29.5 mg, 0.020 mmol) in DMF. The mixture was refluxed at 150-160 °C for 1 h. After that the reaction was cooled down and extracted three times with distilled water. The organic layer was dried over MgSO_4 and concentrated under vacuum. Recrystallization by layering methanol onto concentrated CHCl_3 solution gave Zn(II)-*meso*-tetramethoxycarbonylphenyltetraphenanthroporphyrin (**9**) (27.2 g, 90%) as a dark red solid.

^1H NMR (CDCl_3 , 400 MHz): δ 4.03 (br), 6.822 (br), 7.043 (br), 7.579 (br), 8.26 (br), 8.42 (br), 8.65 (br), 8.75 (br), 8.91 (br); MALDI-TOF-MS (dithranol): m/z $[\text{M}]^+$ Calcd for $\text{C}_{100}\text{H}_{60}\text{N}_4\text{O}_8\text{Zn}$: 1508.370, Found 1510.619; UV-visible (CH_2Cl_2 , nm): λ_{max} nm (ϵ) 595 (45674) (Soret), 746 (11826), 816 (12257) (Q).

2.7.4 Synthesis of *meso*-Tetramethoxycarbonylphenyltetraphenanthroporphyrin (Co-TMCPTPP, **10**)

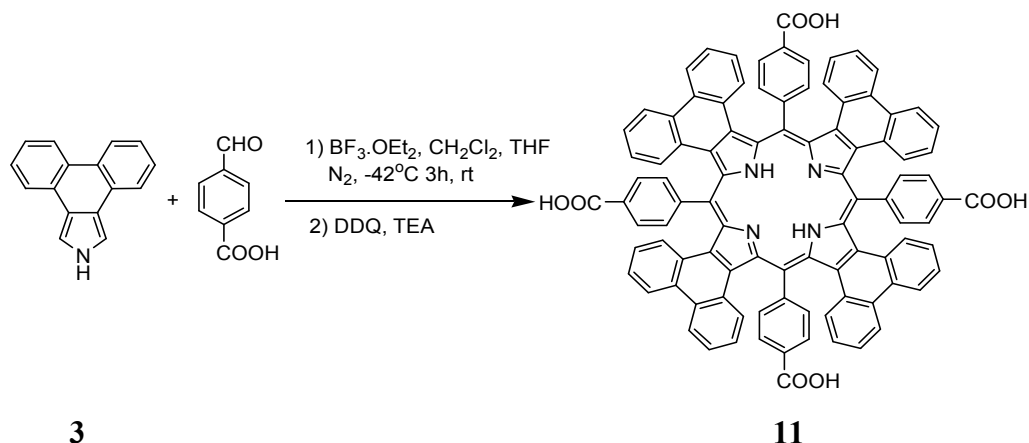


A saturated solution of $\text{Co(OAc)}_2 \cdot 4\text{H}_2\text{O}$ (24.8 mg, 0.10 mmol) in MeOH (2 mL) was added to a boiling solution of *meso*-tetramethoxycarbonylphenyltetraphenanthroporphyrin (TMCPTPP, **7**) (28.2 mg, 0.020 mmol). The mixture was refluxed at 60-70 °C for 7 h. After that the reaction was cooled down and extracted three times with distilled water. The organic layer was dried over MgSO_4 and concentrated under vacuum. Recrystallization by layering methanol onto concentrated CHCl_3 solution gave Co(II)-*meso*-tetramethoxycarbonylphenyltetraphenanthroporphyrin (**10**) (18.8 g, 64%) as a dark green solid.

^1H NMR (CDCl_3 , 400 MHz): δ 3.99 (br), 6.56 (br), 6.96 (br), 8.07 (br), 8.43 (br); MALDI-TOF-MS (dithranol): m/z $[\text{M}]^+$ Calcd for $\text{C}_{100}\text{H}_{60}\text{CoN}_4\text{O}_8$: 1503.374, Found 1503.771; UV-visible (CH_2Cl_2 , nm): λ_{max} nm (ϵ) 523 (34809) (Soret), 703 (9908) (Q).

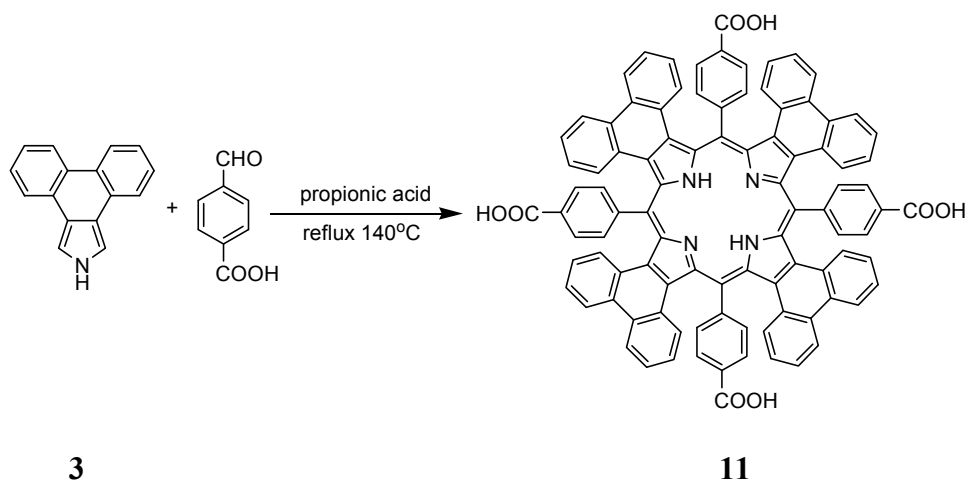
2.8 Synthesis of *meso*-Tetracarboxylphenyltetraphenanthroporphyrin (TCPTPP, 11)

2.8.1 Attempts to use Lindsey's Method



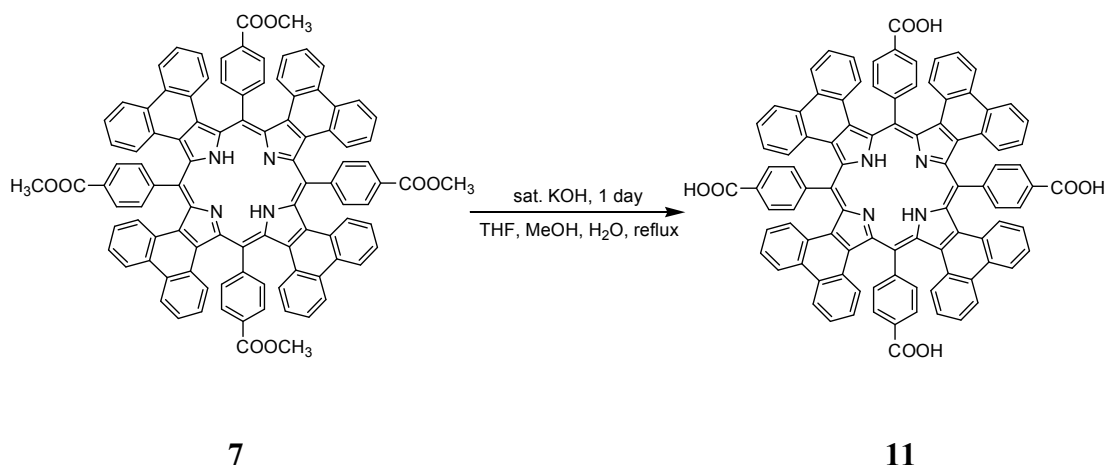
Phenanthro[9,10-*c*]pyrrole (**3**) (0.441 g, 2.03 mmol) was dissolved in 130 mL of CH_2Cl_2 under N_2 in the dark room and was cooled to -45°C (acetonitrile-dry ice bath). The solution of 4-carboxybenzaldehyde (0.308 g, 2.05 mmol) in THF (3 mL) was added dropwise to the mixture, followed by an addition of $\text{BF}_3 \cdot \text{OEt}_2$ (0.26 mL, 2.05 mmol). The mixture was stirred at -45°C for 3 h after which the cool bath was removed. The mixture was left to react at ambient temperature under continuous stirring overnight. DDQ (0.446 g, 1.96 mmol) was added, and the solution stirred for another 2 h. Five drops of triethylamine were then added, and further purified on various separation techniques. Even with normal column chromatography (70-230 mesh silica, CH_2Cl_2 then EtOAc), flash column chromatography (230-400 mesh silica, hexanes:THF 1:1 then 2% MeOH in hexanes:THF 1:1), and Sephadex column chromatography (LH-20, MeOH), the desired product could not be obtained.

2.8.2 Attempts to use Adler-Longo's Method



A solution of 4-carboxybenzaldehyde (0.304 g, 2.03 mmol) in propionic acid (2 mL) was added to a boiling propionic acid (20 mL) and followed by adding a solution of phenanthro[9,10-*c*]pyrrole (**3**) (0.435 g, 2.00 mmol) in propionic acid (2 mL). The mixture was refluxed at 140 °C for 2 h, cooled down to ambient temperature and let stand overnight in a freezer. The resulting solid was collected by suction filtration and washed well with hexanes to give a mixture of *meso*-tetracarboxyphenyltetraphenanthroporphyrin (TCPTPP, **11**) and impurities.

2.8.3 Hydrolysis of *meso*-Tetramethoxycarbonylphenyltetraphenanthroporphyrin (TMCPTPP, **7**)



A mixture of *meso*-tetramethoxyphenyltetraphenanthroporphyrin (TMCPTPP, **7**) (48.9 mg, 0.034 mmol), saturated KOH aqueous solution (1 mL) in THF (8 mL), MeOH (8 mL) and water 0.5 (mL) was refluxed at 60-70 °C with stirring for 1 day. The

solution was evaporated and the residual was dissolved in water (2 mL). After addition of an adequate amount of 0.1 M HCl to acidify the residue, a black precipitate was formed. The resulting black precipitate was washed with water and collected by centrifugation. The product was dried in vacuum to afford *meso*-tetracarboxyphenyl-tetraphenanthroporphyrin (TCPTPP, **11**) (35.4 mg, 75%) as a black solid.

^1H NMR (DMSO, 400 MHz): δ 6.79 (br), 7.41 (br), 8.07 (br), 8.63 (br), 8.72 (br), 8.88 (br); MALDI-TOF-MS (dithranol): m/z $[\text{M}]^+$ Calcd for $\text{C}_{96}\text{H}_{54}\text{N}_4\text{O}_8$: 1390.394, Found 1391.956; UV-visible (0.1% TFA in MeOH, nm): λ_{max} nm (ϵ) 585 (53527) (Soret), 726 (8150), 802 (11036) (Q).

2.9 Investigation of Photophysical Properties

The stock solution of 1.0×10^{-4} M of *meso*-tetraphenyltetraphenanthroporphyrin derivatives and *meso*-tetramethoxycarbonylphenyltetraphenanthroporphyrin derivatives in CH_2Cl_2 were prepared by dissolving porphyrins (1.0×10^{-3} mmol) with CH_2Cl_2 in a 10 mL volumetric flask. *meso*-Tetracarboxyphenyltetraphenanthroporphyrin was prepared the same way but 0.1% TFA in MeOH was used instead of CH_2Cl_2 as a solvent. The exact amounts of each porphyrin which were used in the preparation of the stock solutions are presented in **Table 2.1**.

2.9.1 UV-visible Spectroscopy

A stock solution of porphyrins (100 μL) was added to a 1 cm quartz cuvette and solvent (900 μL) was added to adjust the solution 1 mL by using micropipette. TPTPP derivatives and TMCPTPP derivatives were dissolved in CH_2Cl_2 , whereas TCPTPP was prepared in 0.1 TFA in MeOH. The UV-visible absorption spectra of all porphyrins were measured at 1.0×10^{-5} M and recorded from 350 nm to 900 nm at ambient temperature.

Table 2.1 The amounts of porphyrins which were used in the preparation of the stock solutions.

Porphyrins	MW	weight (mg)	amount (mmol)	concentration of porphyrins (mol/dm ³)
TPTPP, 4	1215.44	1.23	1.0×10^{-3}	1.0×10^{-4}
TMCPTPP, 7	1447.58	1.50	1.0×10^{-3}	1.0×10^{-4}
Cu-TMCPTPP, 8	1509.11	1.55	1.0×10^{-3}	1.0×10^{-4}
Zn-TMCPTPP, 9	1510.96	1.55	1.0×10^{-3}	1.0×10^{-4}
Co-TMCPTPP, 10	1504.50	1.55	1.0×10^{-3}	1.0×10^{-4}
TCPTPP, 11	1391.48	1.40	1.0×10^{-3}	1.0×10^{-4}

2.9.2 Fluorescence Spectroscopy

A stock solution of porphyrin (200 μ L) was added to a 2 cm quartz cuvette and solvent (1800 μ L) was added to adjust the solution 2 mL by using micropipette. TPTPP derivatives and TMCPTPP derivative were used CH₂Cl₂, where as TCPTPP was prepared in 0.1% TFA in MeOH. The fluorescence emission spectra of all porphyrins were measured at 1.0×10^{-5} M and recorded from 400 nm to 1100 nm at ambient temperature.

CHAPTER III

RESULTS AND DISCUSSION

3.1 Concept of Molecular Design

It is known that porphyrin and their metal complexes can be utilized as key dye and pigment materials in various applications such as in optoelectronic devices, photodynamic therapeutic agents, and molecular sensors. However, most porphyrin derivatives display similar optical properties because their π -conjugation are limited in their core ring only. One of the most interesting way to enhance absorption in the near-infrared region is the extension of π -conjugated systems of porphyrins by extending the porphyrin core by fusing it with aromatic fragments.

Owing to this reason, this research is aimed to synthesize porphyrins with exocyclic phenanthrene rings. In addition, the compounds bear various aryl groups at the *meso*-position. The general structure of target molecules is presented in **Figure 3.1**.

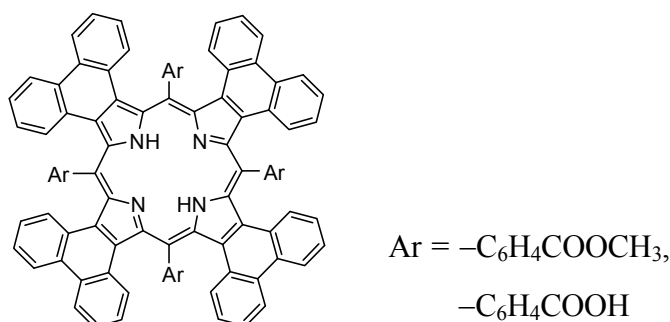


Figure 3.1 The general structure of target molecule

As shown in **Figure 3.1**, there are two parts in the structure which may be modified in order to alter optical properties of the parent porphyrin. These include:

- Exocyclic aromatic rings : It is anticipated that phenanthrene rings which are fused on the tetrapyrrolic fragments would increase the extension of π -conjugated systems of porphyrin. Besides, the synthetic route to the target porphyrin may be done in a one-pot nature.

- Ar group : In this thesis, a phenyl group with two different functional groups at the *para* position are chosen as the target. These aryl groups are connected to the core porphyrin system at the *meso*-position of the porphyrin rings to improve the solubility of the compounds. This is to alleviate difficulties related to low solubility of certain material which affects further manipulation including fabrication process of the material. Moreover, the functional group on the aromatic ring at the *meso*-position are carboxyl group that may improve the solubility in high polar solvents.

3.2 Synthesis of Ring Extended Pyrrole

The summary of a synthetic route to phenanthro[9,10-*c*]pyrrole as a precursor of target porphyrins is shown in **Figure 3.2**.

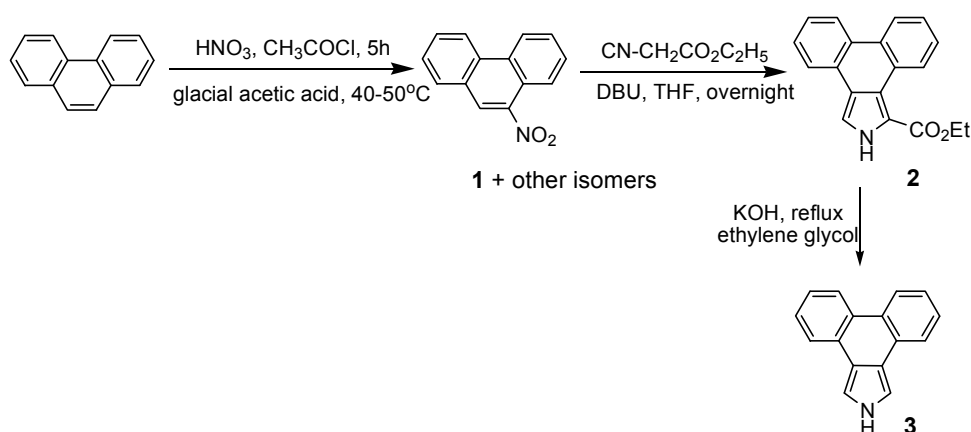


Figure 3.2 Reagents and conditions for the synthesis of phenanthro[9,10-*c*]pyrrole

Nitration of phenanthrene in acetic acid with nitric acid in acetyl chloride led to the formation of all five possible mononitrophenanthrene isomers but chromatography with caution followed by recrystallization from ethanol afforded the desired isomer **1**. However, even after chromatography and recrystallization were introduced, the NMR spectrum still showed small 3-nitrophenanthrene peaks (**Figure 3.3**).

¹H NMR spectra of 9-nitrophenanthrene and 3-nitrophenanthrene exhibited signals of protons corresponding to the structure as shown in **Figure 3.4** and **Figure 3.5**, respectively [32]. The proton NMR spectrum of 9-nitrophenanthrene showed the phenanthrene protons between 7.70-8.78 ppm but the proton of 3-nitrophenanthrene

close to the nitro group at position 4 was further deshielded to 9.60 ppm. Nonetheless, the small amount of 3-nitrophenanthrene did not affect the synthesis in the next step.

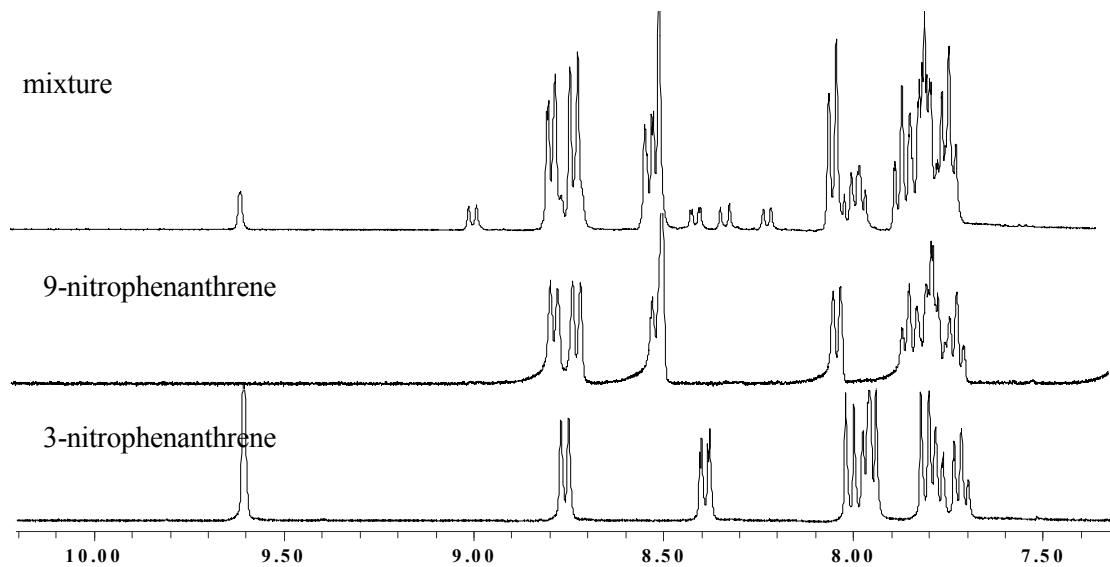


Figure 3.3 The ¹H NMR spectra of mixture, 9-nitrophenanthrene and 3-nitrophenanthrene

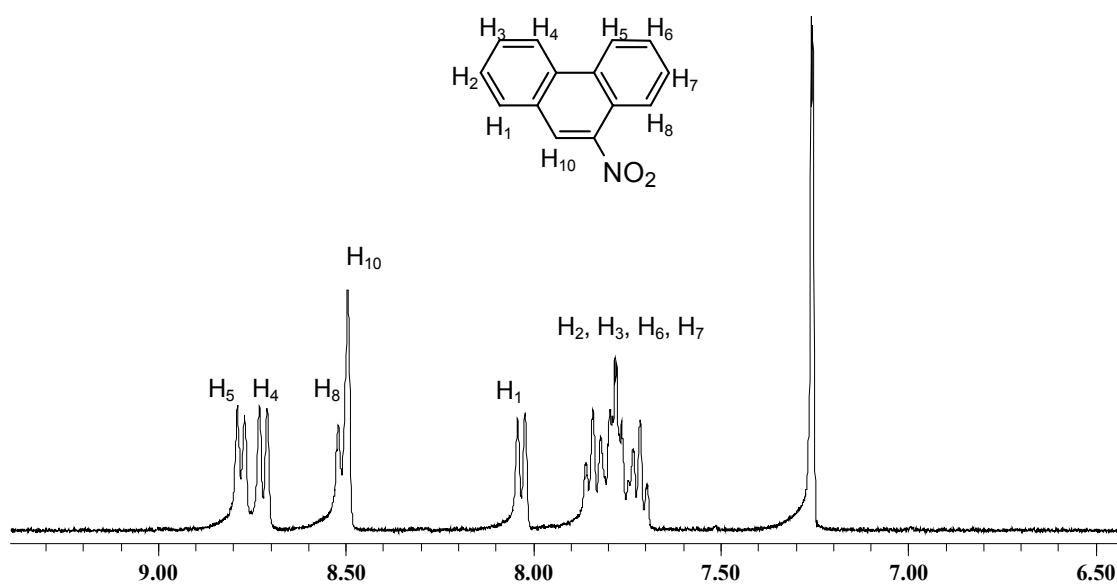


Figure 3.4 The ¹H NMR of 9-nitrophenanthrene (1)

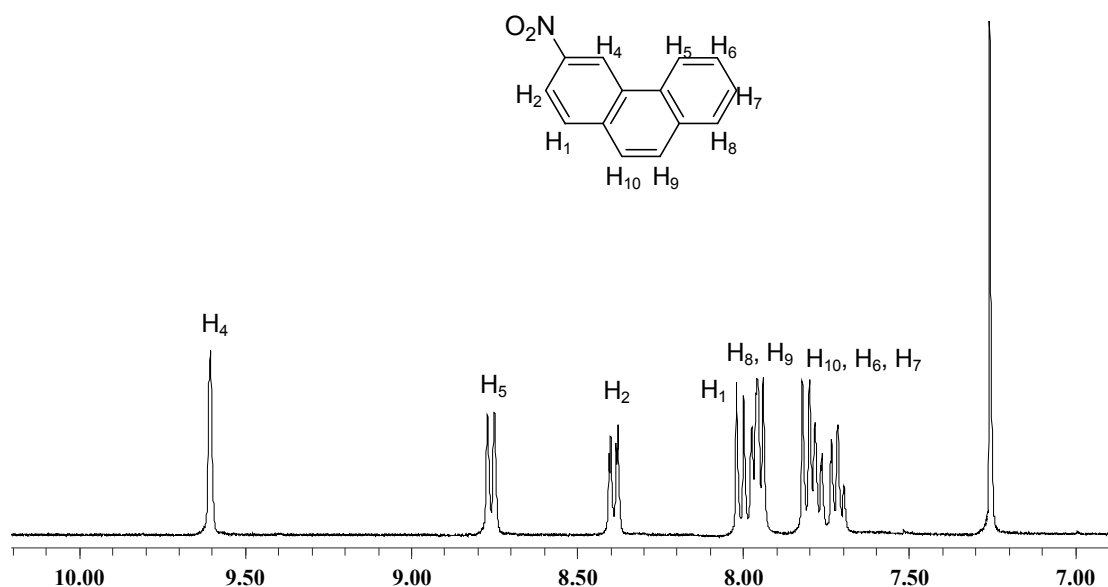


Figure 3.5 The ^1H NMR of 3-nitrophenanthrene

9-Nitrophenanthrene (**1**) has been shown to condense with ethyl isocyanoacetate in the presence of a non-nucleophilic base 1,8-diazabicyclo[5.4.0]undec-7-ene (DBU) *via* Barton-Zard pyrrole condensation. It was found that during recrystallization, the recrystallizing flask should not be placed in an ice bath because the unreacted starting material (9-nitrophenanthrene) and 3-nitrophenanthrene would precipitate out. The proton NMR spectrum of ethyl phenanthro[9,10-*c*]pyrrole-1-carboxylate (**2**) is shown in **Figure 3.6**. The majority of the phenanthrene protons appeared between 7.5-8.6 ppm. However, the proton overlying the carbonyl moiety at position 8 was further deshielded to 9.81 ppm by its close proximity to the secondary π -system. The pyrrole CH gave a doublet ($J = 3.6$ Hz) at 7.70 ppm [30].

Finally, a cleavage of the ester moieties with KOH in refluxing ethylene glycol was performed under two conditions as shown in **Table 3.1**. Both reactions at 195°C (entry 1) and 170°C (entry 2) gave phenanthro[9,10-*c*]pyrrole in good yields (92% and 97% yield, respectively). However, the 170 °C condition was milder than 195 °C condition and the color of the synthesized pyrrole from lower temperature appeared to be more homogeneous than that formed at the higher temperature. After refluxing was finished, the mixture was cooled to room temperature then poured into an iced water. It

is important to let the solution cool down to room temperature otherwise small precipitates would form upon pouring hot solution into an ice bath. These small precipitates would cause difficulty in suction filtration. Phenanthro[9,10-*c*]pyrrole (**3**) was an unstable solid that should be stored in dry place and in a dark room. The proton NMR spectrum of this compound is shown in **Figure 3.7**. The spectrum demonstrated the symmetry of the structure and the absence of a carboxylate unit. Confirmation with ESI-MS showed the anticipated strong molecular ion at m/z 216 (Figure A-8). The overall yield of phenanthro[9,10-*c*]pyrrole is 22%.

Table 3.1 The summary of phenanthro[9,10-*c*]pyrrole synthesis conditions

entry	temperature (°C)	reaction time	Yield (%)
1	195	30 min	92
2	170	2 h	97

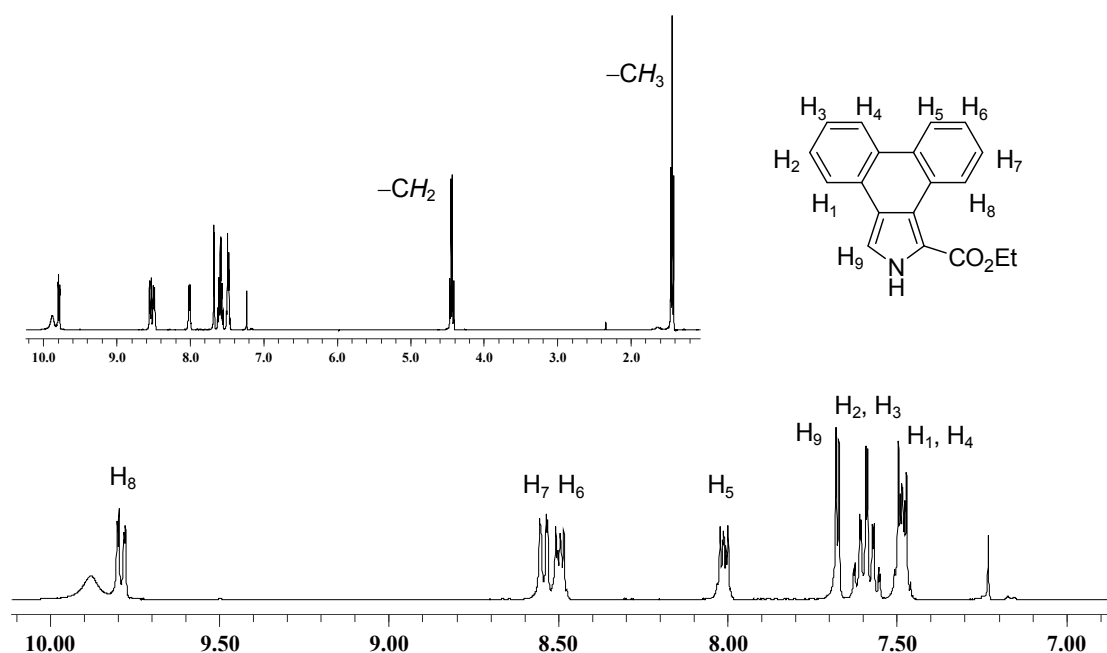


Figure 3.6 The ^1H NMR of ethyl phenanthro[9,10-*c*]pyrrole-1-carboxylate (**2**)

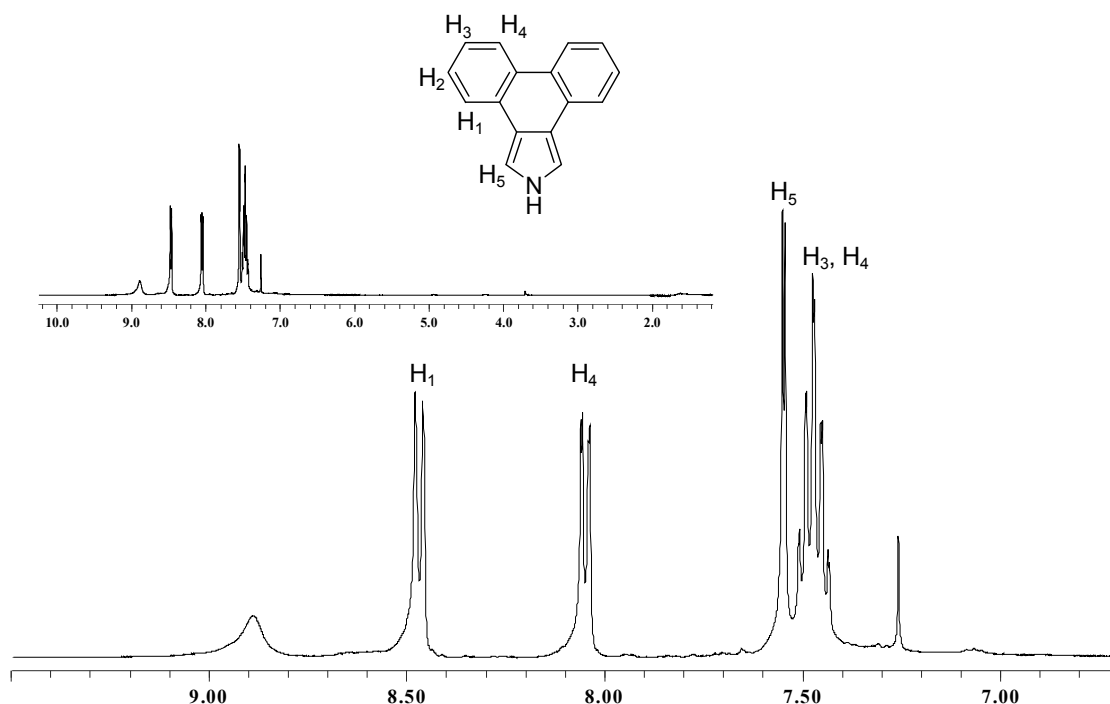


Figure 3.7 The ^1H NMR of phenanthro[9,10-*c*]pyrrole (**3**)

3.3 Synthesis of *meso*-Tetraphenyltetraphenanthroporphyrin Derivatives

3.3.1 Synthesis of *meso*-Tetraphenyltetraphenanthroporphyrin (TTPP, **4**)

Various preparation conditions and purification methods have been applied in the synthesis of TTPP. **Table 3.2** summarizes such conditions.

Table 3.2 The summary of results from different TTPP synthetic conditions

entry	ratio of pyrrole 3 : $\text{BF}_3\cdot\text{OEt}_2$:DDQ	temperature
1	1 : 1 : 2	-42°C then ambient
2	1 : 0.5 : 1	-42°C then ambient
3	1 : 1 : 1	ambient

The preparation of *meso*-tetraphenyltetraphenanthroporphyrin was performed in a two-step reaction. This consisted of condensation of phenanthro[9,10-*c*]pyrrole (**3**) and benzaldehyde using 1.0 equivalent $\text{BF}_3\cdot\text{OEt}_2$ as catalyst to form a porphyrinogen then oxidation with 2.0 equivalents of DDQ (entry 1). Generally, the condensation

yielded predominantly polypyrrolemethane oligomers and the cyclic porphyrinogen. Thus, this reaction was stirred at low temperature ($-42\text{ }^{\circ}\text{C}$) for 3 h to slow down the reaction and increase the selectivity of formation the cyclic porphyrinogen. To complete the reaction, the mixture was stirred at ambient temperature for 2 nights before adding DDQ. In entry 1, the short column chromatography was applied as the first step to purify the crude product. Beginning with a large amount of CH_2Cl_2 (approximately 2.0 L) as an eluent to elute an excess of DDQ following with hexanes:EtOAc (1:1) then EtOAc. The dark red solution was collected and further purified by flash column chromatography (eluent: 1:1 hexanes:EtOAc). Unexpectedly, a flash column chromatographic separation could not be used to isolate the desired TPTPP in a satisfactory purity. Furthermore, Sephadex column chromatography was chosen to purify the product with CH_2Cl_2 :MeOH (6:4) as an eluent but the pure TPTPP could not be obtained. The TLC confirmed that TPTPP was contaminated with impurity and the NMR spectrum could not be identified. On the other hand, the MALDI-TOF mass spectrum showed only one molecular ion peak of the product at 1215.899 (**Figure 3.8**).

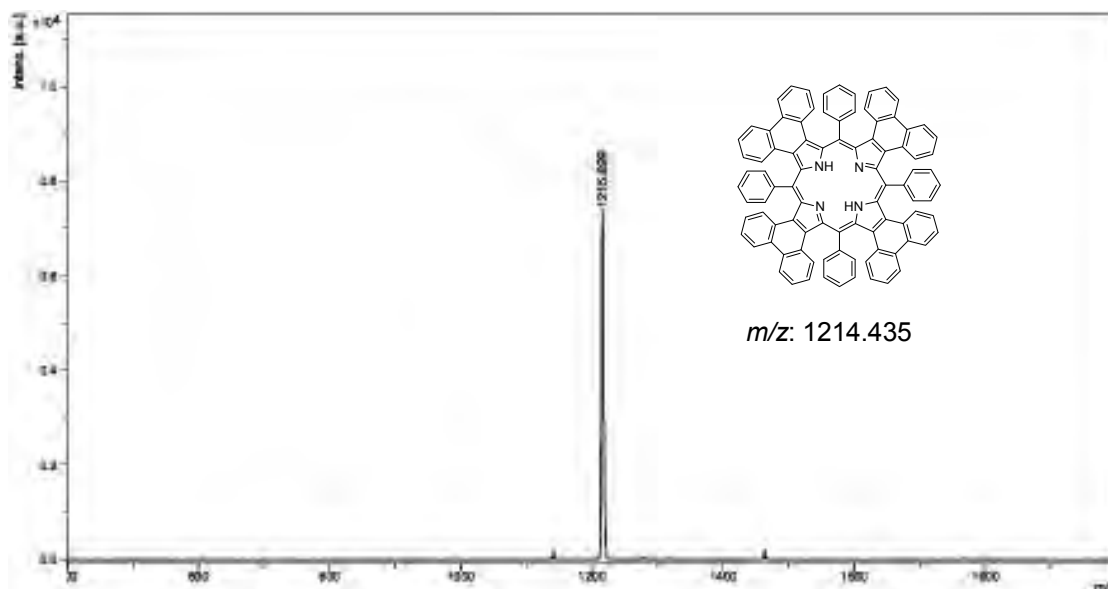


Figure 3.8 The MALDI-TOF mass spectrum of TPTPP from entry 1

In entry 2, where the same synthetic protocol as that in entry 1 was employed, TPTPP was also synthesized from the condensation reaction. In this case the amount of $\text{BF}_3\cdot\text{OEt}_2$ was modified from 1.0 to 0.5 equivalent. It is known that the overall rate of

reaction and ultimate yield of porphyrin are dependent on the concentration of the reactants, the nature of the acid catalyst, and on the concentration of the acid [33]. Because of these factors, the idea of decreasing the equivalent of acid was utilized to enhance the selectivity of cyclization reaction. Moreover, the amount of DDQ was adjusted to 1.0 equivalent to decrease the excess amount of the oxidant. After the reaction was stirred at ambient temperature for 2 nights, the solution was treated with triethylamine followed by base extraction to remove excess DDQ instead of using short column chromatography. After extraction, the crude product was further purified by column chromatography using 4:1 CH_2Cl_2 :petroleum ether and then 1:1 hexanes:EtOAc as eluents. The dark red solution was collected and further crystallized by layering methanol onto concentrated CHCl_3 solution. After filtration, similar results was obtained as in result from entry 1. In addition, the UV-visible absorption spectrum in dichloromethane showed a maximum peak at 579 nm which is typical for Soret band, and two Q-bands were observed at 727 and 804 nm (**Figure 3.9**). These value, in good agreement with what was reported by the You group [15], confirmed that the synthesized TPTPP was occurred.

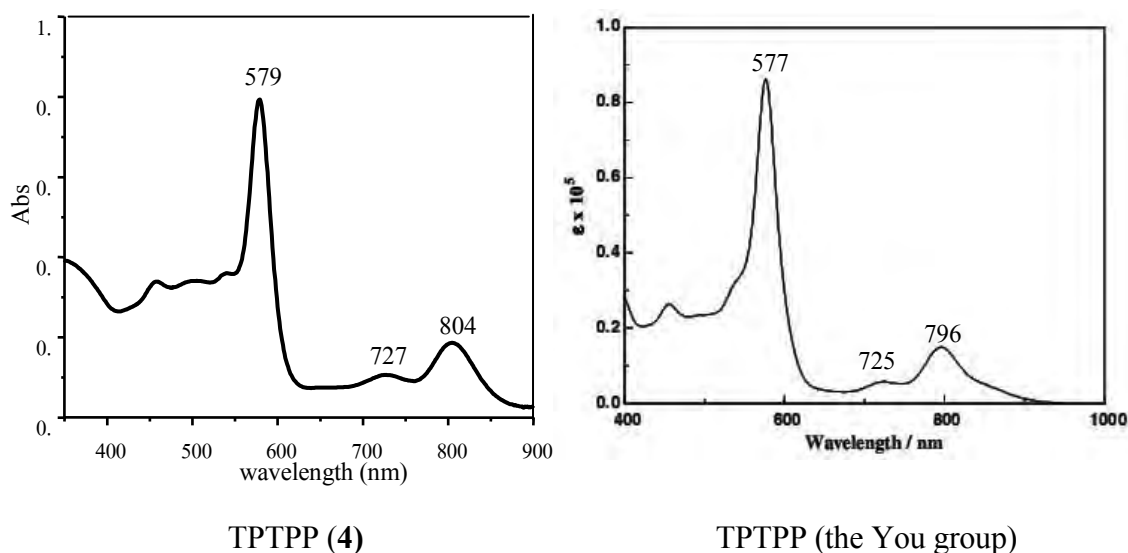


Figure 3.9 The absorption spectra of synthesized TPTPP (4) and TPTPP from the You group in dichloromethane [15]

In entry 3, where the same synthetic protocol, entry 1, was employed, TPTPP was also synthesized from the condensation reaction. This reaction was carried out in an

attempt to synthesize TPTPP at room temperature to confirm that the temperature affected a formation of porphyrinogen. After treatment with triethylamine, the resulting solution was monitored by thin layer chromatography. TLC results indicated that the desired porphyrin could not be completely separated because each component in the mixture has similarly close chromatographic R_f values. TLC results, therefore, supported that formation of cyclic porphyrinogen at low temperature was more selective than at room temperature.

3.3.2 Synthesis of Cu(II)-*meso*-Tetraphenyltetraphenanthroporphyrin (Cu-TPTPP, 5)

To prepare Cu(II)-*meso*-tetraphenyltetraphenanthroporphyrin (Cu-TPTPP, 5), a solution of copper(II) acetate in methanol was added to a refluxing solution of *meso*-tetraphenyltetraphenanthroporphyrin (TPTPP, 4) in CHCl_3 . Copper(II) was inserted easily into the core of free base TPTPP as monitored by the MALDI-TOF mass spectrometry. Within 1 h, TPTPP peak disappeared and only Cu-TPTPP peak observed in the MALDI-TOF mass spectrum (**Figure 3.10**). After a workup, the crude product was further purified by column chromatography using CH_2Cl_2 as eluent and a column chromatography on Sephadex using CH_2Cl_2 :MeOH at 7:3 as eluent. Unfortunately, even with the two types of column chromatography, purification was not successful. The UV-visible absorption spectrum in dichloromethane showed broad signal, which made it uncertain to be identify as the desired product. However, the estimation of a peak at 588 nm which could be a Soret band, and the Q-band signal have decreased from two to one peak at 689 nm compared to a free base TPTPP (**Figure 3.11**).

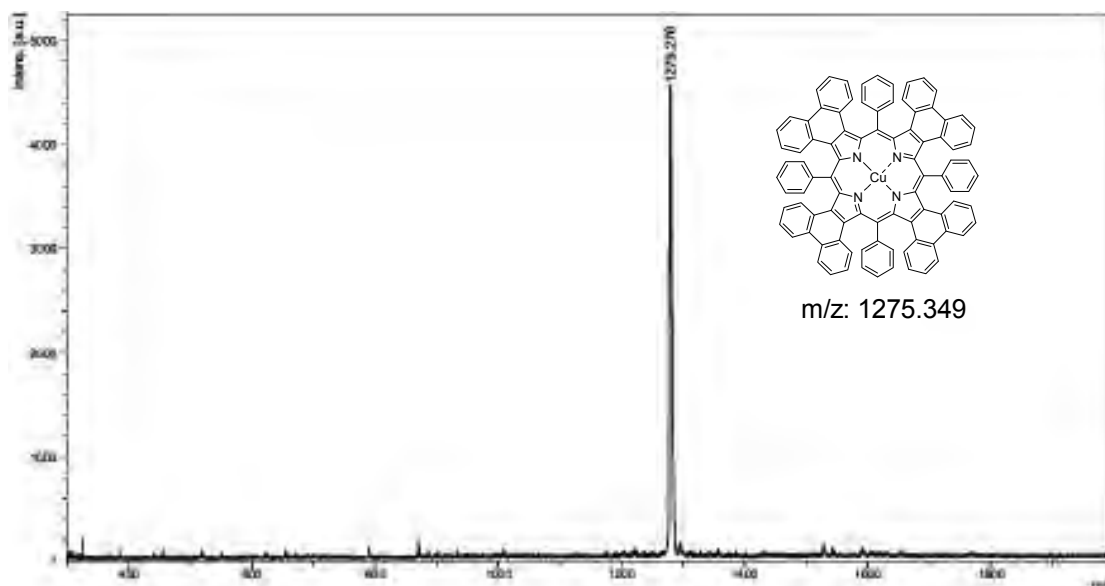


Figure 3.10 The MALDI-TOF mass spectrum of Cu-TPTPP crude

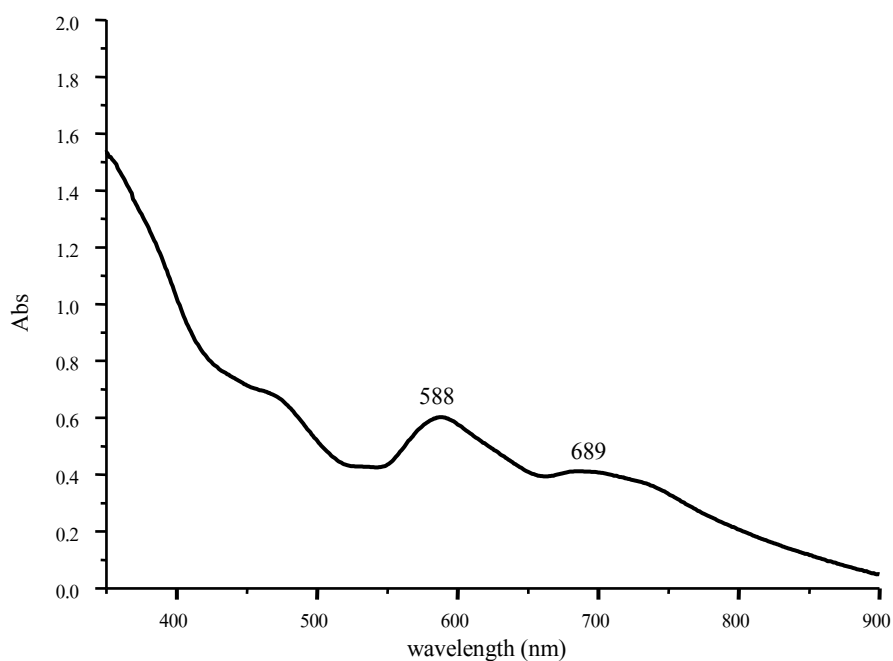


Figure 3.11 The UV-visible absorption spectrum of Cu-TPTPP (5)

3.3.3 Synthesis of Zn(II)-*meso*-Tetraphenyltetraphenanthroporphyrin (Zn-TPTPP, 6)

The synthesis of Zn(II)-*meso*-tetraphenyltetraphenanthroporphyrin (Zn-TPTPP, 6) in method I using 3.5 equivalents of zinc(II) acetate dihydrate in methanol was not completed in one hour. The MALDI-TOF spectrum showed two peaks assigned to

TPTPP and Zn-TPTPP (**Figure 3.12**). The reflux was continued overnight and monitored by MALDI-TOF mass spectrometry at 3 and 16 h. All MALDI-TOF mass spectra are shown in **Figure 3.12**. As the reaction time increased, the intensity ratio of Zn-TPTPP and TPTPP at 16 h was better. Although the reaction time was increased, the starting material; TPTPP, was still present in higher amount than the product; Zn-TPTPP. Even if the amount of zinc(II) acetate dihydrate was increased from 3.5 to 6.7 equivalents, similar result was obtained. Alternatively, metallation solvents of porphyrin was changed to dimethylformamide (DMF) (method II). The reaction was refluxed at higher temperature than when chloroform was used as a solvent in method I. The MALDI-TOF mass spectrum is shown in **Figure 3.13**. The starting material peak at 1215.835 appeared in a low intensity together with many other peaks while none of the Zn-TPTPP peak was detected. Perhaps these other components resulted from the pre-existing impurities from previous steps.

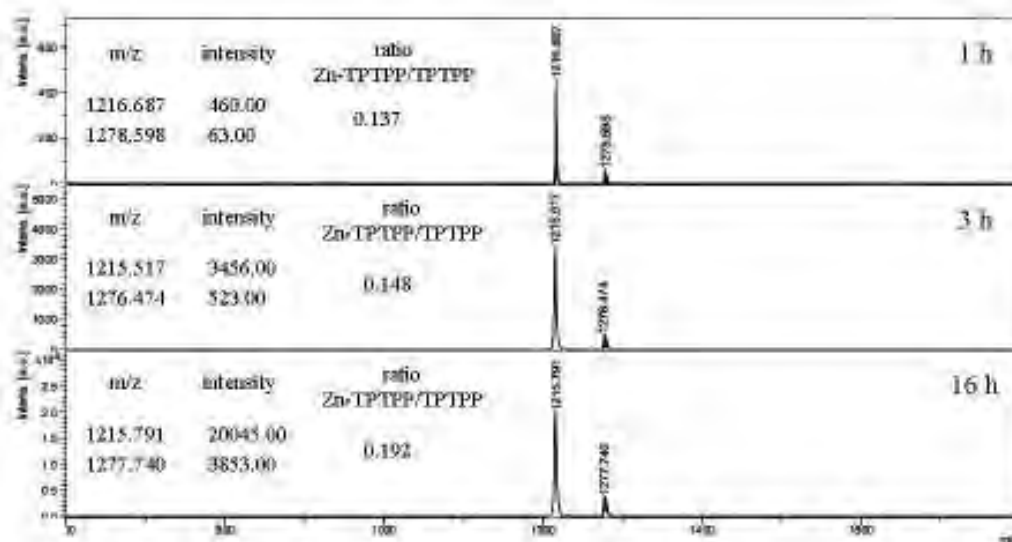


Figure 3.12 The MALDI-TOF mass spectrum of Zn-TPTPP by using CHCl_3 as a solvent

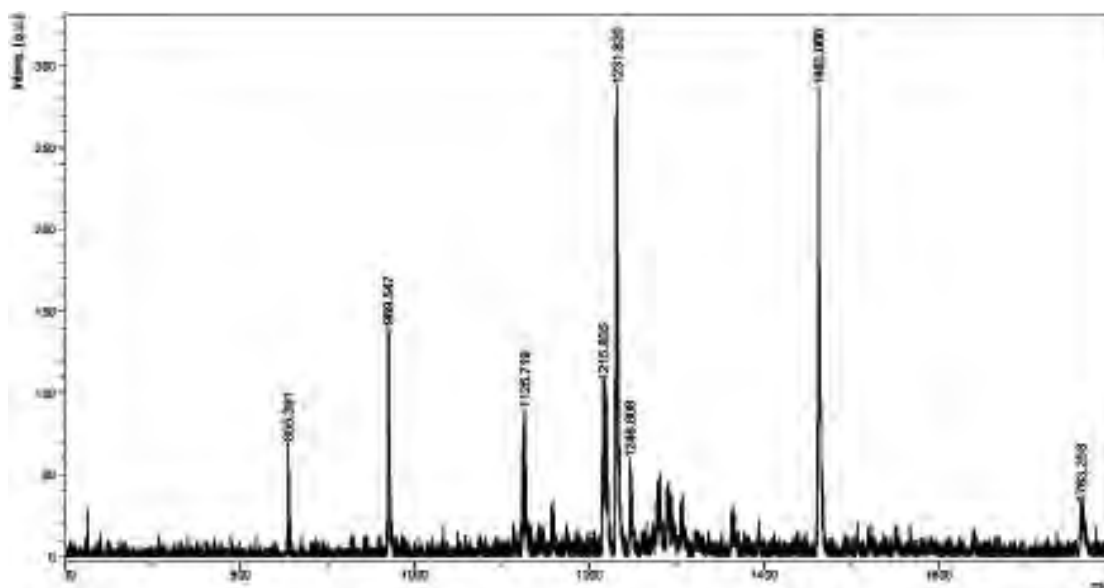


Figure 3.13 The MALDI-TOF mass spectrum of Zn-TPTPP by using DMF as a solvent

3.4 Synthesis of *meso*-Tetramethoxycarbonylphenyltetraphenanthroporphyrin Derivatives

3.4.1 Synthesis of *meso*-Tetramethoxycarbonylphenyltetraphenanthroporphyrin (TMCPTPP, 7)

Various preparation conditions and purification methods have been applied in the synthesis of TMCPTPP. **Table 3.3** summarizes such conditions. From **Table 3.3**, *meso*-tetramethoxycarbonylphenyltetraphenanthroporphyrin (TMCPTPP, 7) was also synthesized from Lindsey condensation between pyrrole **3** and methyl-4-formylbenzoate. A similar amount of DDQ at 1.0 equivalent was used. After column chromatography, the dark violetish-red solution was collected and then purified with flash column chromatography (eluent : hexanes:CH₂Cl₂ at 1:5, 1:10, then pure CH₂Cl₂, and finally 0.5% AcOH in CH₂Cl₂). Subsequently, column chromatography (eluent : 5% MeOH in CH₂Cl₂) on Sephadex was carried out. Unfortunately, purification was not successful. Alternatively, preparative thin layer chromatography was used to separate the product. TLC plate was developed in the chamber saturated with hexanes:EtOAc (1:1) consecutively six times. This resulted in a blue individual product band. The product was obtained in 1% yield (entry 1).

Table 3.3 The conditional summary of TMCPTPP synthesis

entry	ratio of pyrrole 3:aldehyde:BF ₃ ·OEt ₂	the amount of CH ₂ Cl ₂ (mL)	Reaction time at ambient temperature (h)	yield (%)
1	1 : 1 : 1	80	24	1
2	1 : 1 : 1	350	24	1
3	1 : 1 : 0.5	200	24	3
4	1 : 1 : 0.5	200	48	4
5	1 : 1 : 0.5	400	48	6

Firstly, an attempt to improve the yield by increasing the amount of solvent in entry 2 was applied. Moreover, the purification method was developed. The resulting solution was extracted with base followed by column chromatography. The dark violetish-red solution was collected and further purified by flash column chromatography (eluent : CH₂Cl₂:petroleum ether at 19:1 then 0.5% AcOH in CH₂Cl₂). In entry 2, flash column chromatography was used. However, it was quite difficult to optimize the suitable eluent for column chromatography. It was found that CH₂Cl₂:petroleum ether at 19:1 was a good eluent to remove some low polar impurities at the beginning of the chromatography but the second eluent system still needed to be optimized. In entry 2, attempts have been made to use 0.5% AcOH in CH₂Cl₂ as the second eluent. The order of the fractions eluted out were a red solution, a violetish-blue solution, and followed immediately with a green solution. A large amount of violetish-blue solution was mixed with the green solution and they were difficult to separate. After collecting the violetish-blue solution, recrystallization gave a product in 1% yield.

Secondly, a ratio between the starting materials and acid catalyst was modified. Generally, the ratio of starting material to BF₃·OEt₂ was 1:1. This ratio in entry 3 was decreased to 1:0.5 (**Table 3.3**). It was anticipated that a decrease in the amount of acid catalyst would raise the formation of cyclic porphyrinogen instead of polypyrrolemethane oligomeric formation. Moreover, the reaction flask was let stand in the dark because it was noticed earlier that phenanthro[9,10-*c*]pyrrole (**3**) could

moderately decompose with light in a solution. Due to partial decomposition of the starting material, the amount of porphyrinogen was decreased and many components which caused difficulties in purification were generated. After the reaction was stirred overnight, the resulting solution was extracted with 5% NaHCO₃ and further purified by column chromatography. Initially, a CH₂Cl₂:petroleum ether (19:1) eluent was used followed with hexanes:EtOAc at 1:1, 3:7 and EtOAc, respectively. This mobile phase system would elute all impurities and elute the blue solution at last. Some product was lost to the green solution but the main part of product could be separated in the end. The yield was 3% in this case.

From **Table 3.3**, it was followed the same synthetic condition but a period of reaction time at ambient temperature was extended to 48 h (entry 4). The resulting solution was monitor by MALDI-TOF mass spectrometry. The only one molecular ion peak at 1447.173 was TMCPTPP (**Figure 3.14**). After purification was similar to entry 3, the desired porphyrin was a dark red solid in 4% yield.

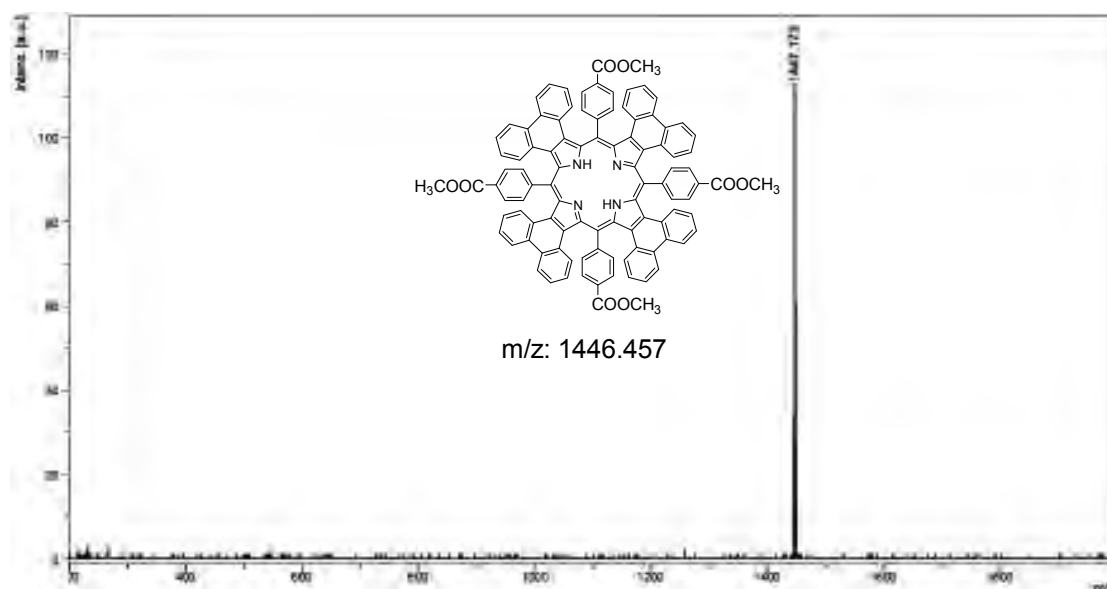


Figure 3.14 The MALDI-TOF mass spectrum of the resulting solution in the entry 4

Here in, we optimized the ratio of starting material to acid catalyst and the reaction time at ambient temperature. Thus, these optimum conditions were used in the entry 5 as shown in **Table 3.3**. The yield was improved by an increase in the amount of solvent used. The purification was carried out following the details in entry 3 but the

second eluent in column chromatography was changed to EtOAc for an acceleration in the rate of product elution. In this case, the yield was raised to 6% was the highest yield so far.

The proton NMR spectrum of TMCPTPP in TFA-deuteriochloroform (**Figure 3.15**) is consistent with the proposed structure of this highly symmetrical porphyrin and shows five separate sets of signals corresponding to the three distinct types of phenanthrene protons and the two types of phenyl substituent protons. The eight phenanthrene protons closest to the phenyl subunit were shielded by the adjacent phenyl rings and gave an upfield signal at 6.75 ppm [15]. The *ortho* protons on the phenyl substituents were directed toward the porphyrin macrocycle and were consequently deshielded by the macrocyclic ring current, giving a doublet for 8H at close to 9 ppm [12]. The remaining protons fell into a typical aromatic range, with chemical shifts lying between 7.2-8.5 ppm. The chemical shift of the internal NH appeared at 1.23 ppm, indicating that this porphyrin had a highly distorted conformation in solution. The structure was further supported by MALDI-TOF mass spectrometry, which gave the expected $[M+H]^+$ peak at $m/z = 1447.173$.

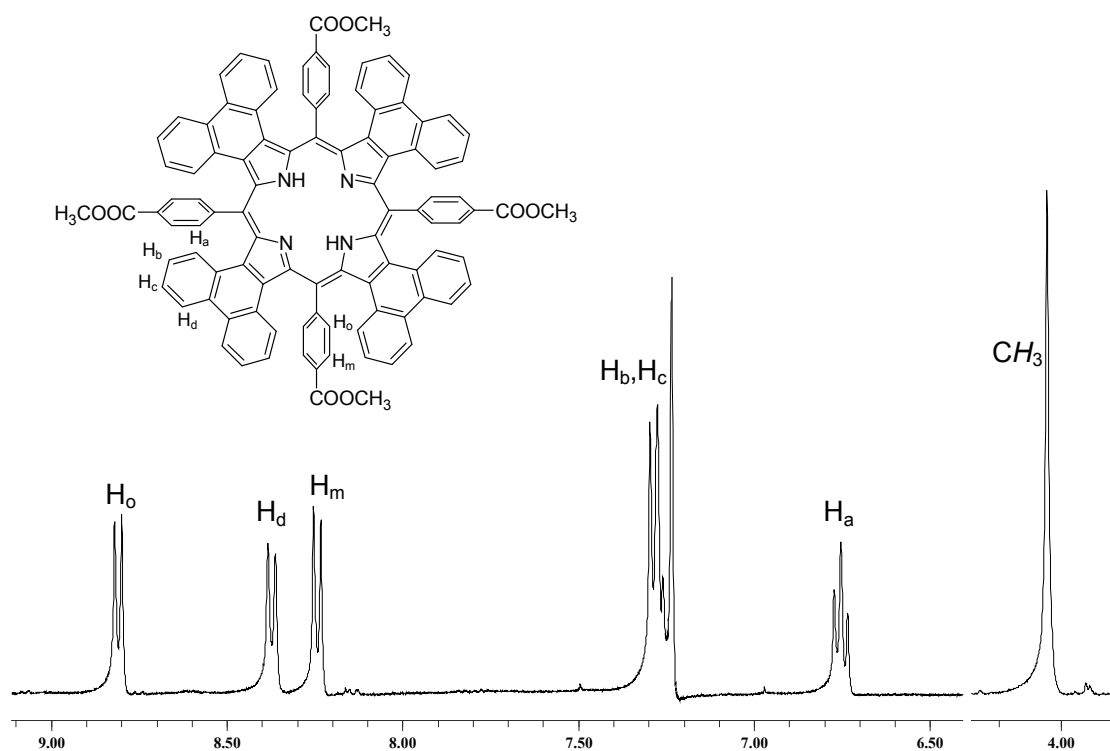


Figure 3.15 The ^1H NMR spectrum of TMCPTPP (**7**) in deuteriochloroform

3.4.2 Synthesis of Cu(II)-*meso*-Tetramethoxycarbonylphenyltetraphenanthroporphyrin (Cu-TMCPTPP, **8**)

Cu(II)-*meso*-tetramethoxycarbonylphenyltetraphenanthroporphyrin (Cu-TMCPTPP, **8**) was synthesized by adding copper(II) acetate in methanol into a CHCl₃ solution of TMCPTPP. Only after 1 h of reflux, copper(II) ion has inserted very easily into the core of the free base TMCPTPP as monitored by MALDI-TOF mass spectrometry. The MALDI-TOF mass spectrum exhibited the expected [M]⁺ peak at $m/z = 1507.758$ which was consistent with calculated molecular ion of 1507.371. After a routine workup, the dark violet solid was obtained in 92% yield. The product was further characterized by ¹H-NMR spectroscopy and UV-visible spectroscopy. The ¹H NMR spectrum (Figure A-16) showed broad signals of aromatic protons resonance at δ 8.59, 7.86 and 6.79 ppm. The absent signal of internal NH protons around 1.2 ppm was a clear indication. In addition, the absence of free base porphyrin peak at $m/z = 1447$ in MALDI-TOF mass spectrum (Figure A-17) strongly supported that copper(II) ion had completely replaced the inner protons.

3.4.3 Synthesis of Zn(II)-*meso*-Tetramethoxycarbonylphenyltetraphenanthroporphyrin (Zn-TMCPTPP, **9**)

An attempt to synthesis of Zn(II)-*meso*-tetramethoxycarbonylphenyltetraphenanthroporphyrin (Zn-TMCPTPP, **9**) in CHCl₃ using 5.0 equivalents of zinc(II) acetate dihydrate in methanol was not complete in one hour as in the case of Zn-TPTPP. The MALDI-TOF mass spectrum showed two peaks assigned to TMCPTPP and Zn-TMCPTPP (Figure 3.16). As mentioned before, the reaction was continued to reflux overnight and monitored by MALDI-TOF mass spectrometry at 2, 14 and 16 h (Figure 3.16). Still, although the reaction time was increased, the starting material; TMCPTPP (calcd $m/z = 1446.457$), was still present in a higher amount than the product; Zn-TMCPTPP (calcd $m/z = 1508.370$). Thus, metallation solvents of porphyrin was changed to dimethylformamide (DMF). As a result, the reaction was completed within 1 h. After a routine workup and recrystallization, dark red solid was obtained in 90% yield. The product was further characterized by ¹H-NMR spectroscopy, MALDI-TOF mass spectrometry and UV-visible spectroscopy.

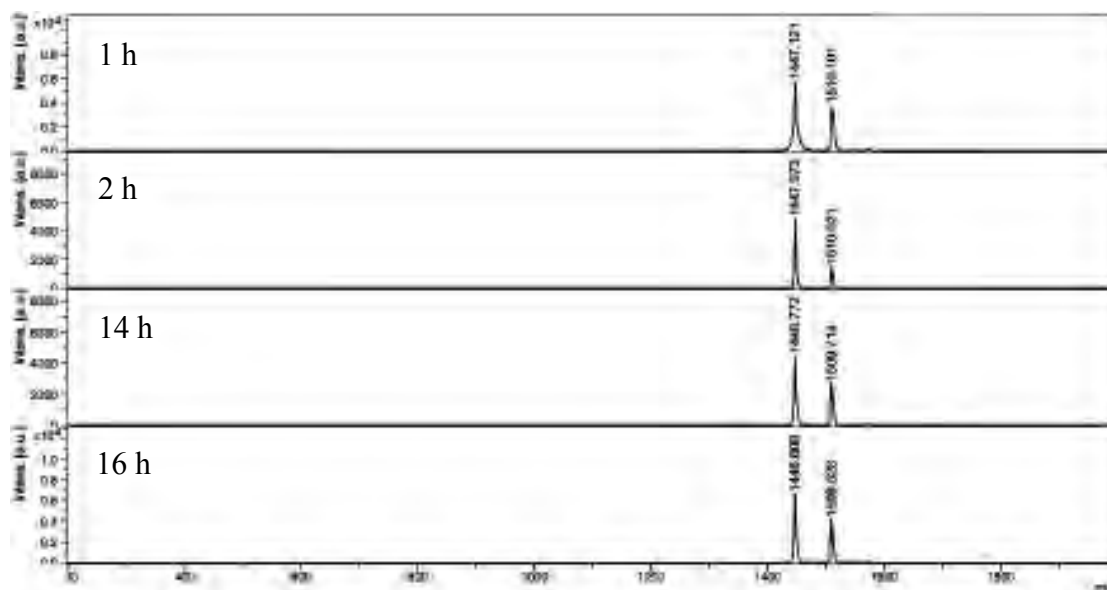


Figure 3.16 The MALDI-TOF mass spectrum of Zn-TMCPTP from CH₂Cl₂/methanol method

The ¹H NMR spectrum (Figure A-19) showed broad signals of aromatic protons resonance at δ 6.82-8.91 ppm. The absent signal of internal NH protons around 1.2 ppm was a good confirmation. However, the absence of the free base porphyrin peak at m/z = 1447 in MALDI-TOF mass spectrum (Figure A-20) strongly supported that zinc(II) ion had completely replaced the inner protons.

3.4.4 Synthesis of Co(II)-*meso*-Tetramethoxycarbonylphenyltetraphenanthroporphyrin (Co-TMCPTP, **10**)

Co(II)-*meso*-tetramethoxycarbonylphenyltetraphenanthroporphyrin (Co-TMCPTP, **10**) was synthesized by adding cobalt acetate tetrahydrate in methanol into a CHCl₃ solution of TMCPTP. After 2 h of reflux, the reaction was monitored by MALDI-TOF mass spectrometry. The MALDI-TOF mass spectrum showed two molecular ion peaks at 1446.700 and 1503.654 (**Figure 3.17**). The latter peak referred to Co-TMCTP which was consistent with a calculated molecular ion of 1503.374. The reaction was continued at reflux and the monitoring maintained by MALDI-TOF mass spectrometry (**Figure 3.17**). Finally, cobalt(II) ion was inserted into the core of the free base TMCPTP as confirmed by MALDI-TOF mass spectrometry at 7 h. After a routine workup and recrystallization, the dark green solid was obtained in 64% yield.

The product was further characterized by $^1\text{H-NMR}$ spectroscopy and UV-visible spectroscopy.

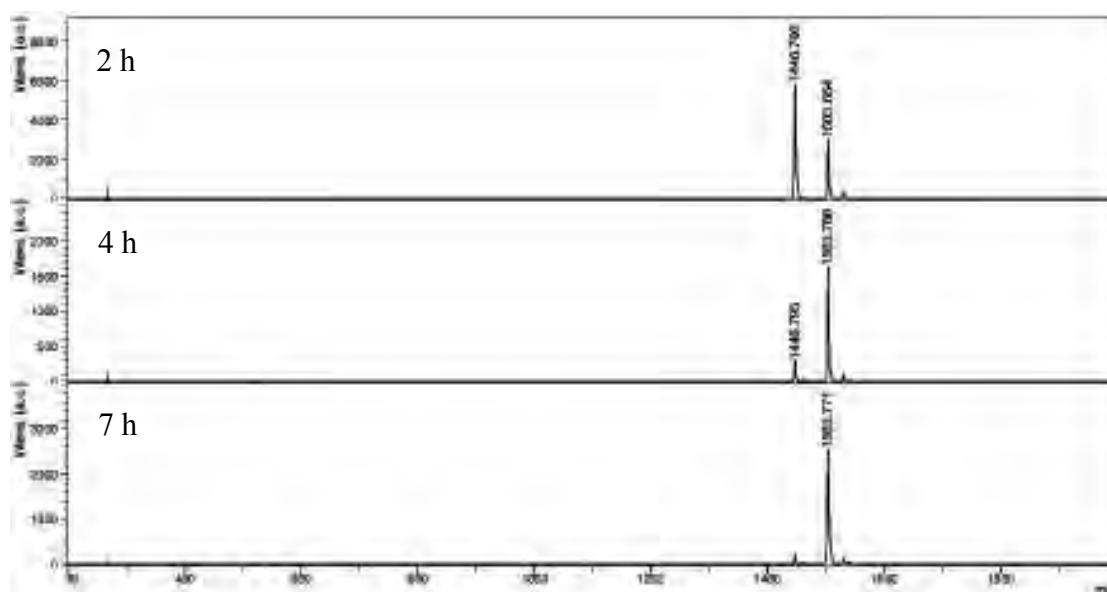


Figure 3.17 The MALDI-TOF mass spectrum of Co-TMCPTPP at 2 h, 4 h and 7 h

The $^1\text{H NMR}$ spectrum (Figure A-22) showed broad signals of aromatic protons resonance at δ 6.55-8.43 ppm. The disappearance of the internal NH proton signal around 1.2 ppm was a clear affirmation. Moreover, the absence of free base porphyrin peak at $m/z = 1447$ in MALDI-TOF mass spectrum (Figure A-23) strongly supported that copper(II) ion had completely replaced the inner protons.

3.5 Synthesis of *meso*-Tetracarboxyphenyltetraphenanthroporphyrin (TCPTPP, 11)

The synthesis *via* direct routes, namely, the Lindsey's and the Adler-Longo's method were carried out in order to prepare *meso*-tetracarboxyphenyltetraphenanthroporphyrin. Unfortunately, neither method has provided the desired product.

Since attempts to synthesize TCPTPP by Lindsey condensation and Adler-Longo's method failed to give the desired porphyrin, an alternative route was performed *via* a hydrolysis of *meso*-tetramethoxycarbonylphenyltetraphenanthroporphyrin (TMCPTPP, 7). This was conducted using a saturated aqueous potassium hydroxide solution in a mixed solvents of tetrahydrofuran, methanol, and water. The mixture was refluxed at 60-70 °C for 1 day and THF and methanol was removed. After

the addition of enough 1 M HCl to acidify the reaction mixture, a black precipitate was formed. After centrifugation, *meso*-tetramethoxycarbonylphenyltetraphenanthroporphyrin (TCPTPP, **11**) was obtained in a good yield (75 %). This porphyrin was insoluble in most of organic solvents, but its dication $11H_2^{2+}$ was soluble in CH_2Cl_2 . Thus, the formation of TCPTPP was confirmed by MALDI-TOF mass spectrometry which using TFA- CH_2Cl_2 as a solvent to dissolve the porphyrin. The MALDI-TOF mass spectrum showed molecular ion peak at $m/z = 1391.956$, relatively close to the calculated dication TCPTPP molecular ion of 1392.409 (**Figure 3.18**). The product was further characterized by 1H -NMR spectroscopy and UV-visible spectroscopy.

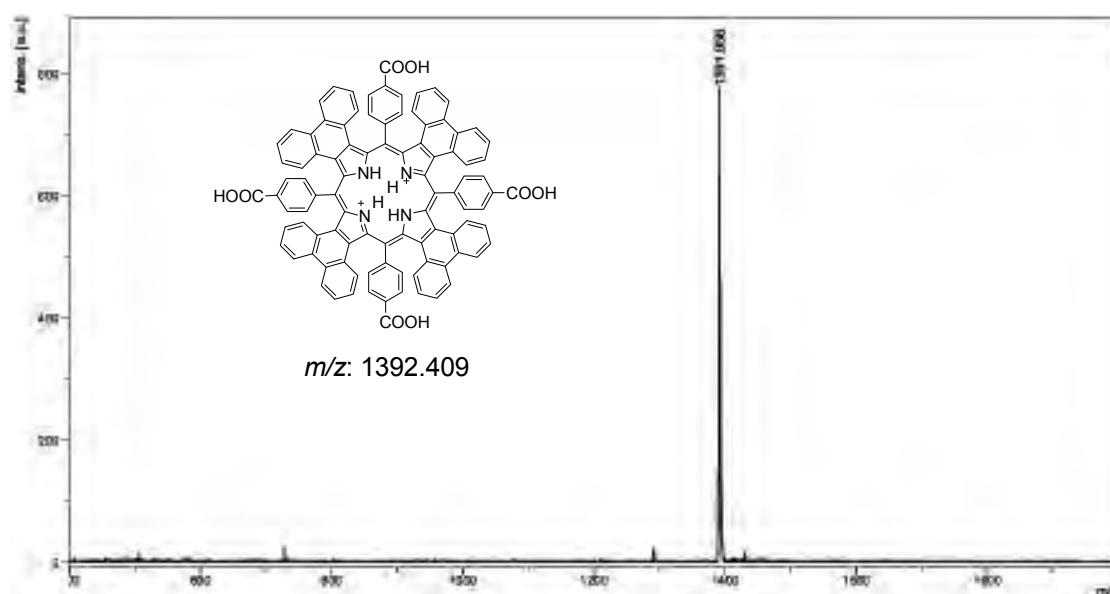


Figure 3.18 The MALDI-TOF mass spectrum of dication TCPTPP

The 1H NMR spectrum in deuterated dimethyl sulfoxide (Figure A-25) showed broad signals of aromatic protons resonance at δ 6.79-8.88 ppm. The complete disappearance of the proton signal of CH_3 ester moieties at 4.00 ppm strongly supported that TCPTPP was completely formed.

Finally, all of the synthesized *meso*-tetraaryltetraphenanthroporphyrin derivatives were characterized by MALDI-TOF mass spectrometry. The result of characterization is shown in **Table 3.4**.

Table 3.4 The MALDI-TOF mass data of synthesized *meso*-tetraaryltetraphenanthroporphyrin derivatives

porphyrins	calculated exact mass	molecular ion peak
TPTPP, 4	1214.435	1215.889
TMCPTPP, 7	1446.457	1447.173
Cu-TMCPTPP, 8	1507.371	1507.758
Zn-TMCPTPP, 9	1508.370	1510.619
Co-TMCPTPP, 10	1503.374	1503.771
H ₂ ²⁺ TCPTPP, H ₂ ²⁺ 11	1392.409	1391.956

3.6 Solubility of *meso*-tetraaryltetraphenanthroporphyrin series

The solubility of all derivatives in various organic solvents for the purpose of further manipulation was summarized in **Table 3.5**.

Table 3.5 The solubility of all synthesized porphyrins

porphyrins	Hexanes	Et ₂ O	CH ₂ Cl ₂	THF	CHCl ₃	EtOAc	Acetone	DMF	DMSO	MeOH	H ₂ O
4	-	-	+++	+++	+++	+	+	+++	+++	-	-
7	-	-	+++	+++	+++	++	+	+++	+++	-	-
8	-	-	+++	+++	+++	-	+	+++	+++	-	-
9	-	-	+++	+++	+++	+	+	+++	+++	-	-
10	-	-	+++	+++	+++	+	+	+++	+++	-	-
11	-	-	-	-	-	-	-	+++	+++	-	-

+++ completely soluble; ++ mostly soluble; + slightly soluble; - insoluble

The results from **Table 3.5** revealed that TPTPP and TMCPTPP derivatives were insoluble in non-polar solvents such as hexanes and diethyl ether and soluble in

low polar solvents (CH_2Cl_2 , THF and CHCl_3). Compared to *meso*-tetraphenanthroporphyrin (**Figure 3.19**), that was virtually insoluble in most organic solvents [14, 30]. The main reason for low solubility in the case of *meso*-tetraphenanthroporphyrin may be attributed to π - π stacking interactions between porphyrin molecules (**Figure 3.20**). In the case of *meso*-tetraphenanthroporphyrin, each molecule can be stacked closely because there is no substituents at the *meso*-positions. On the other hand, phenyl groups at *meso*-positions in TPTPP and TMCPTPP derivatives are relatively bulky groups. This leads to an out of the plane twist of the substituted phenyl rings to avoid steric interactions with the core phenanthrene rings of the porphyrins. As a consequence, decreasing in π - π stacking interactions and, hence an increase in the solubility can be observed. The attached phenyl moieties at *meso*-position conquer the problem of solubility. Nevertheless, TCPTPP were insoluble in most organic solvents but it was soluble in DMF, DMSO and 1% TFA-methanol.

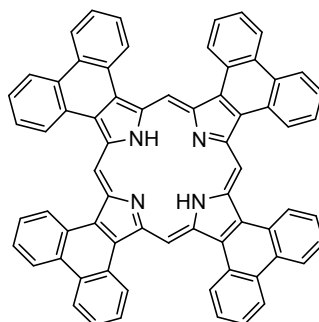


Figure 3.19 The structure of *meso*-tetraphenanthroporphyrin

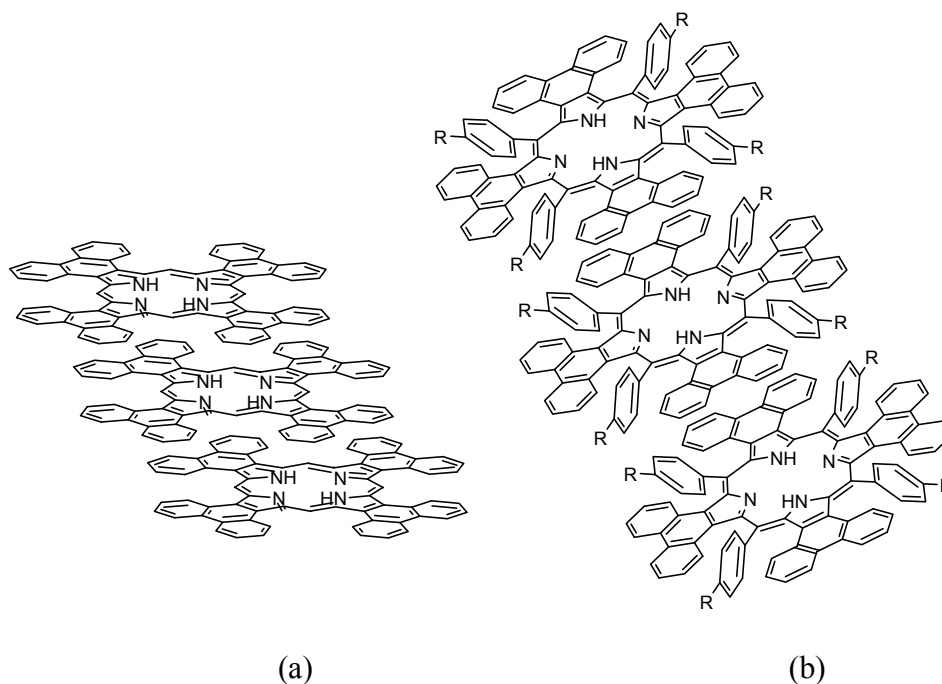


Figure 3.20 The difference in degree of π - π stacking interactions between (a) *meso*-tetraphenanthroporphyrin and (b) *meso*-tetraarylporphyrin

3.7 Investigation of Photophysical Properties

One of the more interesting aspects about a basic structure theme of tetrapyrrolic macrocycle; porphyrins, is a large π -conjugated system that exhibit extraordinary photophysical properties. As a result, it leads to a wide diversity of several applications. Moreover, the modified π -conjugated porphyrins display remarkably red-shifted absorption bands that is generally useful for those biomedical applications, near-infrared dyes and organic semiconductors.

In this research, photophysical properties of all synthesized porphyrins were investigated by UV-visible absorption spectroscopy and fluorescence emission spectroscopy. Furthermore, effects of extended via conjugation with exocyclic aromatic rings and metal ion were also discussed.

3.7.1 UV-visible Spectroscopy

The UV-visible absorption spectra of synthesized TPTPP derivatives and TMCPTPP derivatives were measured at a 10^{-5} M concentration in CH_2Cl_2 solution,

whereas TCPTPP was measured in 0.1% TFA in MeOH. The summary of the absorption maxima at Soret band and Q bands in the solution of porphyrin and the color of each solution are shown in **Table 3.6**.

Table 3.6 Absorption maxima of the solutions of all synthesized porphyrins at a 10^{-5} M concentration and their color in solution

Porphyrins	absorption maxima, λ_{\max}/nm ($\epsilon/10^4 \text{ M}^{-1} \text{ cm}^{-1}$)		color
	Soret band	Q bands	
TPTPP, 4 ^a	579 (6.43)	727 (0.86), 804 (1.51)	purple
TMCPTPP, 7 ^a	586 (6.19)	719 (1.04), 797 (1.30)	blue
Cu-TMCPTPP, 8 ^a	599 (5.24)	670 (1.26)	purple
Zn-TMCPTPP, 9 ^a	595 (4.57)	746 (1.18), 816 (1.23)	greenish-blue
Co-TMCPTPP, 10 ^a	523 (3.48)	703 (0.99)	pink
TCPTPP, 11 ^b	585 (5.35)	726 (0.82), 802 (1.10)	greenish-blue

^a measured in CH_2Cl_2 ; ^b measured in 0.1% TFA in methanol

A comparison between the absorption spectrum of free base TPTPP and free base TMCPTPP in dichloromethane is revealed in **Figure 3.21**. The typical UV-visible absorption spectrum of TMCPTPP exhibited characteristic Soret and Q bands. Two Q bands were observed at 719 and 797 nm in a far red region corresponding to the weak $\pi\text{-}\pi^*$ transition to the first excited state ($S_0 \rightarrow S_1$), while the Soret band observed at 586 nm was ascribed to the strong $\pi\text{-}\pi^*$ transition to the second excited state ($S_0 \rightarrow S_2$) [3]. The UV-visible spectrum of TMCPTPP closely resembled a spectrum obtained for TPTPP, and a bathochromic shift for the major λ_{\max} values were only 7 nm. The most red shifted band (Q_1) of TMCPTPP was relatively weak and appeared at 797 nm, compared to a value of 804 nm in TPTPP case. Besides, TCPTPP proved to be too insoluble in organic solvents to give a UV-visible spectrum, but in 0.1% TFA-methanol the corresponding dication gave a Soret band at 585 nm which was comparable to TPTPP and TMCPTPP. These results suggest that different substituents on *meso*-aryl groups had minor additional influence on the porphyrin electronic properties.

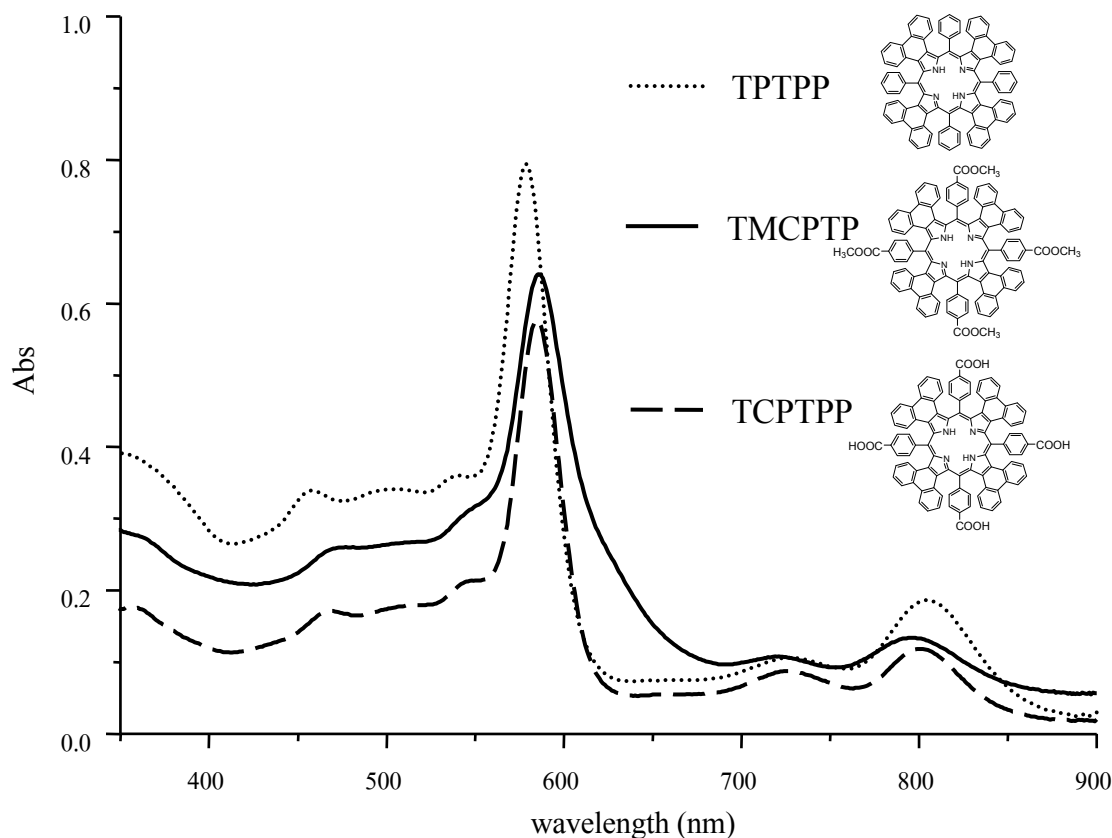


Figure 3.21 UV-visible absorption spectra of TPTPP, TMCPTP and TCPTP in dichloromethane

Moreover, free base *meso*-tetramethoxycarbonylphenyltetraphenanthroporphyrin (TMCPTP, 7) in 1% TFA-chloroform is shown the Soret band at 592 nm and two Q bands at 731 and 806 nm (Figure 3.22). Compared to a regular *meso*-tetraphenanthroporphyrin, which is *meso*-unsubstituted porphyrin, a UV-visible spectrum in 1% TFA-chloroform exhibit Soret band at 482 nm and two Q bands at 615 and 688 nm (Figure 3.22) [14]. The Q-band I of synthesized TMCPTP are significantly red shifted in respect to the Q-band I of *meso*-tetraphenanthroporphyrin by 118 nm. While the positions the Soret maxima are also red shifted notably high by 110 nm. A question arises whether the differences in these basic photophysical properties of *meso*-substituted tetraphenanthroporphyrins vs *meso*-unsubstituted tetraphenanthroporphyrin are perhaps caused by the severe conformational distortions of the former induced by the *meso*-aryl subunits with the relatively wider phenanthrene rings [15].

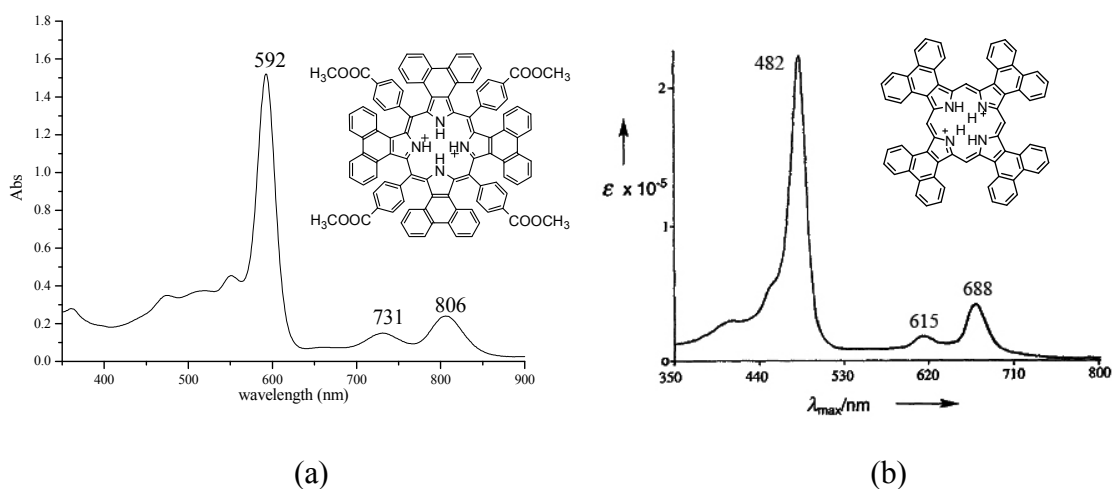


Figure 3.22 UV-visible absorption spectra of (a) TMCPTPP and (b) *meso*-tetraphenanthroporphyrin [14] in 1% TFA-chloroform

Furthermore, four porphyrins including free base TMCPTPP, Cu-TMCPTPP, Zn-TMCPTPP and Co-TMCPTPP were chosen to examine the effect of metal ions on the absorption spectra.

As shown in **Figure 3.23**, Zn-TMCPTPP displays a similar spectrum to that of free base TMCPTPP. A Soret band appeared at 595 nm, and two smaller Q bands were evident at 746 and 816 nm. Remarkably, the Soret band of Zn-TMCPTPP slightly red-shifted by 9 nm, whereas, the two Q bands significantly red-shifted by about 20-30 nm compared to the corresponding bands of free base TMCPTPP. In contrast, the absorption spectra of Cu-TMCPTPP and Co-TMCPTPP exhibited Soret bands at 559 and 523 nm respectively and only one Q band at 670 and 703 nm respectively. This demonstrated that when Cu(II) ion was inserted into the porphyrin core, the Soret band blue-shifted by 27 nm as well as the Q band degenerated from two peaks to one peak. Moreover, the Soret band of Co-TMCPTPP highly blue-shifted by 63 nm and the Q band degenerated from two peaks to one peak as well. These characteristic properties of porphyrin copper complexes and cobalt complexes [34] which can be explained relying on the fact that when the metal ion coordinates with the N atoms, the symmetry of the molecule increases and the number of Q bands therefore decreases [5].

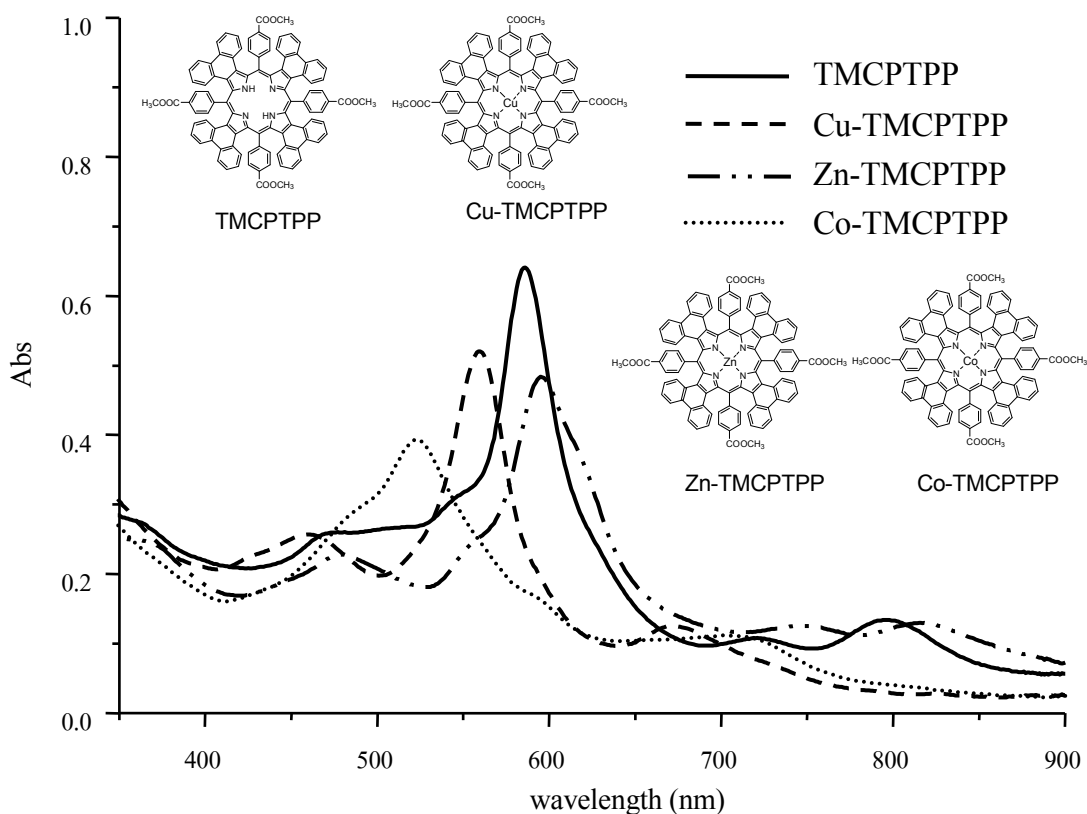


Figure 3.23 UV-visible absorption spectra of TMCPTPP, Cu-TMCPTPP, Zn-TMCPTPP and Co-TMCPTPP in dichloromethane

In general, the central part of the metalloporphyrin ring is occupied by a metal ion linked to a pyrrole ring. The metal ion accepts the lone pair electrons of the nitrogen atoms of the pyrrole ring, while electrons of the metal ion can be donated back to the porphyrin ring leading to the formation of delocalized π -bonds which permit the easy flow of electrons within the delocalized π -system. Based on this concept, the delocalized π -bonds of porphyrin zinc complexes, including Zn-TMCPTPP, increased the average electron density of the porphyrin, which lower the energy for electronic transition. As a result, a red shift in the Soret band is observed. In the case of the delocalized π -bonds of porphyrin copper complexes and cobalt complexes including Cu-TMCPTPP and Co-TMCPTPP, decreased the average electron density of the porphyrin ring which increased the energy available for electronic transition, leading to a blue shift in the Soret band [5]. Besides, synthesized porphyrins show high molar extinction coefficients, which could also allow for application in organic solar cells.

3.7.2 Fluorescence Spectroscopy

The fluorescence emission spectra of synthesized TPTPP derivatives and TMCPTPP derivatives were measured at a 10^{-5} M concentration in CH_2Cl_2 solution, whereas TCPTPP was measured in 0.1% TFA in MeOH. Disappointingly, none of the synthesized porphyrins showed fluorescence emission. For comparison, tetraphenyltetraphenanthroporphyrin that reported by Xu group [15] was investigated only a UV-visible spectrum, whereas a fluorescence spectrum was not reported. Until now, no report of fluorescence emission data are available for tetraaryltetraphenanthroporphyrin series and other fused phenanthrene units on porphyrin such as monophenanthroporphyrin and diphenanthroporphyrin [14, 30, 31]. Perhaps, none of these porphyrins show fluorescence emission or they may be under investigation. Thus, the answer of all these questions require more caution experiment and investigation to describe the electronic properties.

CHAPTER IV

CONCLUSION

A series of symmetrically fused phenanthrene porphyrins with *meso*-aryl substituted have been successfully synthesized by Lindsey's condensation reaction in low yield (5-12%). However, their metal complexes were obtained in moderate to excellent yields (64-99%). Pyrrole with fused phenanthrene ring as a precursor of porphyrins was available through the synthesis from phenanthrene and can be converted into pyrrole derivatives in three additional steps with moderate overall yields (22%). All of the synthesized porphyrin derivatives were characterized by ^1H NMR spectroscopy and MALDI-TOF mass spectrometry. Moreover, UV-visible spectroscopy and fluorescence spectroscopy were also used to investigate their photophysical properties. It has been demonstrated that *meso*-substituents bearing electron withdrawing groups did not affect the electronic absorption of porphyrins, whereas central metal ions affected the electronic absorption of porphyrins. The UV-visible absorption spectra for these tetraaryltetraphenanthroporphyrins revealed higher bathchromic shifts and this suggests that fused phenanthrene porphyrins and their metal complexes may find potential applications as photosensitizer in photodynamic therapy as well as dye-sensitized solar cell. In addition, other potential applications are currently under investigation.

Suggestion and Future works:

A high red-shifted *meso*-tetracarboxyphenyltetraphenanthroporphyrin appears as a candidate for dye-sensitized solar cells (DSSCs) because of the presence of carboxylic groups which can anchor to TiO_2 surface. Thus, the future works will be investigation of electrochemical, and photoelectrochemical properties for DSSCs. Moreover, their metal complexes of this porphyrin should be synthesized and be investigated their properties for DSSCs as well.

REFERENCES

- [1] Milgrom, L. R. *The Colours of Life: An Introduction to the Chemistry of Porphyrins and Related Compounds*. Oxford: OUP: 1997.
- [2] Meng, G. G.; James, B. R. Porphyrin Chemistry Pertaining to the Design of Anti-Cancer Drugs; Part 2, the Synthesis and *in vitro* Tests of Water-Soluble Porphyrins Containing, in the *meso* Positions, the Functional Groups: 4-Methylpyridinium, or 4-Sulfonatophenyl, in Combination with Phenyl, 4-Pyridyl, 4-Nitrophenyl, or 4-Aminophenyl. *Can. J. Chem.* 72 (1994): 2447-2457.
- [3] Anderson, H. L. Building Molecular Wires from the Colours of Life: Conjugated Porphyrin Oligomers. *Chem. Commun.* (1999): 2323-2330.
- [4] Kadish, K. M.; Smith, K. M.; Guilard, R. *The Porphyrin Handbook: Volume 18 Multiporphyrins, Multiphthalocyanines and Arrays*. Academic Press: New York, 2003.
- [5] Zheng, W.; Shan, N.; Yu, L.; Wang, X. UV-visible, Fluorescence and EPR Properties of Porphyrins and Metalloporphyrins. *Dyes Pigm.* 77 (2008): 153-157.
- [6] Hiroto, S.; Shinokubo, H.; Osuka, A. Porphyrin Synthesis in Water Provides New Expanded Porphyrins with Direct Bipyrrrole Linkages: Isolation and Characterization of Two Heptaphyrins. *J. Am. Chem. Soc.* 128 (2006): 6568-6569.
- [7] Kadish, K. M.; Smith, K. M.; Guilard, R., *The Porphyrin Handbook*. Academic Press, New York: 2000.
- [8] Shen, Z.; Uno, H.; Shimizu, Y.; Ono, N. Controlling Conformations and Physical Properties of *meso*-Tetrakis(phenylethynyl)porphyrins by Ring Fusion: Synthesis, Properties and Structural Characterizations. *Org. Biomol. Chem.* 2 (2004): 3442-3447.
- [9] Finikova, O. S.; Cheprakov, A. V.; Carroll, P. J.; Vinogradov, S. A. Novel Route to Functionalized Tetraaryltetra[2,3]naphthaloporphyryns via Oxidative Aromatization. *J. Org. Chem.* 68 (2003): 7517-7520.

- [10] Murashima, T.; Tsujimoto, S.; Yamada, T.; Miyazawa, T.; Uno, H.; Ono, N.; Sugimoto, N. Synthesis of Water-Soluble Porphyrin and the Corresponding Highly Planar Benzoporphyrin without *meso*-Substituents. *Tetrahedron Lett.* 46 (2005): 113-116.
- [11] Filatov, M. A.; Lebedev, A. Y.; Vinogradov, S. A.; Cheprakov, A. V. Synthesis of 5,15-Diaryltetrabenzoporphyrins. *J. Org. Chem.* 73 (2008): 4175-4185.
- [12] Lash, T. D.; Chandrasekar, P. Synthesis of Tetraphenyltetraacenaphthoporphyrin: A New Highly Conjugated Porphyrin System with Remarkably Red-Shifted Electronic Absorption Spectra. *J. Am. Chem. Soc.* 118 (1996): 8767-8768.
- [13] Spence, J. D.; Lash, T. D. Porphyrins with Exocyclic Rings. 14.1 Synthesis of Tetraacenaphthoporphyrins, a New Family of Highly Conjugated Porphyrins with Record-Breaking Long-Wavelength Electronic Absorptions. *J. Org. Chem.* 65 (2000): 1530-1539.
- [14] Lash, T. D.; Novak, B. H. Tetraphenanthro[9,10-*b*:9,10-*g*:9,10-*l*:9,10-*q*]porphyrin, a New Highly Conjugated Porphyrin System. *Angew. Chem., Int. Ed. Engl.* 34 (1995): 683-685.
- [15] Xu, H.-J.; Shen, Z.; Okujima, T.; Ono, N.; You, X.-Z. Synthesis and Spectroscopic Characterization of *meso*-Tetraarylporphyrins with Fused Phenanthrene Rings. *Tetrahedron Lett.* 47 (2006): 931-934.
- [16] Yamada, H.; Kuzuhara, D.; Takahashi, T.; Shimizu, Y.; Uota, K.; Okujima, T.; Uno, H.; Ono, N. Synthesis and Characterization of Tetraanthroporphyrins. *Org. Lett.* 10 (2008): 2947-2950.
- [17] Lash, T. D.; Werner, T. M.; Thompson, M. L.; Manley, J. M. Porphyrins with Exocyclic Rings. 16.1 Synthesis and Spectroscopic Characterization of Fluoranthoporphyrins, a New Class of Highly Conjugated Porphyrin Chromophores. *J. Org. Chem.* 66 (2001): 3152-3159.
- [18] Campbell, W. M.; Burrell, A. K.; Officer, D. L.; Jolley, K. W. Porphyrins as Light Harvesters in the Dye-Sensitised TiO₂ Solar Cell. *Coord. Chem. Rev.* 248 (2004): 1363-1379.

- [19] Xu, X.; Chen, H.; Cai, X. R.; Li, Y.; Jiang, Q. Synthesis and Properties of Polyfluorene Copolymers Bearing Thiophene and Porphyrin. *Chin. Chem. Lett.* 18 (2007): 879-882.
- [20] Montes, V. A.; Perez-Bolivar, C.; Agarwal, N.; Shinar, J.; Anzenbacher, P. Molecular-Wire Behavior of OLED Materials: Exciton Dynamics in Multichromophoric Alq₃-Oligofluorene-Pt(II)porphyrin Triads. *J. Am. Chem. Soc.* 128 (2006): 12436-12438.
- [21] Kim, D. U.; Paik, S.-H.; Kim, S.-H.; Tak, Y.-H.; Kim, S.-D.; Han, Y.-S.; Kim, T.-J.; Ko, T.-H.; Yoon, U.-C.; Mariano, P. S. Electroluminescent Characteristics of Novel Platinum-Porphyrin Complex. *Colloids Surf. A* 313-314 (2008): 444-447.
- [22] D'Amico, A.; Di Natale, C.; Paolesse, R.; Macagnano, A.; Mantini, A. Metalloporphyrins as Basic Material for Volatile Sensitive Sensors. *Sens. Act. B* 65 (2000): 209-215.
- [23] Ma, X.; Sun, J.; Wang, M.; Hu, M.; Li, G.; Chen, H.; Huang, J. Effects of Fluorination in the Ring of Zinc Tetraphenylporphyrin on its Gas-Response to Volatiles at Room Temperature. *Sens. Actuators B* 114 (2006): 1035-1042.
- [24] Kubo, Y.; Yamamoto, M.; Ikeda, M.; Takeuchi, M.; Shinkai, S.; Yamaguchi, S.; Tamao, K., A Colorimetric and Ratiometric Fluorescent Chemosensor with Three Emission Changes: Fluoride Ion Sensing by a Triarylborane-Porphyrin Conjugate. *Angew. Chem., Int. Ed.* 42 (2003): 2036-2040.
- [25] Ko, Y.-J.; Yun, K.-J.; Kang, M.-S.; Park, J.; Lee, K.-T.; Park, S. B.; Shin, J.-H. Synthesis and in vitro Photodynamic Activities of Water-Soluble Fluorinated Tetrapyridylporphyrins as Tumor Photosensitizers. *Bioorg. Med. Chem. Lett.* 17 (2007): 2789-2794.
- [26] Weimin, S.; Gen, Z.; Guifu, D.; Yunxiao, Z.; Jin, Z.; Jingchao, T. Synthesis and in vitro PDT Activity of Miscellaneous Porphyrins with Amino Acid and Uracil. *Bioorg. Med. Chem.* 16 (2008): 5665-5671.
- [27] Bonnett, R. Photosensitizers of the Porphyrin and Phthalocyanine Series for Photodynamic Therapy. *Chem. Soc. Rev.* 24 (1995): 19-33.

- [28] Stilts, C. E.; Nelen, M. I.; Hilmey, D. G.; Davies, S. R.; Gollnick, S. O.; Oseroff, A. R.; Gibson, S. L.; Hilf, R.; Detty, M. R. Water-Soluble, Core-Modified Porphyrins as Novel, Longer-Wavelength-Absorbing Sensitizers for Photodynamic Therapy. *J. Med. Chem.* 43 (2000): 2403-2410.
- [29] Sessler, J. L.; Weghorn, S. J. *Expanded, Contracted & Isomeric Porphyrins*. Pergamon: 1997; Vol. 15.
- [30] Novak, B. H.; Lash, T. D. Porphyrins with Exocyclic Rings. 11.1 Synthesis and Characterization of Phenanthroporphyrins, a New Class of Modified Porphyrin Chromophores. *J. Org Chem.* 63 (1998): 3998-4010.
- [31] Lash, T. D.; Chandrasekar, P.; Osuma, A. T.; Chaney, S. T.; Spence, J. D. Porphyrins with Exocyclic Rings. 13.1 Synthesis and Spectroscopic Characterization of Highly Modified Porphyrin Chromophores with Fused Acenaphthylene and Benzothiadiazole Rings. *J. Org. Chem.* 63 (1998): 8455-8469.
- [32] Fukuhara, K.; Takei, M.; Kageyama, H.; Miyata, N. Di- and Trinitrophenanthrenes: Synthesis, Separation, and Reduction Property. *Chem. Res. Toxicol.* 8 (1995): 47-54.
- [33] Geier Iii, G. R.; Lindsey, J. S. Effects of Aldehyde or Dipyrromethane Substituents on the Reaction Course Leading to *meso*-Substituted Porphyrins. *Tetrahedron* 60 (2004): 11435-11444.
- [34] Arunwattanachok, T. Synthesis of Pyridylporphyrin metal complexes. Chulalongkorn University, 2006.

APPENDIX

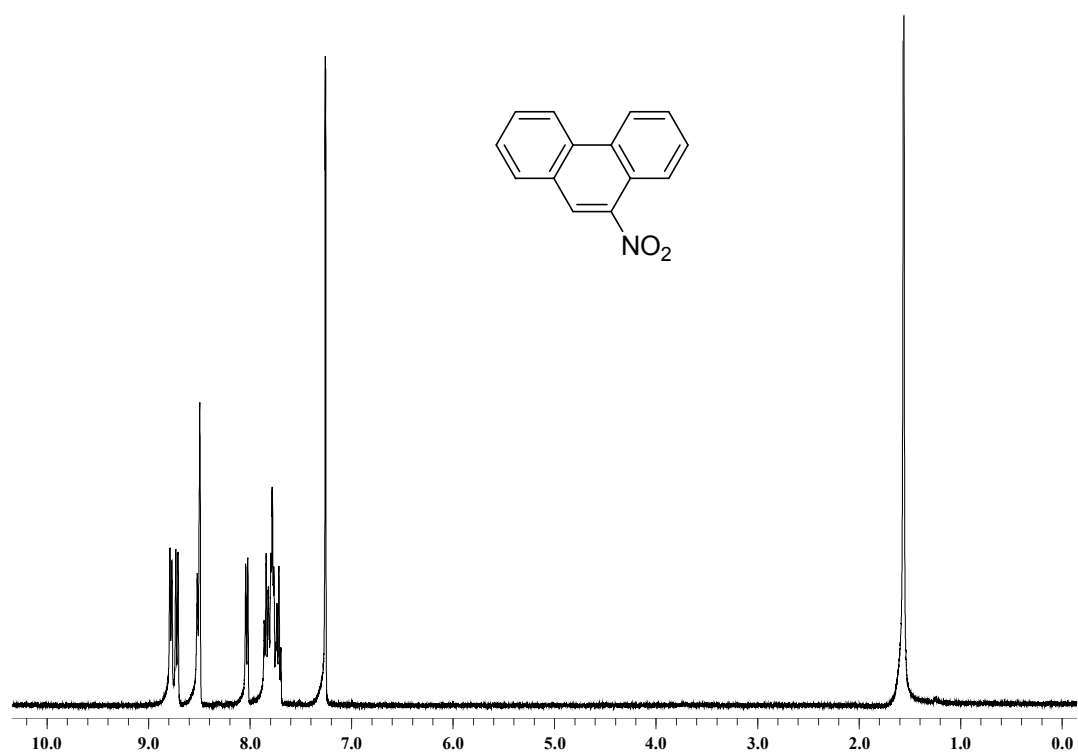


Figure A-1 The $^1\text{H-NMR}$ spectrum of 9-nitrophenanthrene (1)

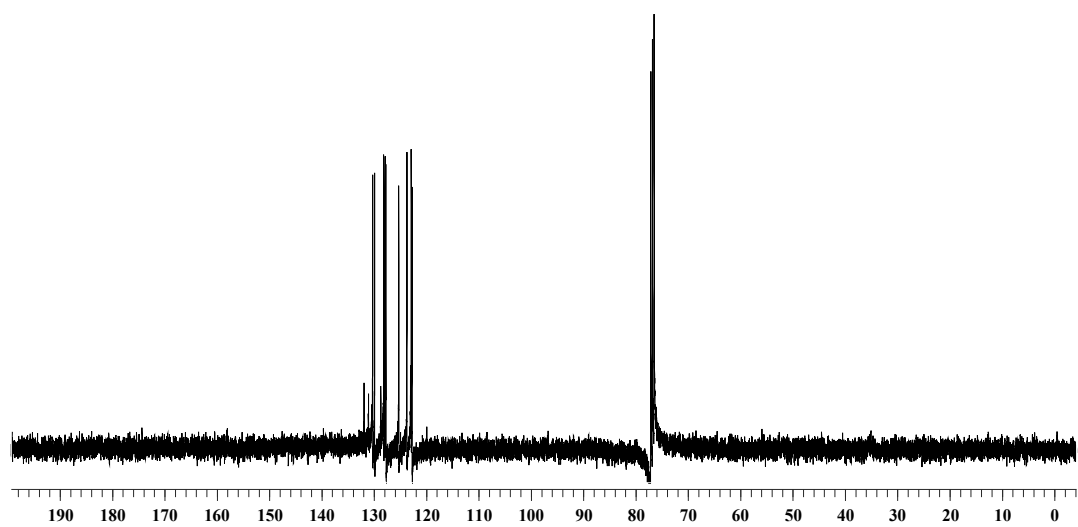


Figure A-2 The $^{13}\text{C-NMR}$ spectrum of 9-nitrophenanthrene (1)

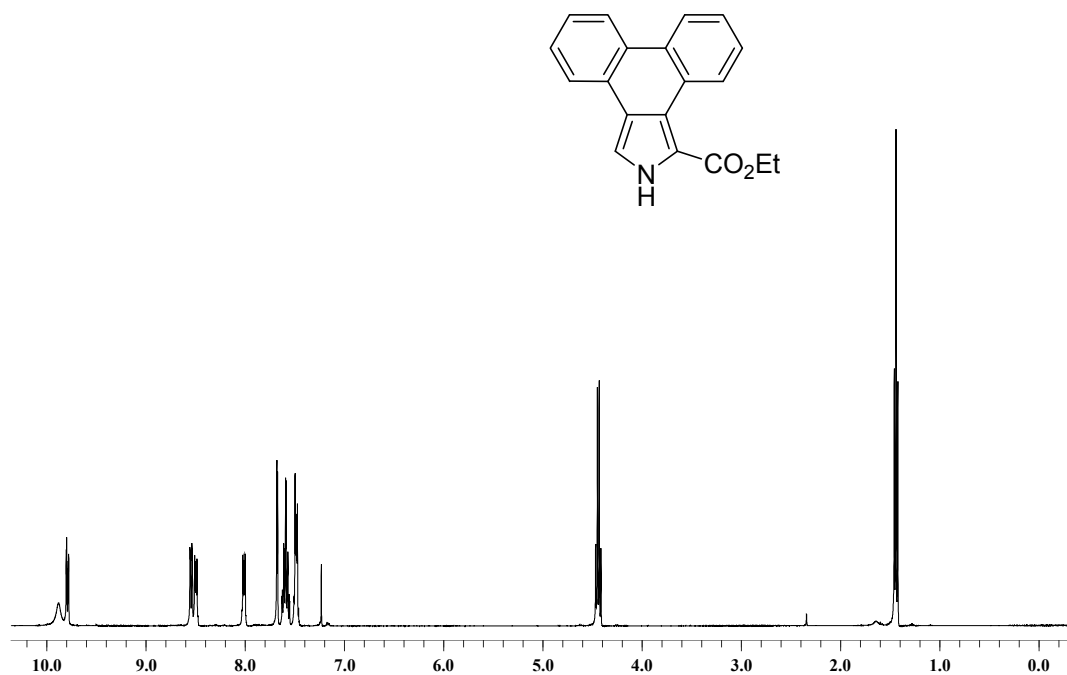


Figure A-3 The ¹H-NMR spectrum of ethyl phenanthro[9,10-*c*]pyrrole-1-carboxylate (2)

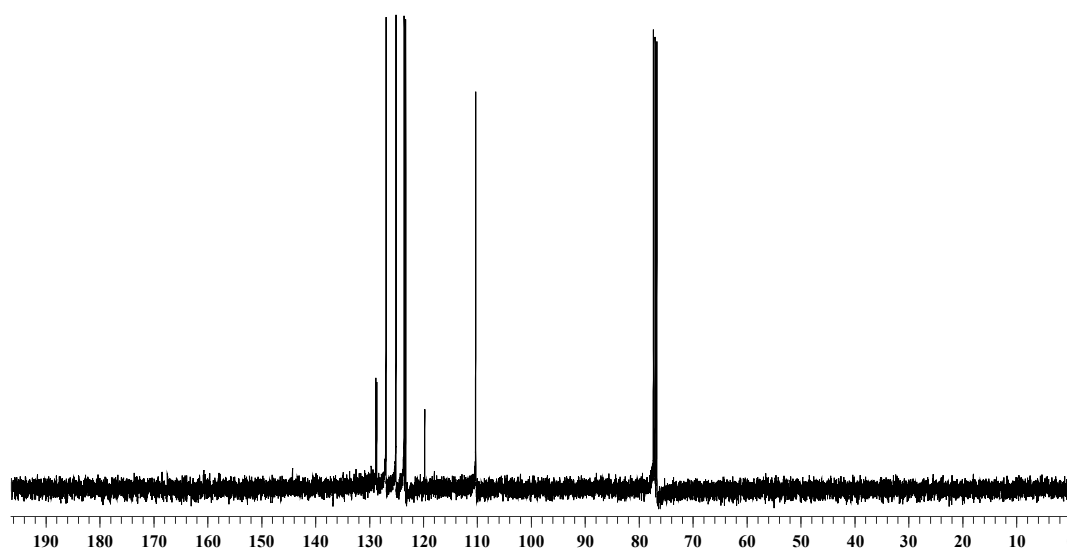


Figure A-4 The ¹³C-NMR spectrum of ethyl phenanthro[9,10-*c*]pyrrole-1-carboxylate (2)

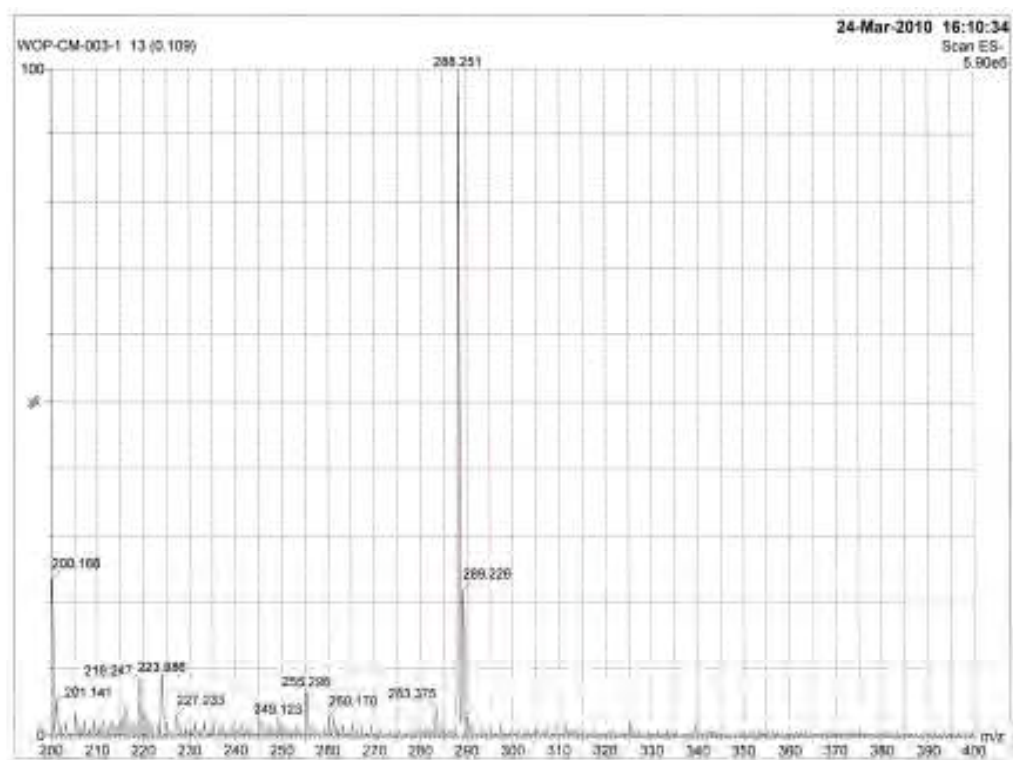


Figure A-5 The ESI mass spectrum of ethyl phenanthro[9,10-*c*]pyrrole-1-carboxylate (2)

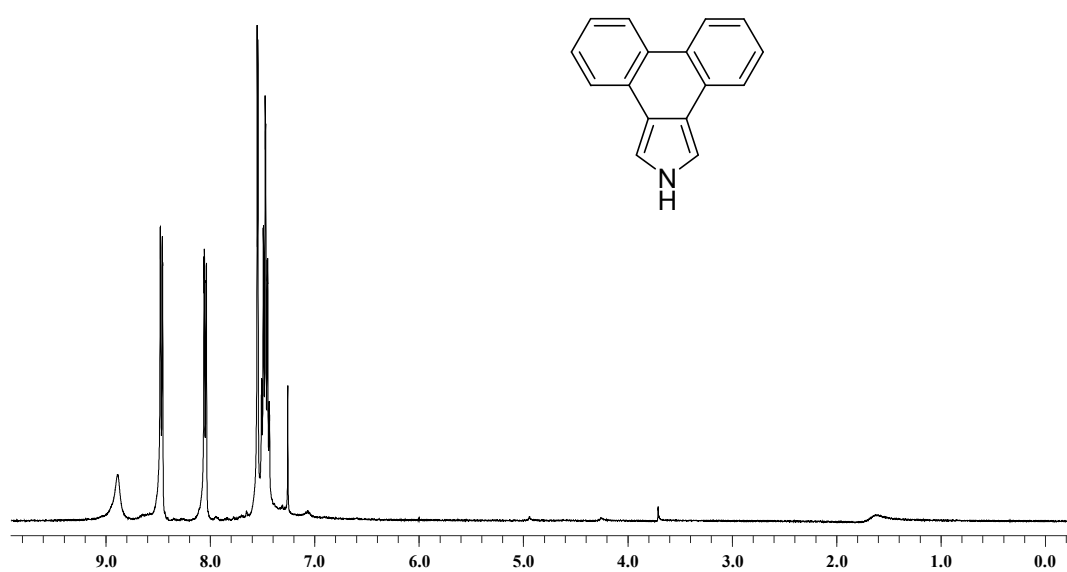


Figure A-6 The ^1H -NMR spectrum of phenanthro[9,10-*c*]pyrrole (3)

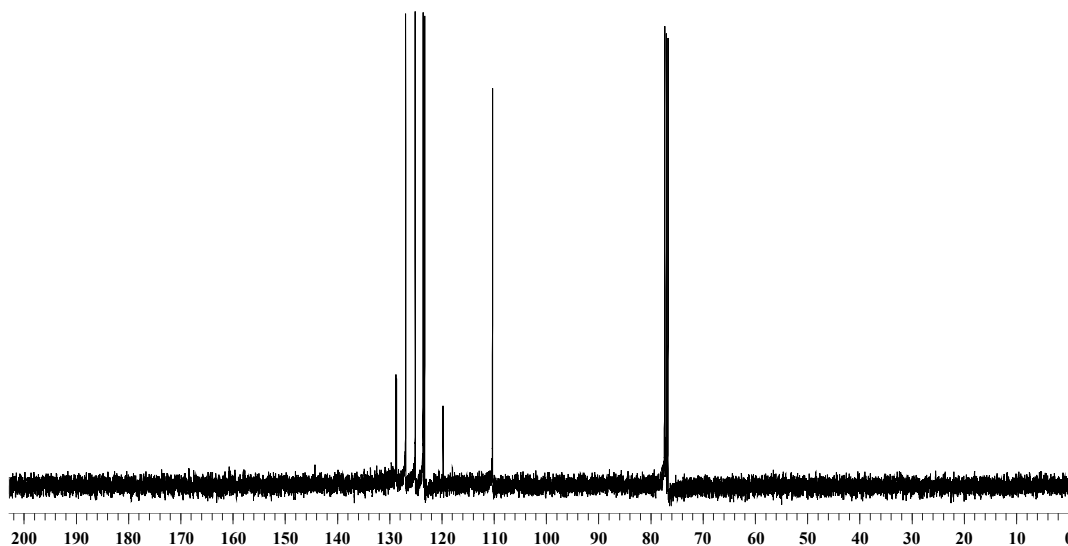


Figure A-7 The ^{13}C -NMR spectrum of phenanthro[9,10-*c*]pyrrole (3)

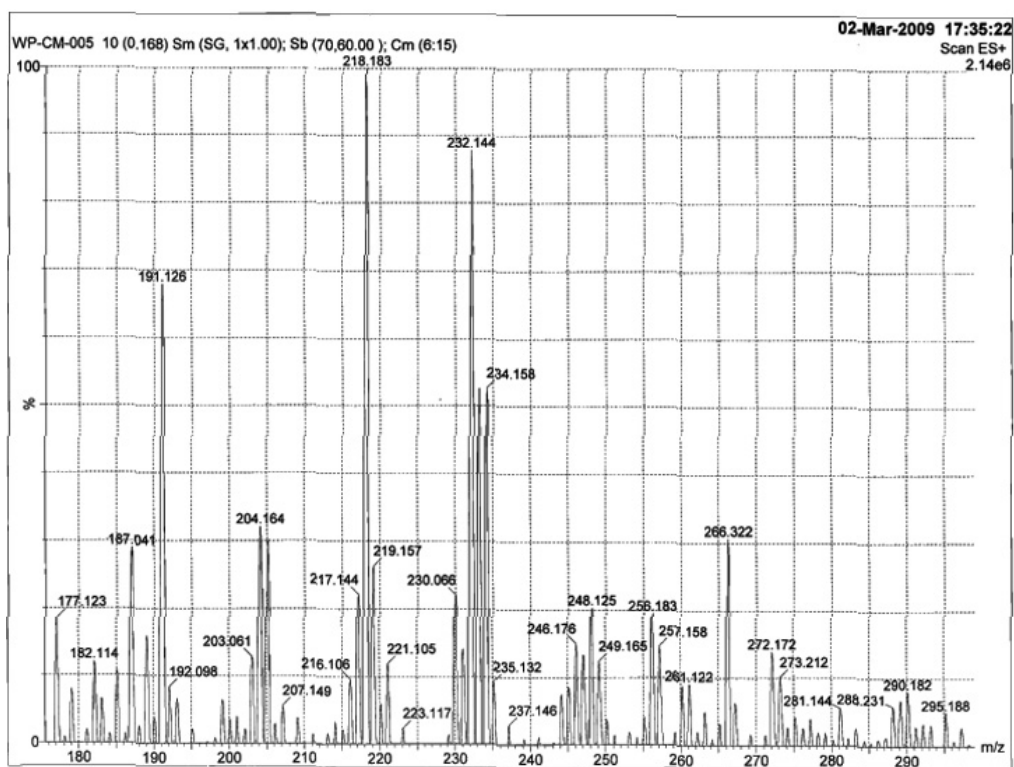


Figure A-8 The ESI mass spectrum of phenanthro[9,10-*c*]pyrrole (3)

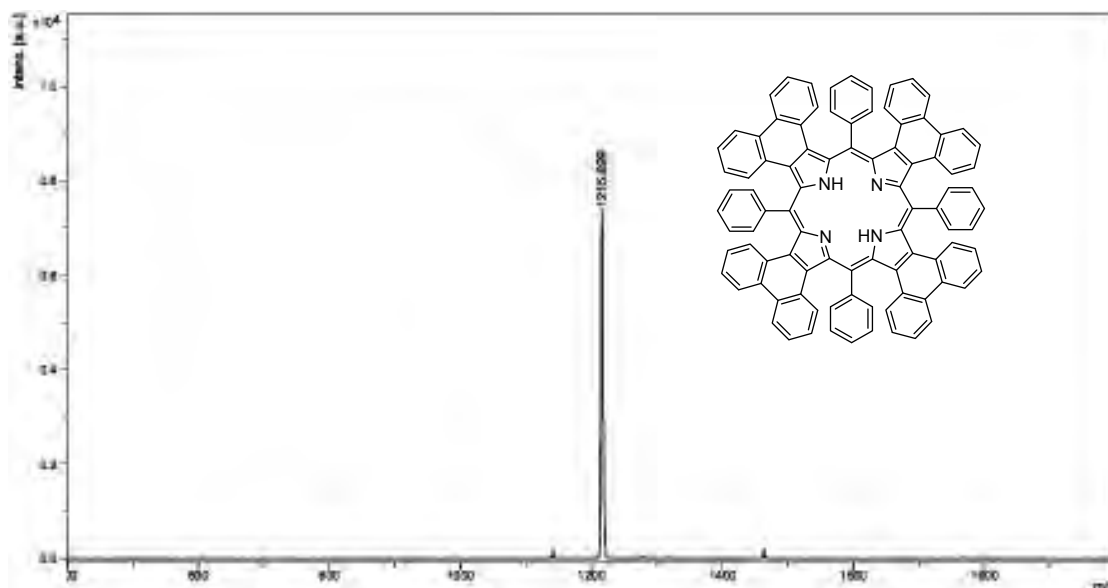


Figure A-9 The MALDI-TOF mass spectrum of TPTPP (4)

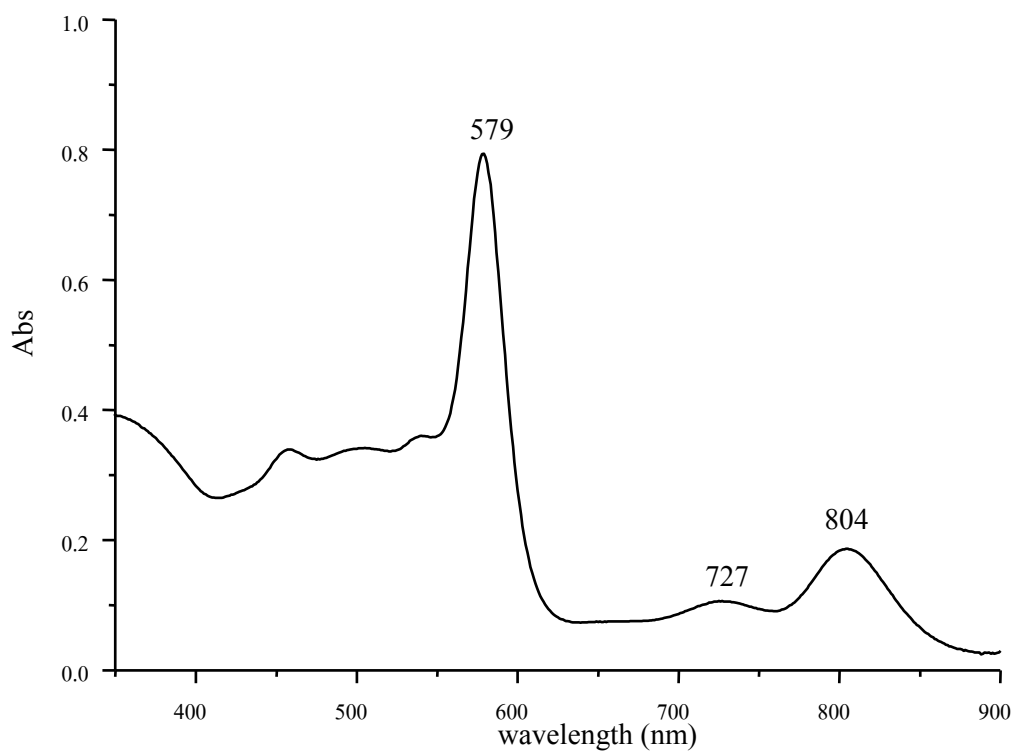


Figure A-10 The UV-visible mass spectrum of TPTPP (4)

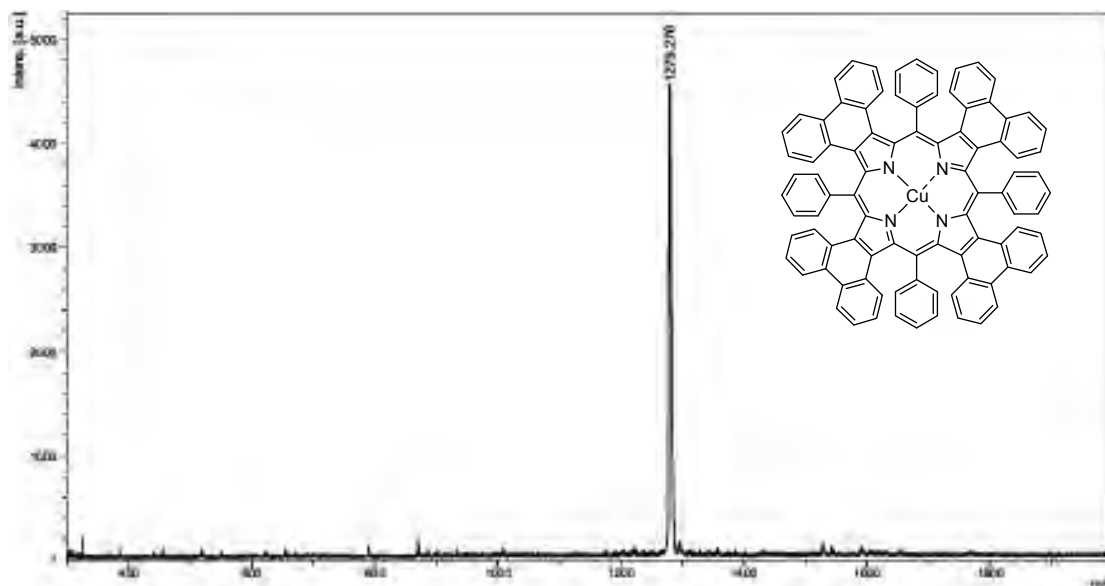


Figure A-11 The MALDI-TOF mass spectrum of Cu-TPTPP (5)

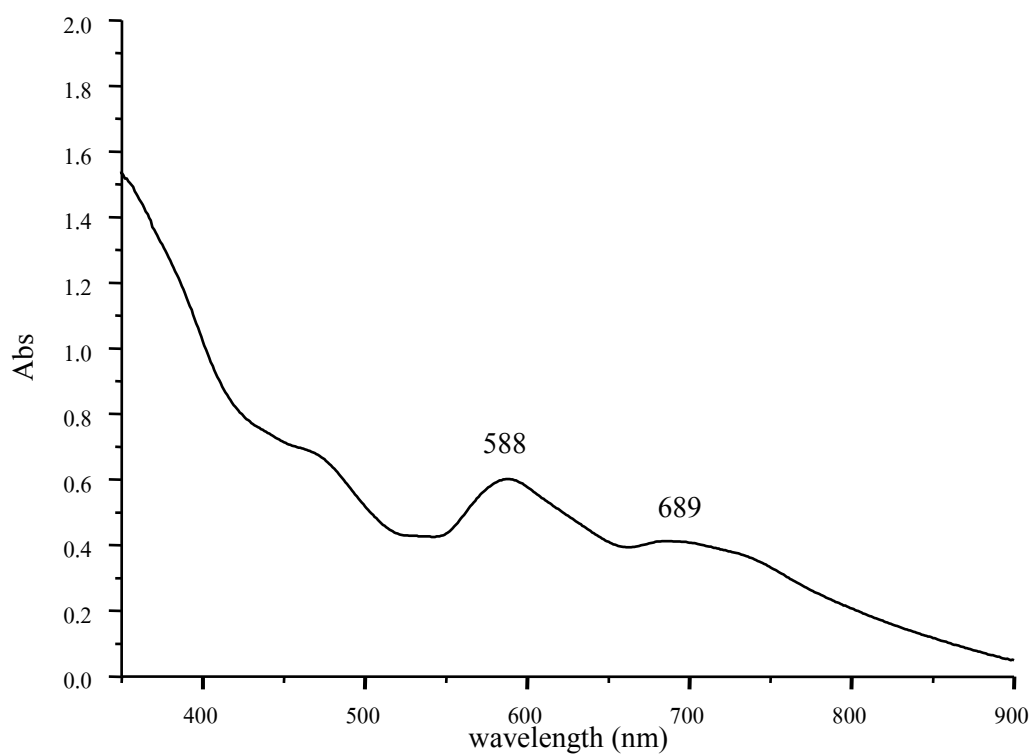


Figure A-12 The UV-visible mass spectrum of Cu-TPTPP (5)

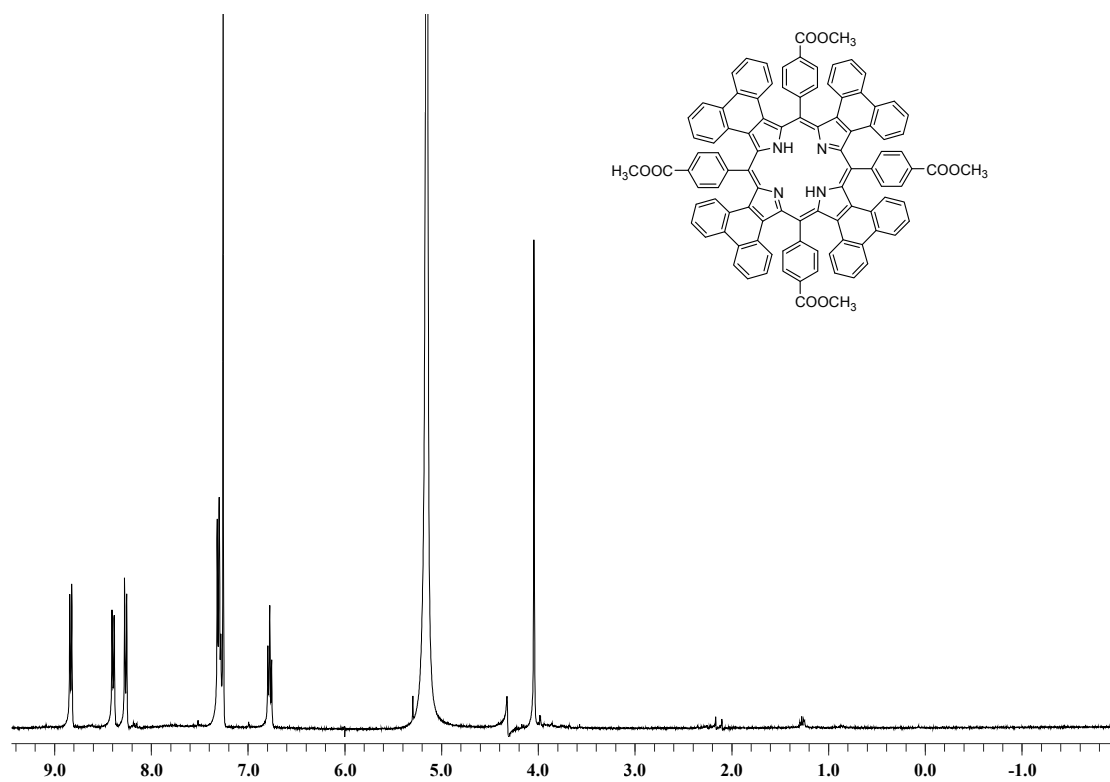


Figure A-13 The $^1\text{H-NMR}$ spectrum of TMCPTP (7)

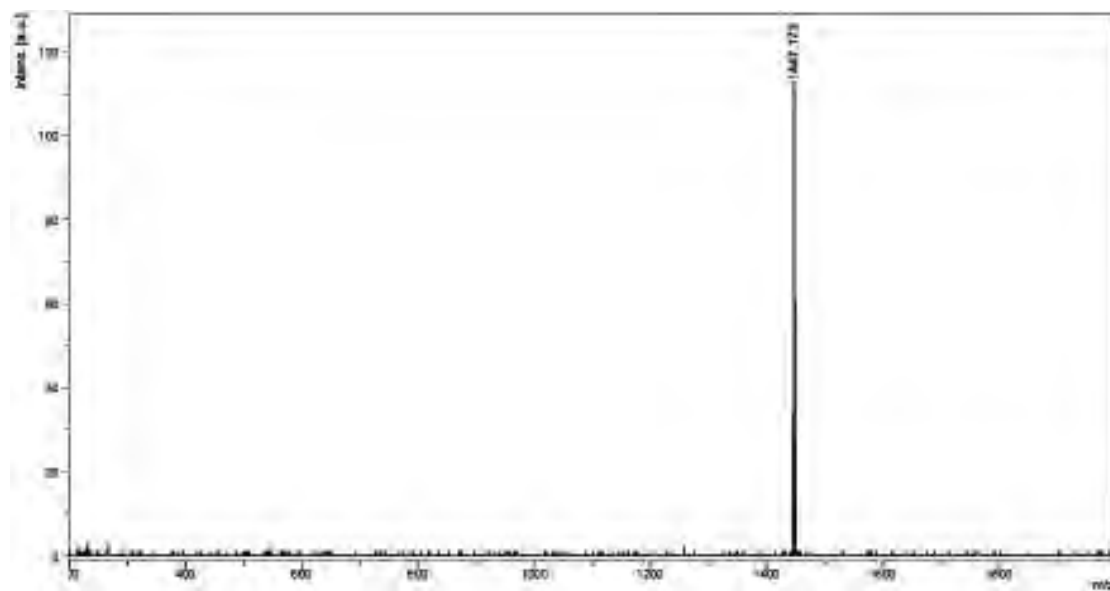


Figure A-14 The MALDI-TOF mass spectrum of TMCPTP (7)

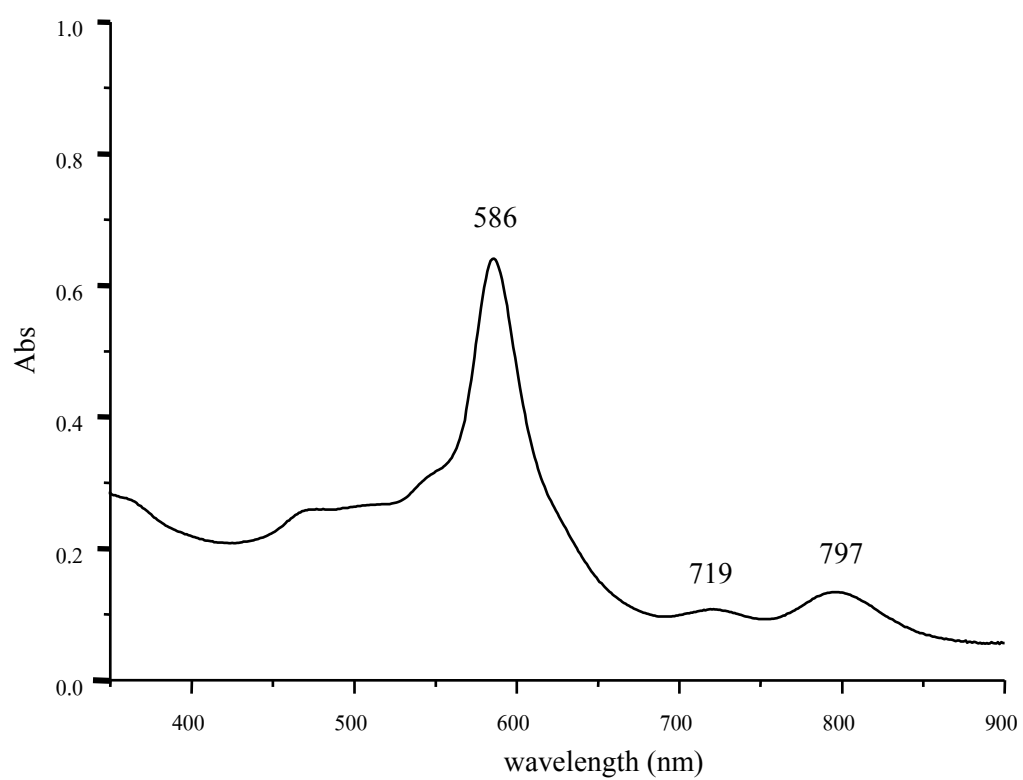


Figure A-15 The UV-visible mass spectrum of TMCPTPP (7)

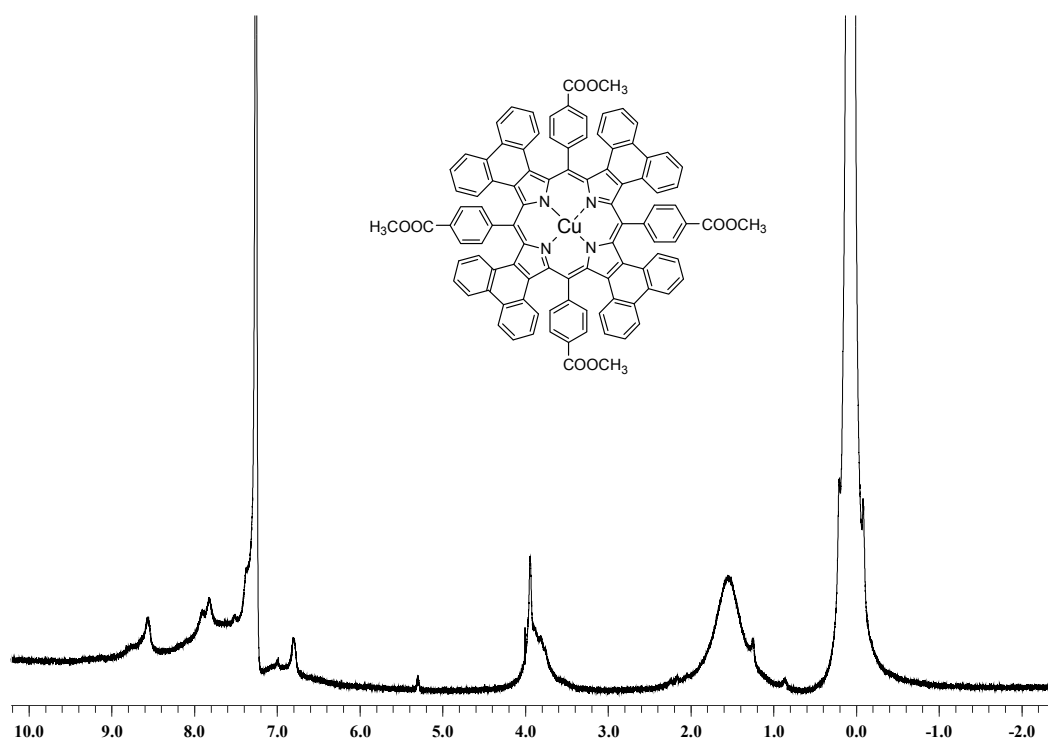


Figure A-16 The $^1\text{H-NMR}$ spectrum of Cu-TMCPTPP (8)

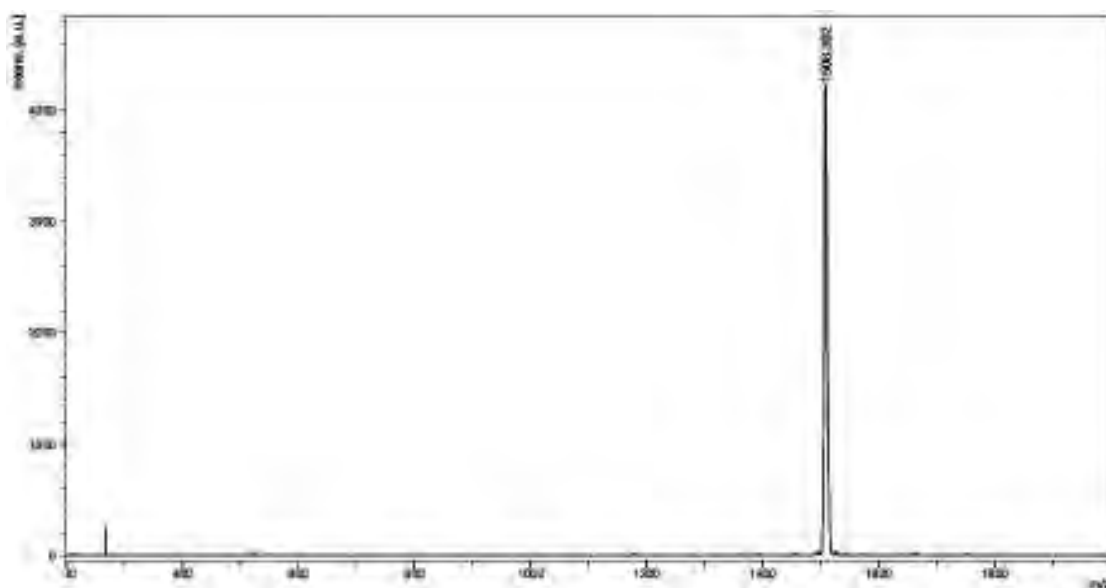


Figure A-17 The MALDI-TOF mass spectrum of Cu-TMCPTPP (**8**)

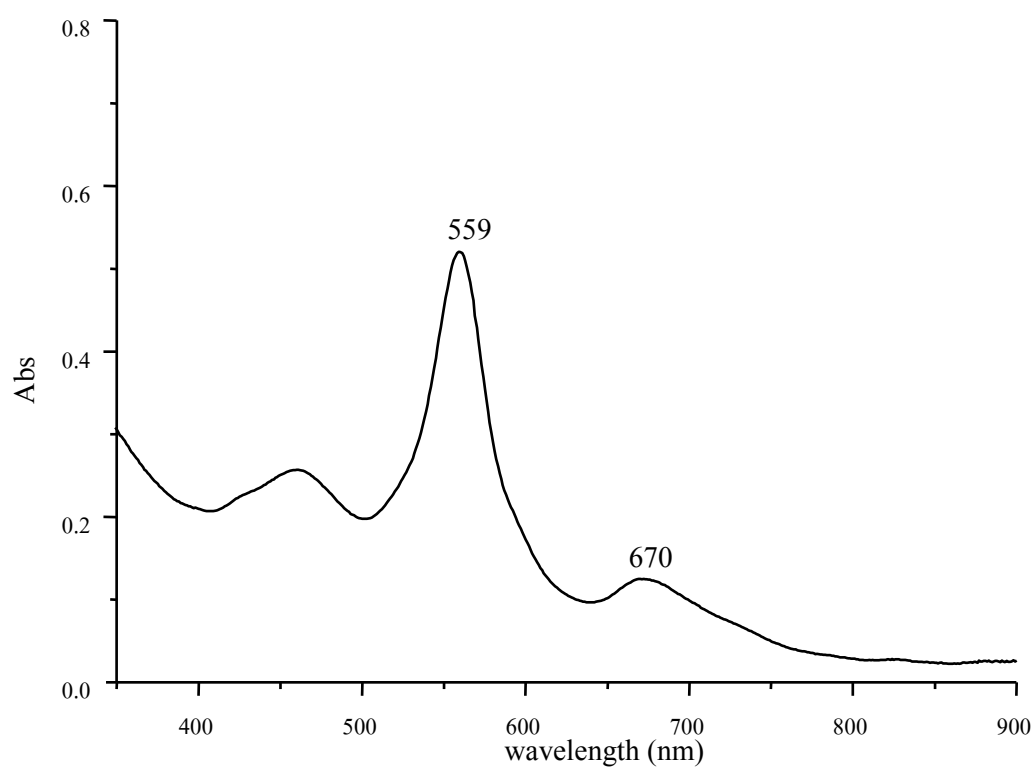


Figure A-18 The UV-visible mass spectrum of Cu-TMCPTPP (**8**)

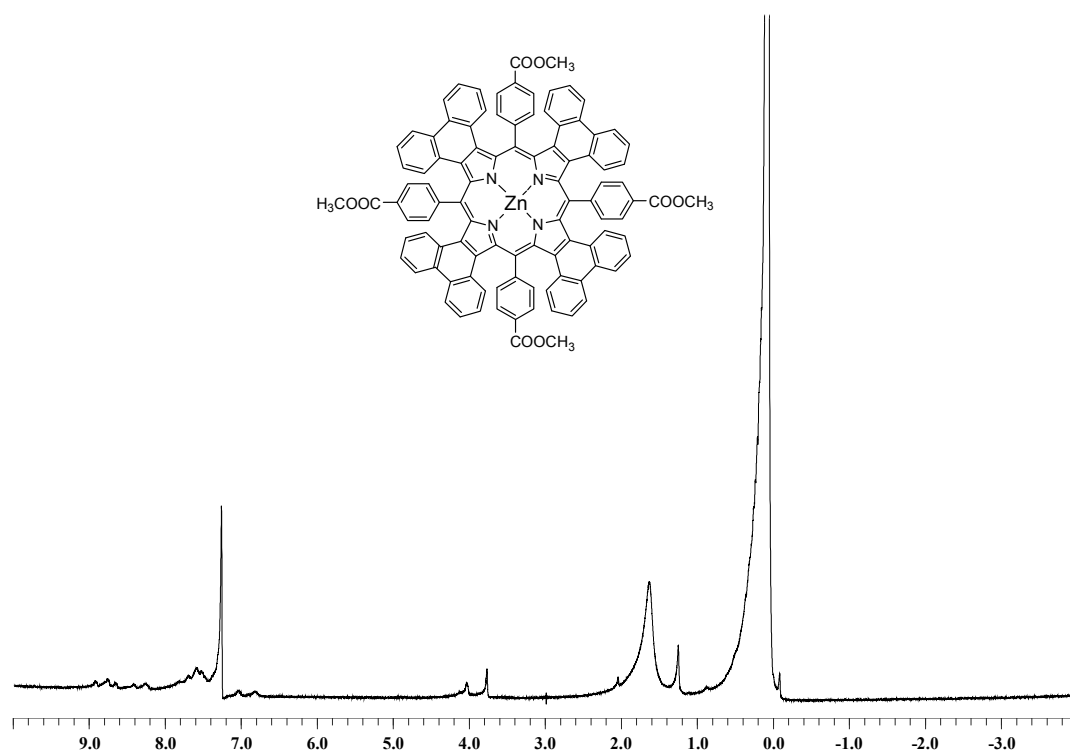


Figure A-19 The ¹H-NMR spectrum of Zn-TMCPTP (9)

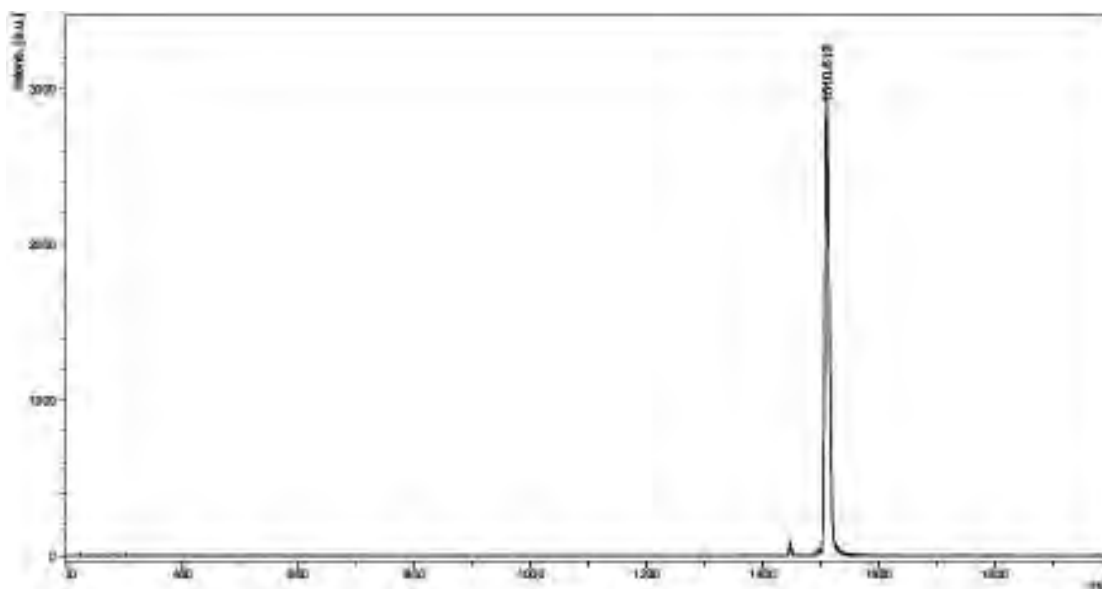


Figure A-20 The MALDI-TOF mass spectrum of Zn-TMCPTP (9)

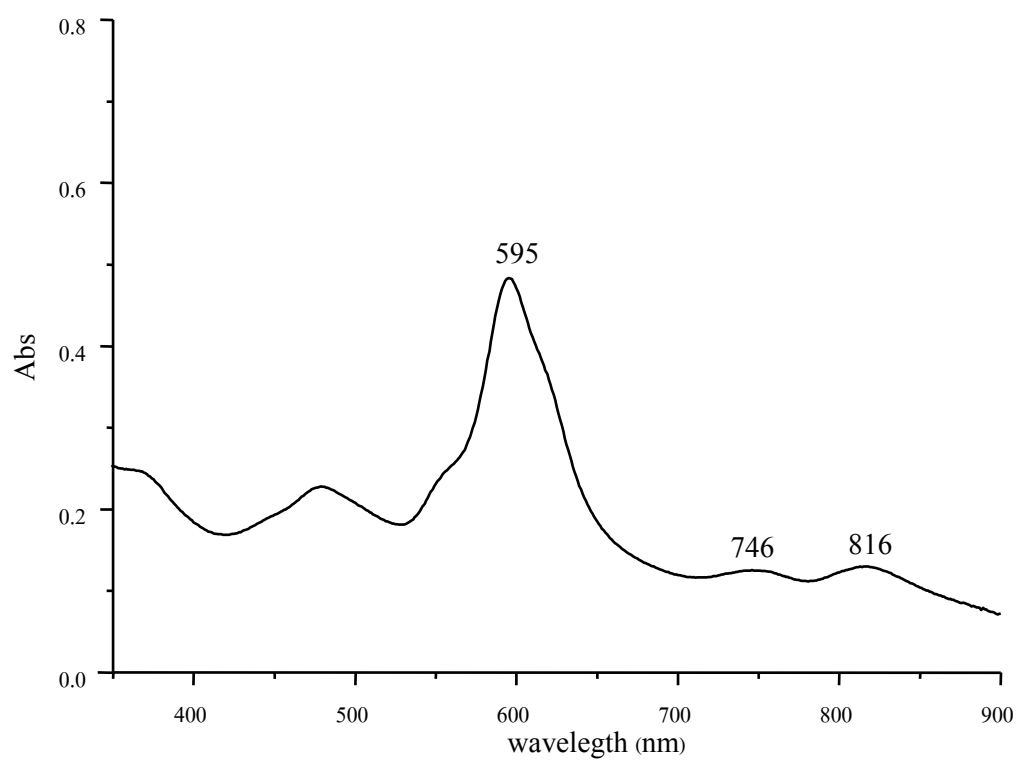


Figure A-21 The UV-visible mass spectrum of Zn-TMCPTP (9)

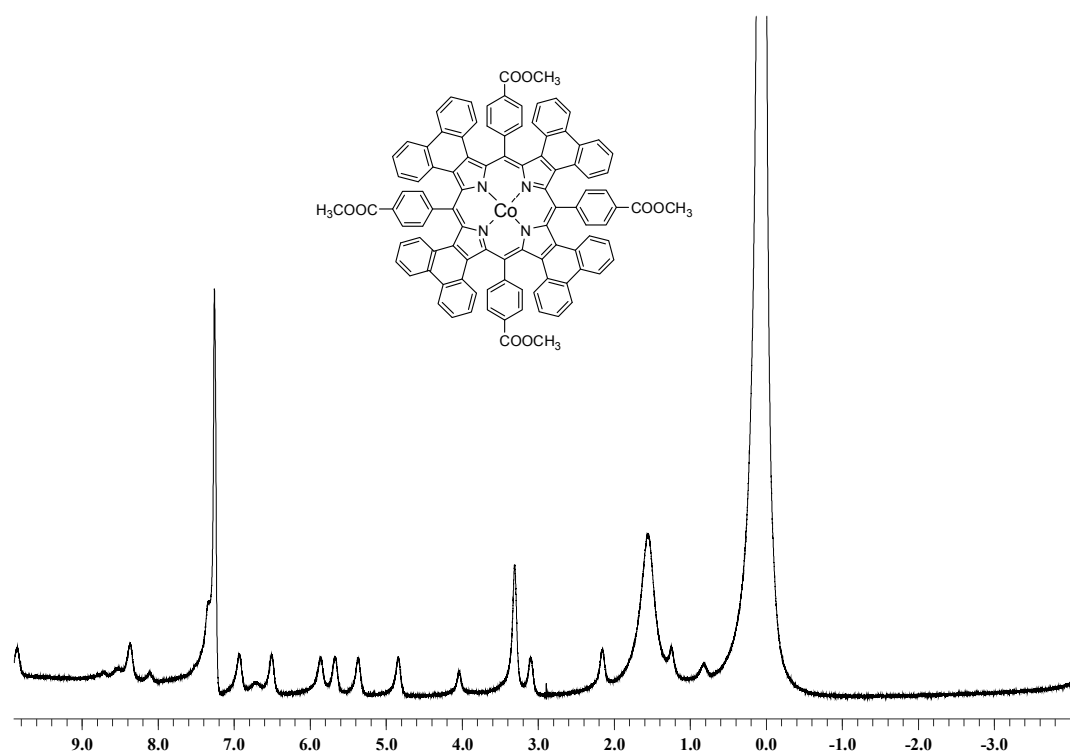


Figure A-22 The ¹H-NMR spectrum of Co-TMCPTP (10)

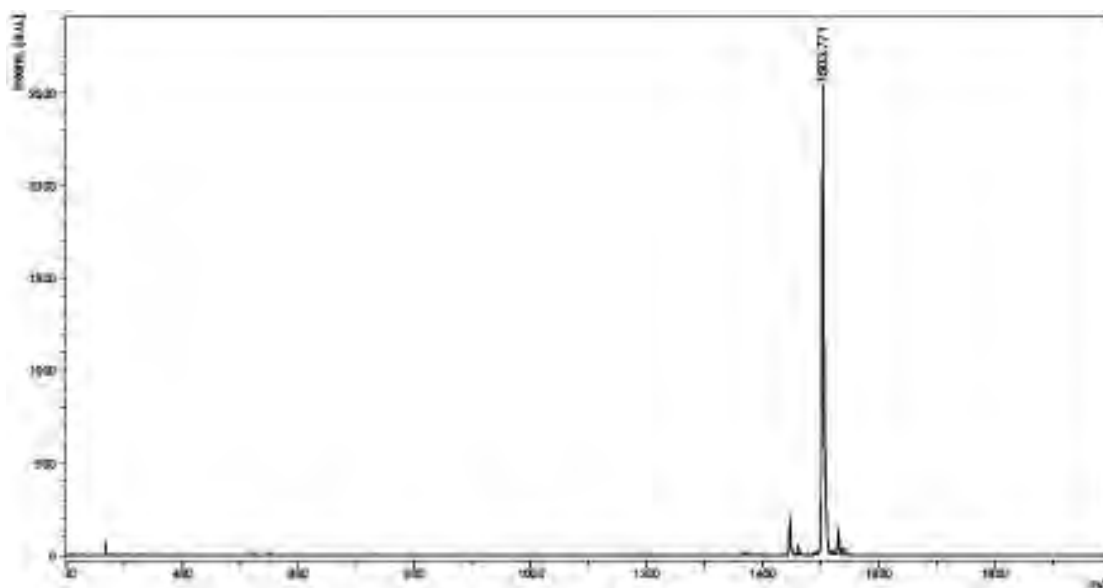


Figure A-23 The MALDI-TOF mass spectrum of Co-TMCPTP (**10**)

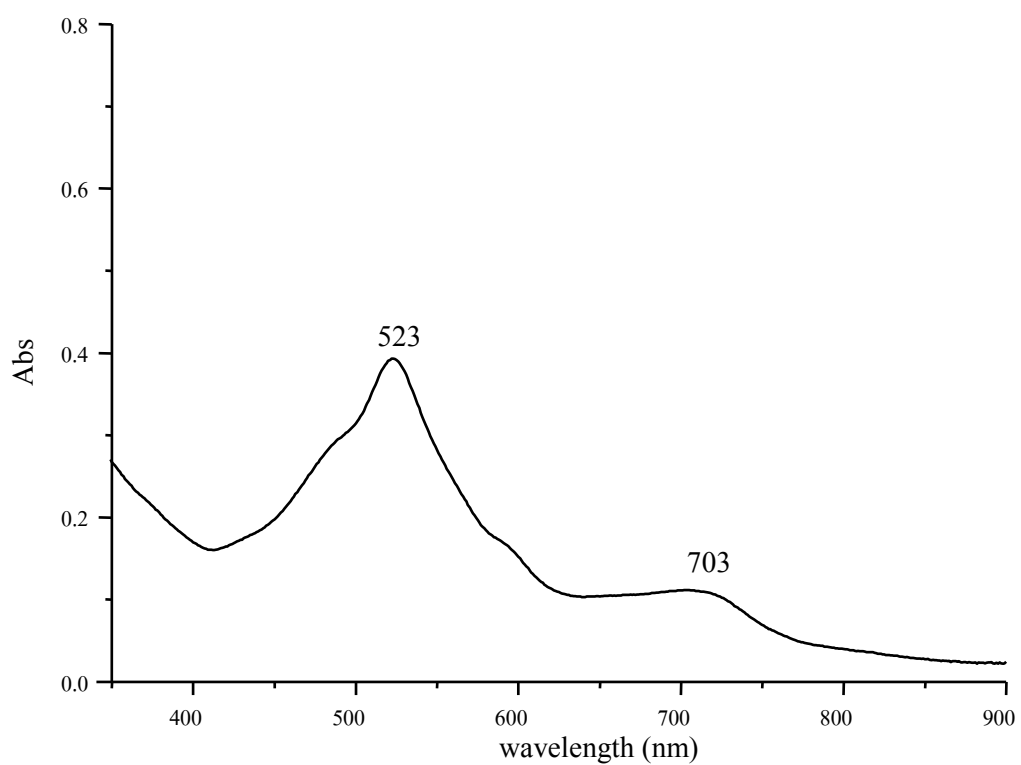


Figure A-24 The UV-visible mass spectrum of Co-TMCPTP (**10**)

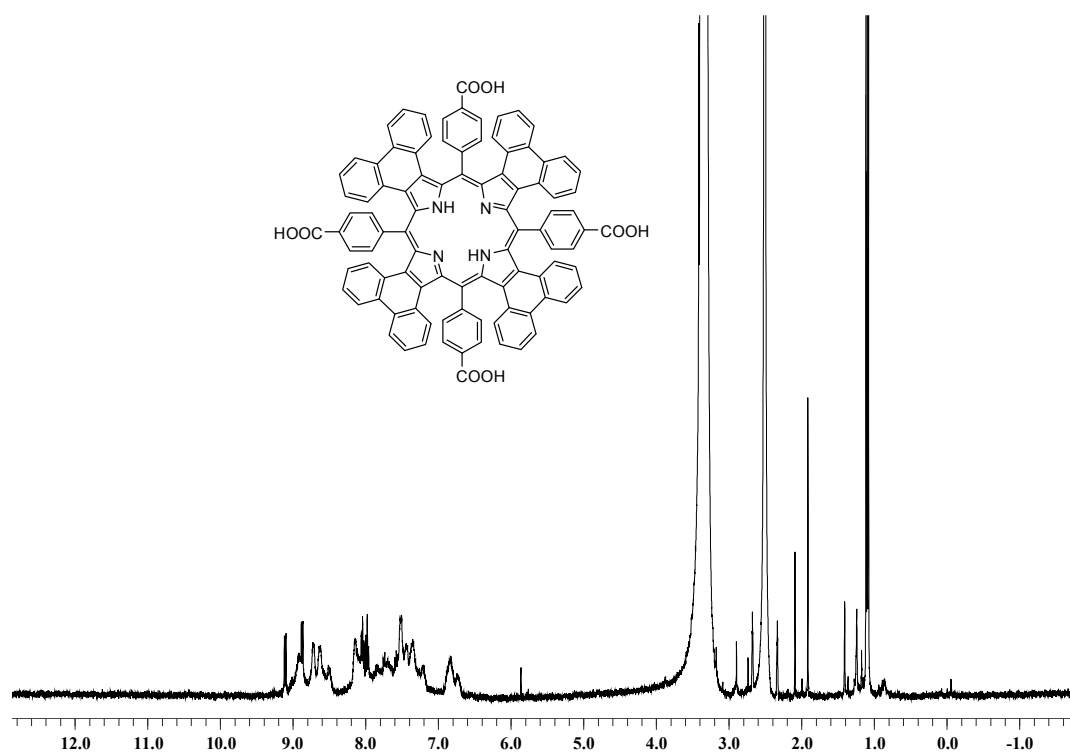


Figure A-25 The ¹H-NMR spectrum of TCPTP (11)

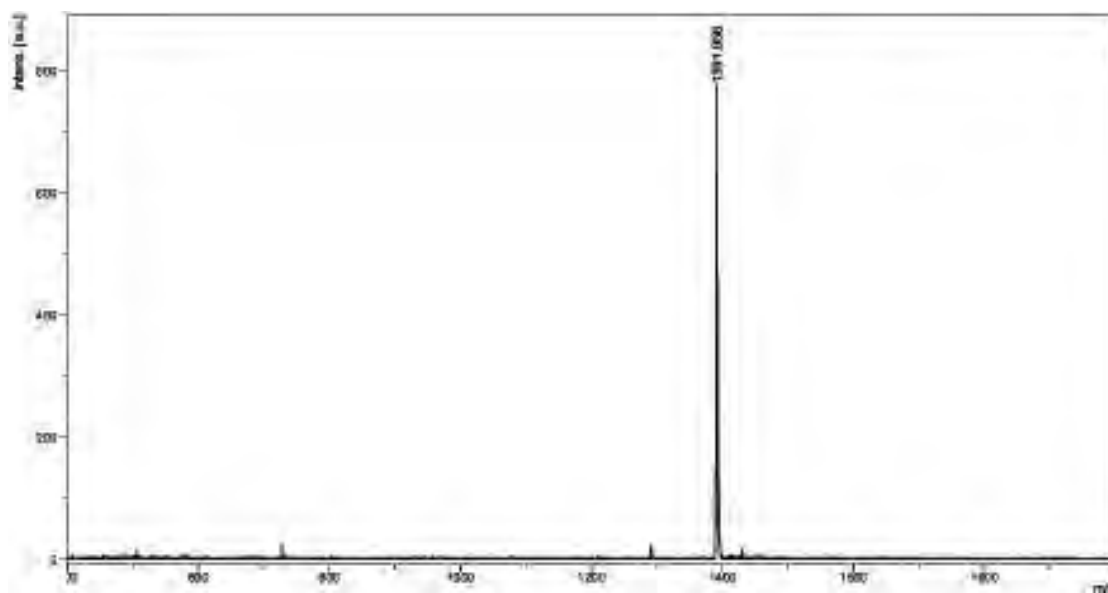


Figure A-26 The MALDI-TOF mass spectrum of TCPTP (11)

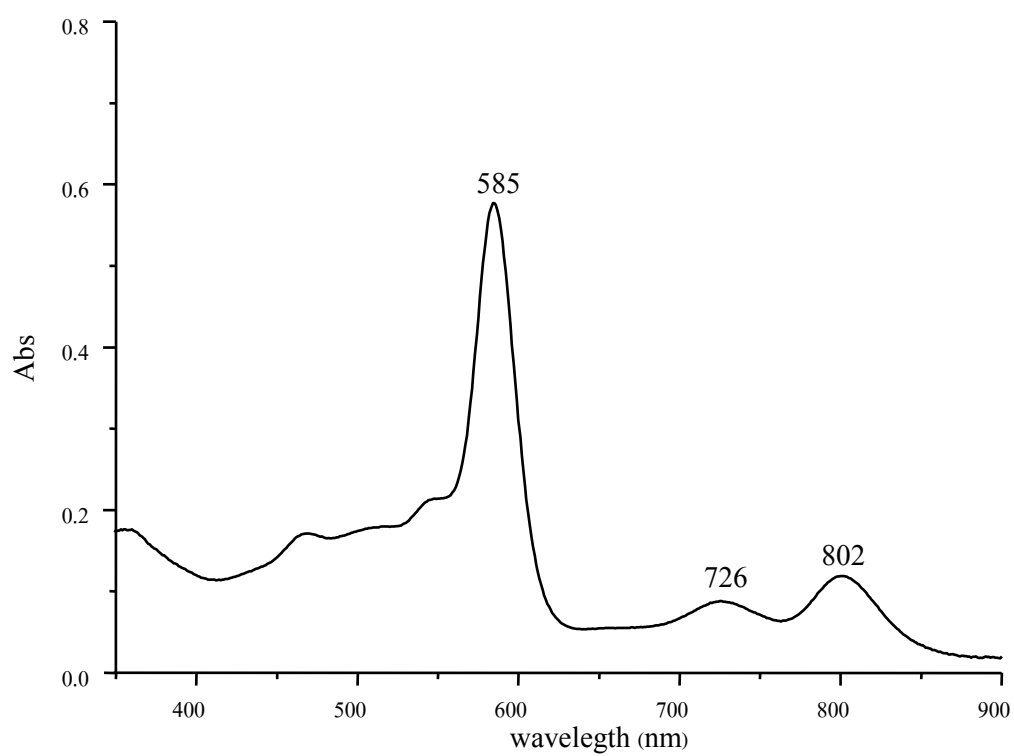


Figure A-27 The UV-visible mass spectrum of TCPTP (11)

VITAE

Miss Chommapat Mettaprasert was born on 14 November 1984 in Bangkok, Thailand. Her present address is 14/17 Ganjanapisek Street, Salatummasop sub-district, Taviwattana District, Bangkok, 10170. She began her study in Rajini School. Then, she received a Bachelor Degree of Science, majoring in Chemistry from Faculty of Science, Chulalongkorn University in 2006 under the support from Human Resource Development in Science Project. Upon her graduation, she received a scholarship from the Center for Petroleum, Petrochemicals and Advanced Materials at Chulalongkorn University to do Master's degree in Organic Chemistry at Department of Chemistry, Faculty of Science, Chulalongkorn University.

Presentation in Conference:

- | | |
|---------------|--|
| November 2009 | The 11 th International Kyoto Conference on New Aspects of Organic Chemistry (IKCOC-11), Rihga Royal Hotel, Kyoto, Japan. |
| November 2009 | The 6 th International Symposium on Advanced Materials in Asia-Pacific Rim (ISAMAP), Faculty of Science, Chulalongkorn University, Bangkok, Thailand. |
| March 2010 | The 18 th Science Forum, Faculty of Science, Chulalongkorn University, Bangkok, Thailand. |

Publication in proceeding: “Synthesis and Characterization of Tetrakis ((methoxy-carbonyl)phenyl)tetraphenanthroporphyrin” The 6th International Symposium on Advanced Materials in Asia-Pacific Rim (ISAMAP), Faculty of Science, Chulalongkorn University, Bangkok, Thailand, November 21-23, 2009, pp 71-74.